# Temperature and Polarization Spectra

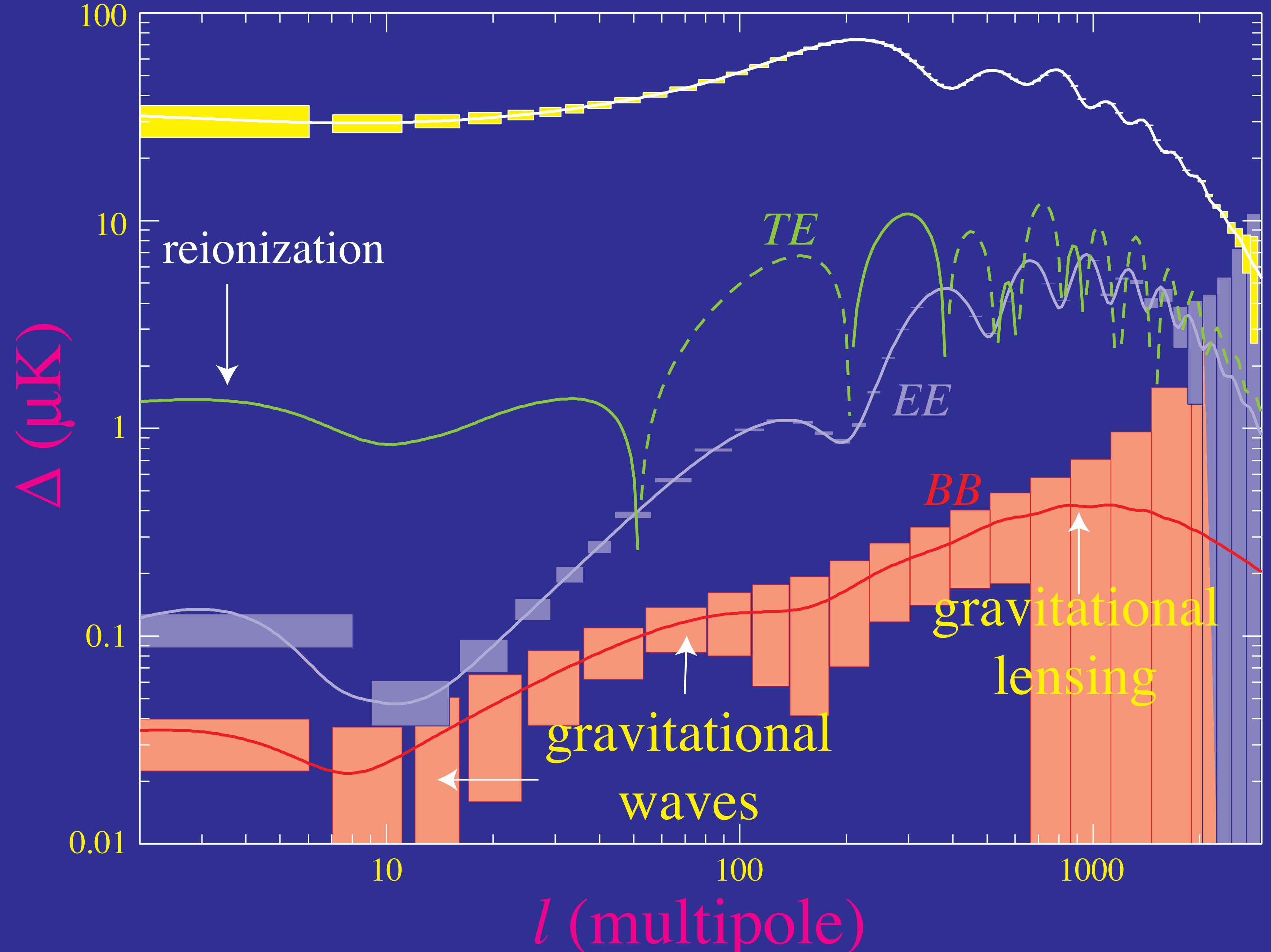

# Physics of Secondary Anisotropies

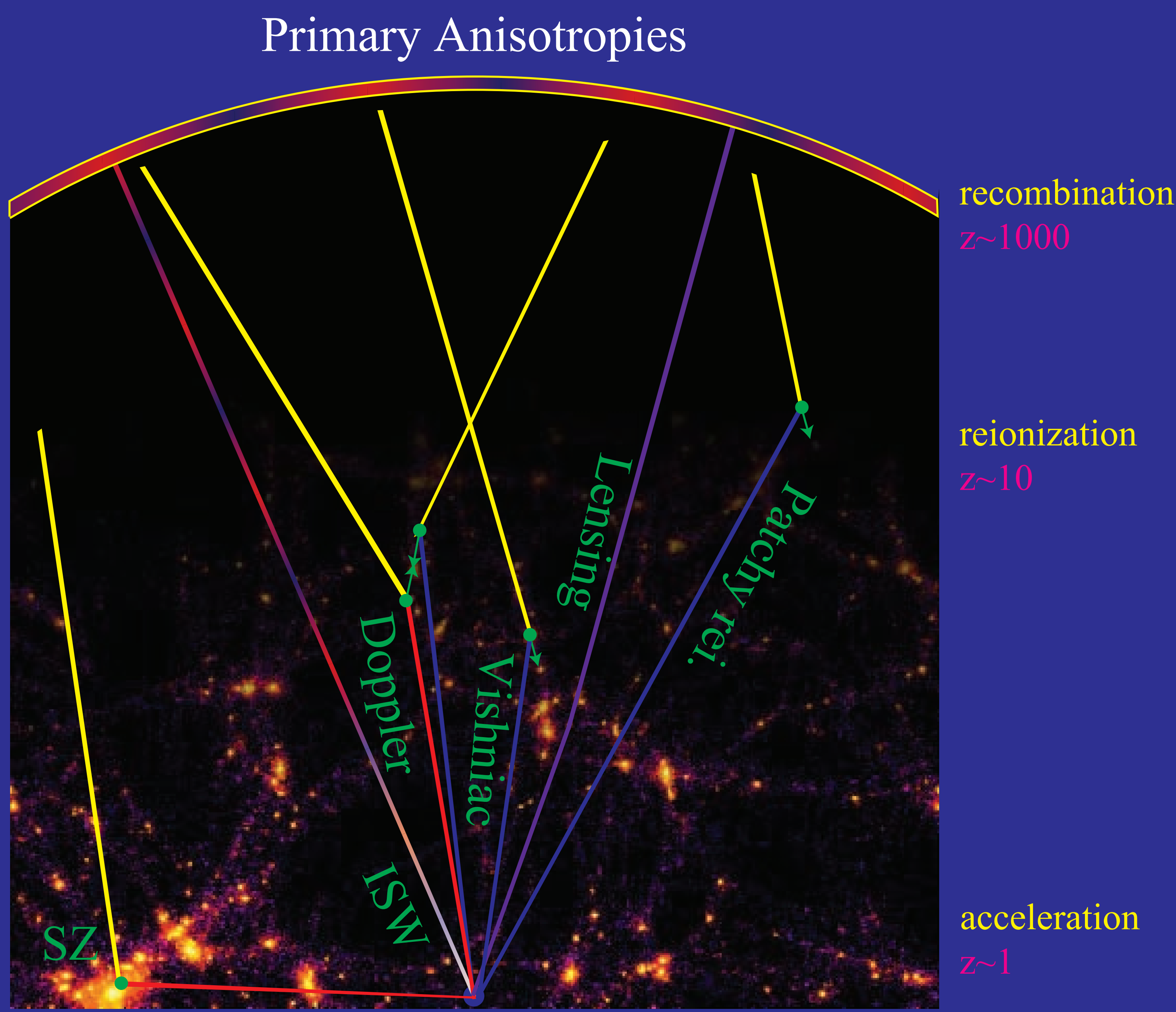

# Scattering Secondaries

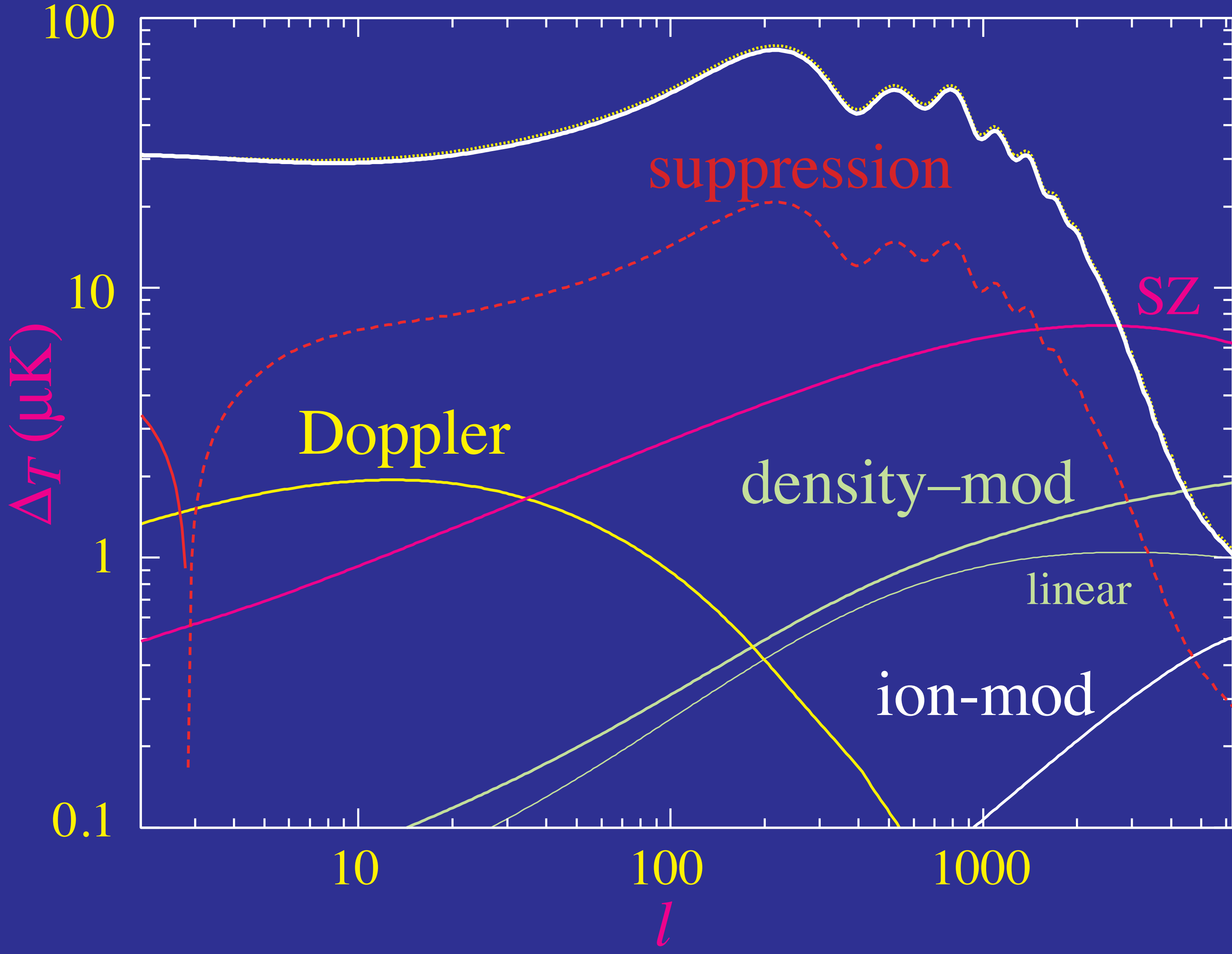

# Anisotropy Suppression

- A fraction $\tau$~0.1 of photons rescattered during reionization out of line of sight and replaced statistically by photon with random temperature flucutuation - suppressing anisotropy as $e^{-\tau}$

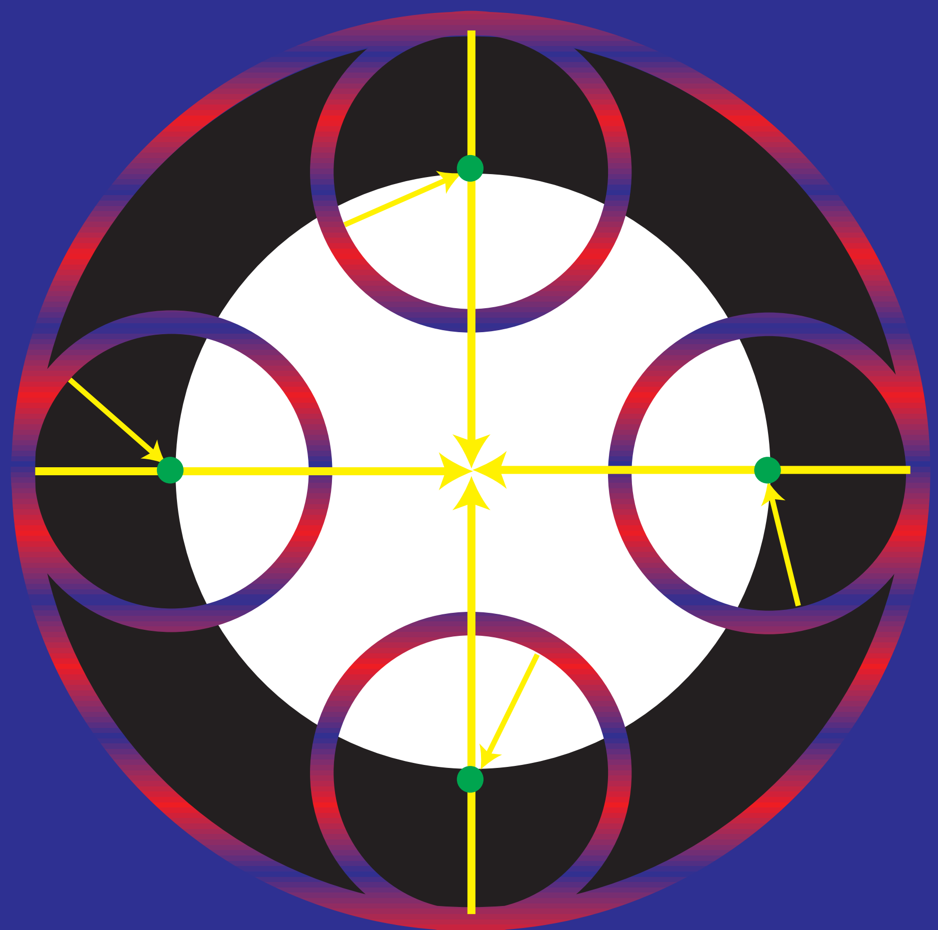

# Reionization Suppression

- Rescattering suppresses primary temperature and polarization anisotropy according to optical depth, fraction of photons rescattered

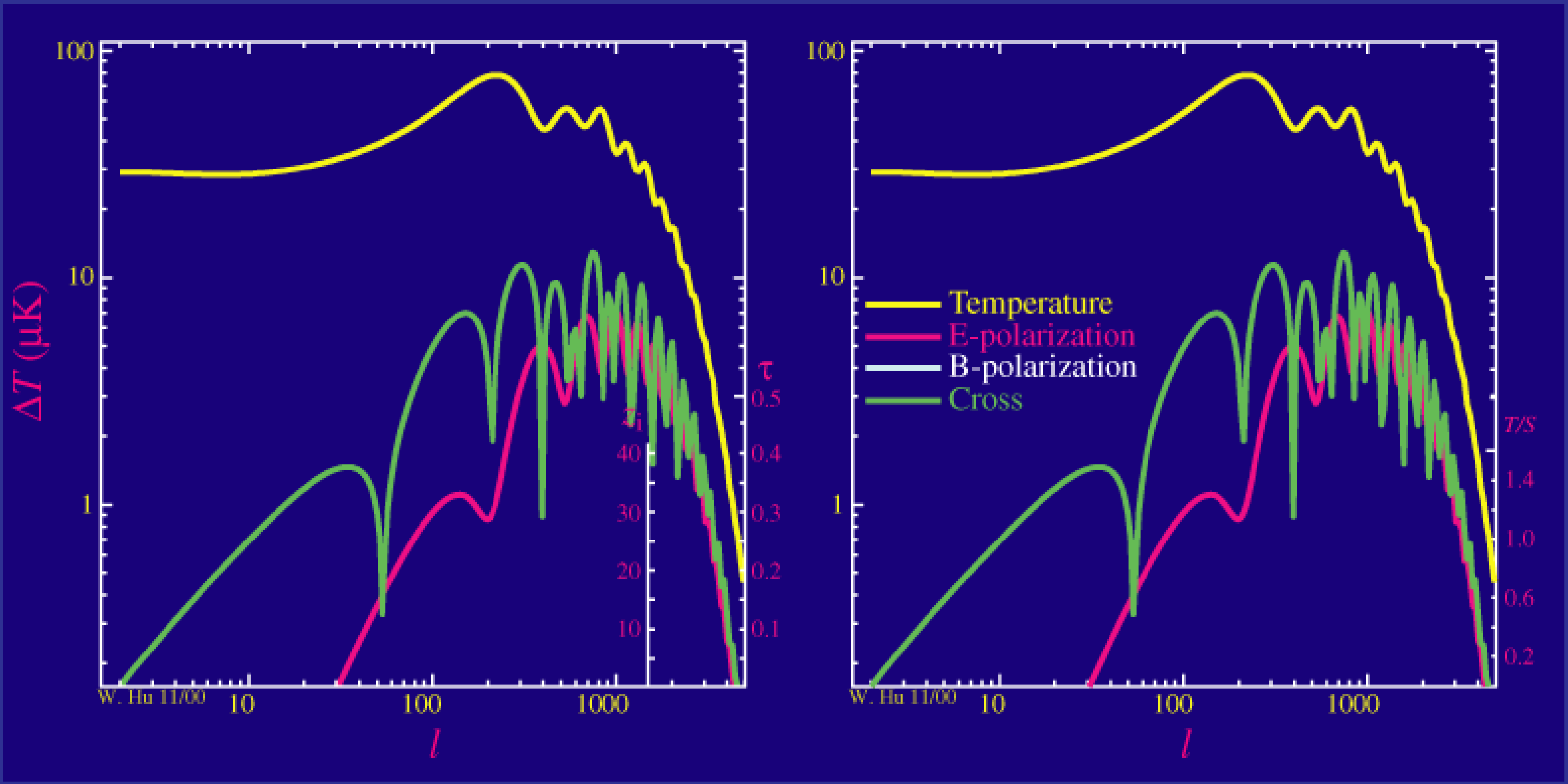

# Tilt-$\tau$ Degeneracy

- Only anisotropy at reionization (high k), not isotropic temperature fluctuations (low k) - is suppressed leading to effective tilt for WMAP (not Planck)

Spergel et al (2006)

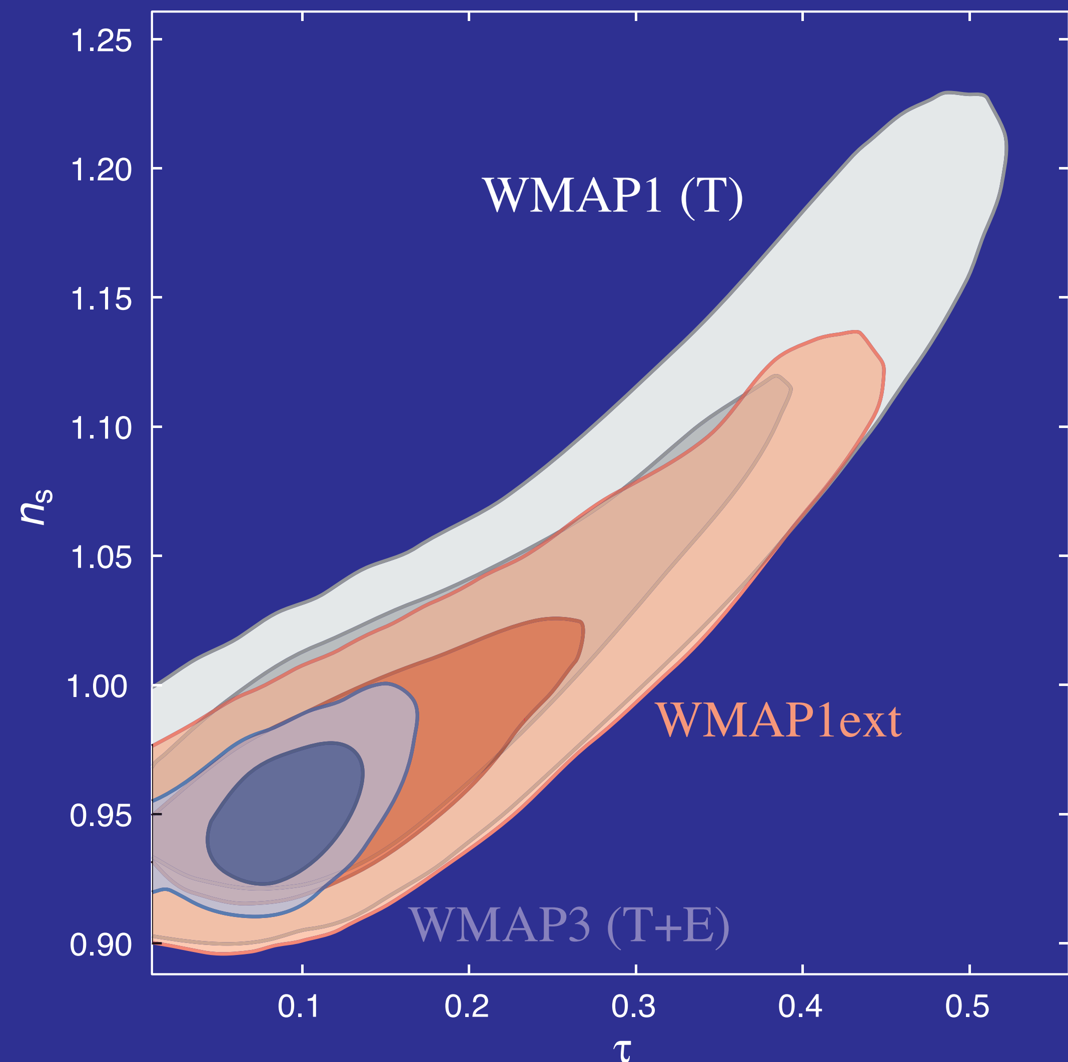

# Scattering Secondaries

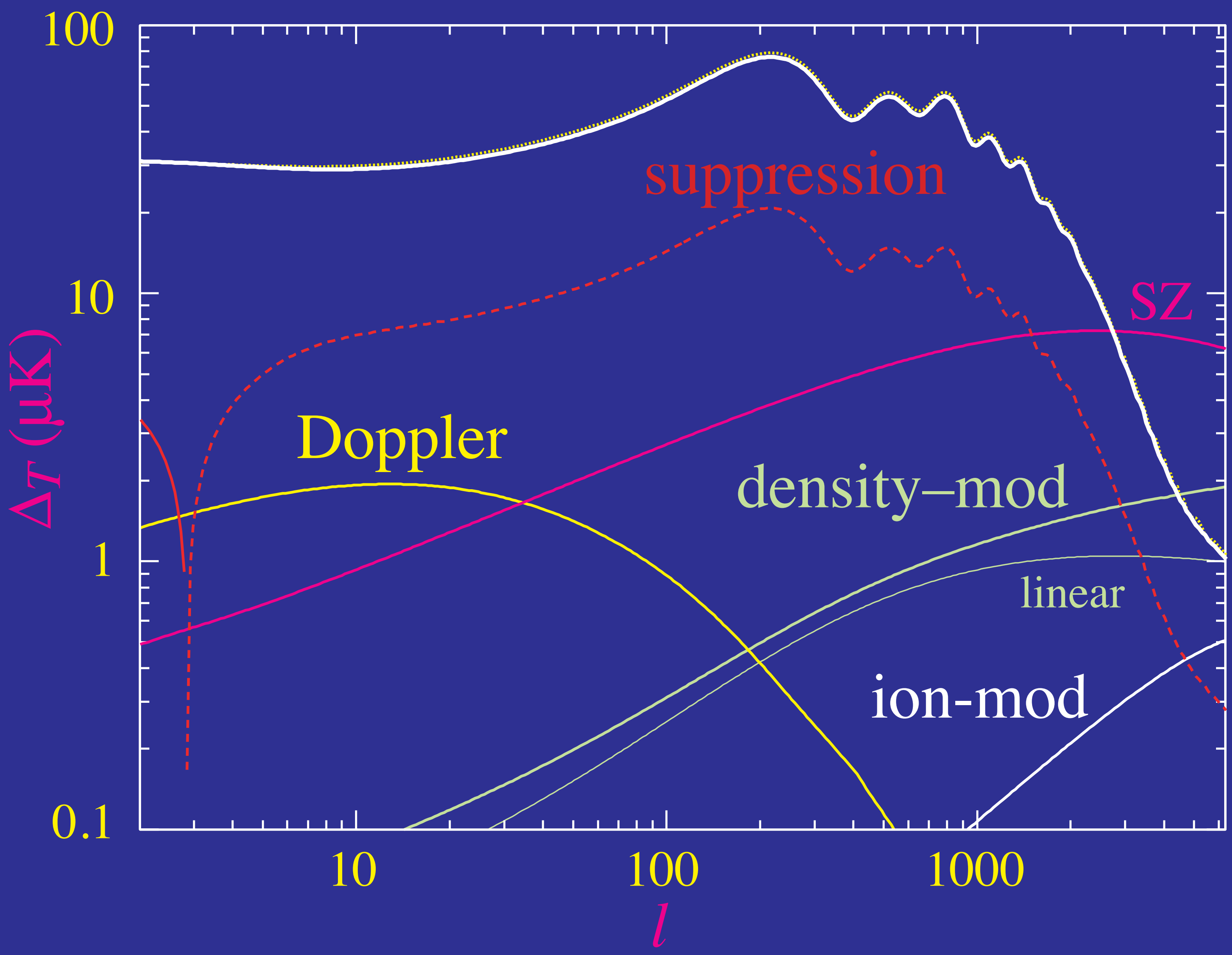

# Why Are Secondaries So Smalll?

- Original anisotropy replaced by new secondary sources
- Late universe more developed than early universe

  Density fluctuations nonlinear not $10^{-5}$

  Velocity field $10^{-3}$ not not $10^{-5}$
- Shouldn't $\Delta T/T \sim \tau v \sim 10^{-4}$?
- Limber says no!
- Spatial and angular dependence of sources contributing and cancelling broadly in redshift

# Anisotropy Suppression and Regeneration

- Recombination sources obscured and replaced with secondary sources that suffer Limber cancellation from integrating over many wavelengths of the source
- Net suppression despite substantially larger sources due to growth of structure except beyond damping tail <10'

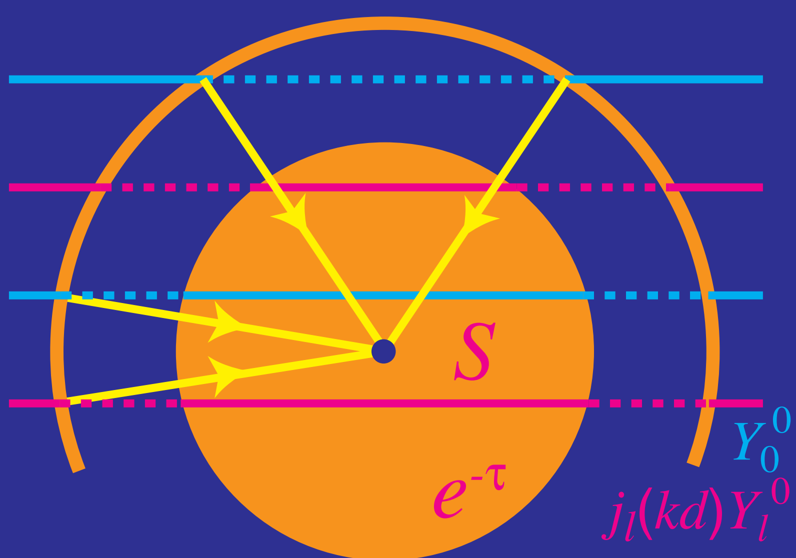


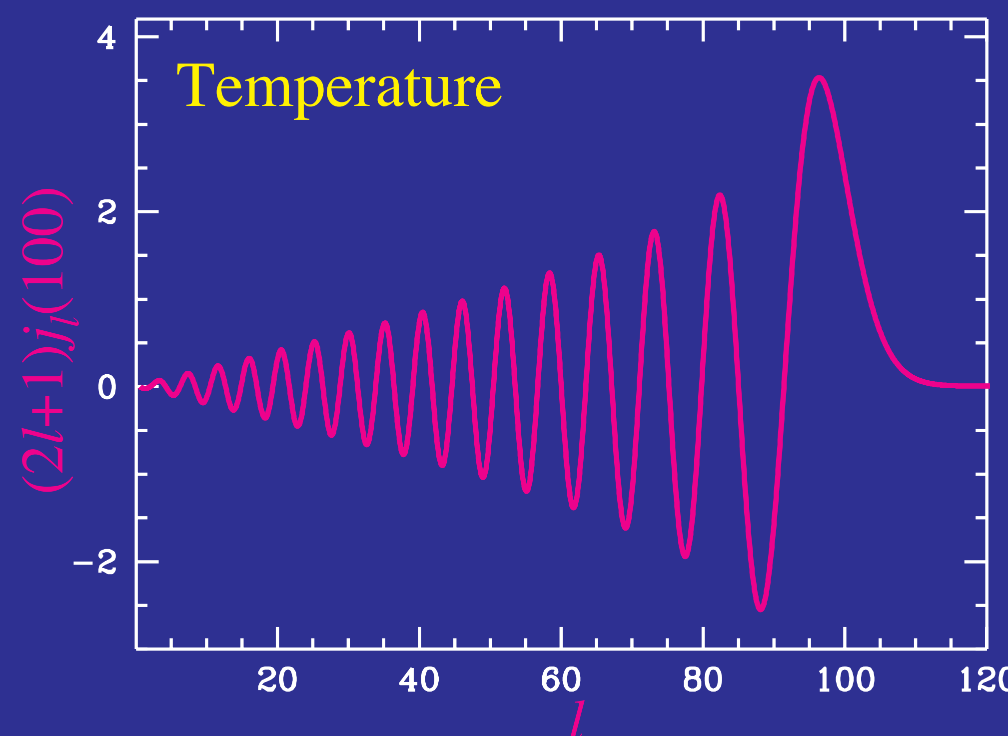

# Doppler Effect in Limber Approximation

- Only fluctuations transverse to line of sight survive in Limber approx but linear Doppler effect has no contribution in this direction

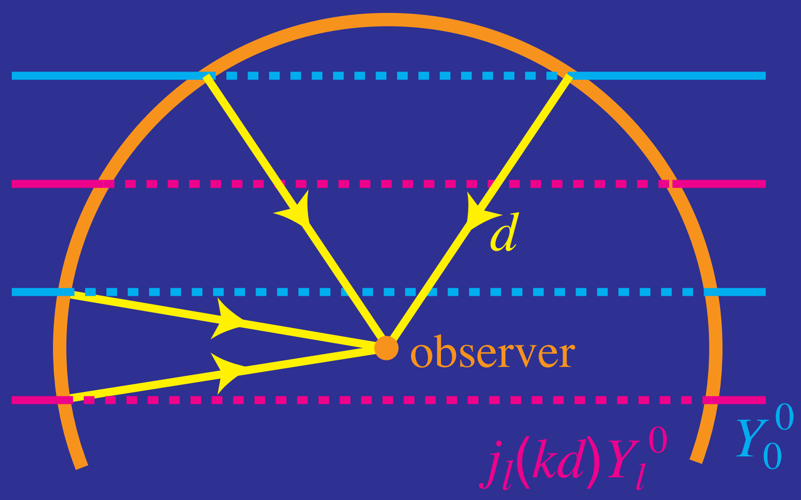


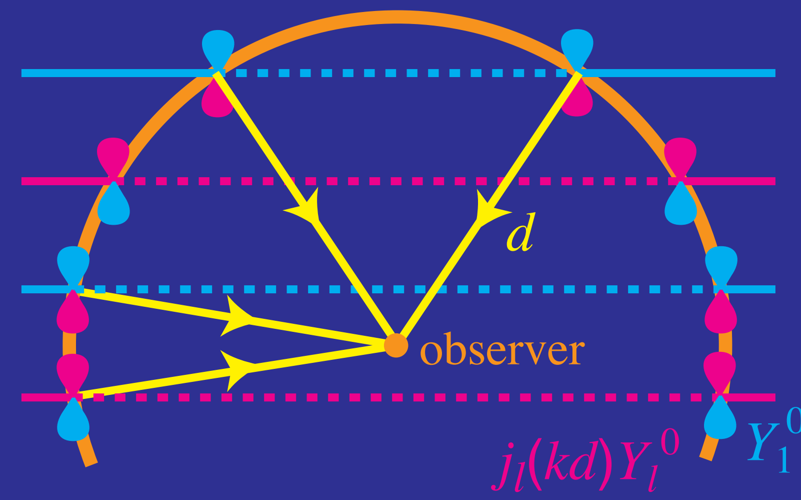


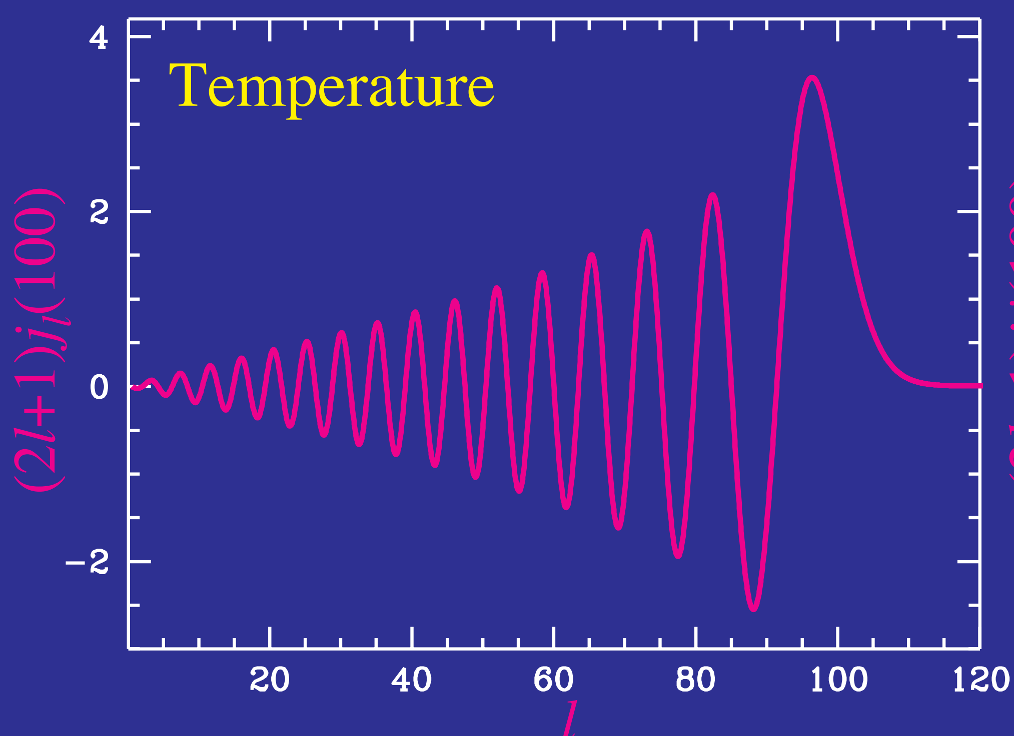


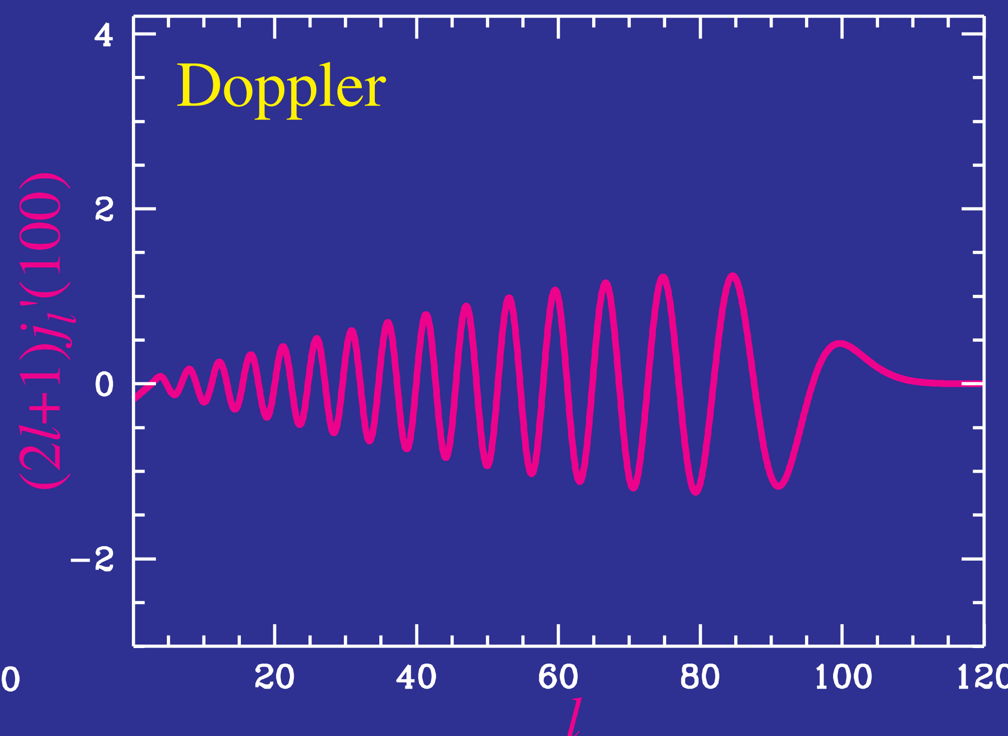

# Cancellation of the Linear Effect

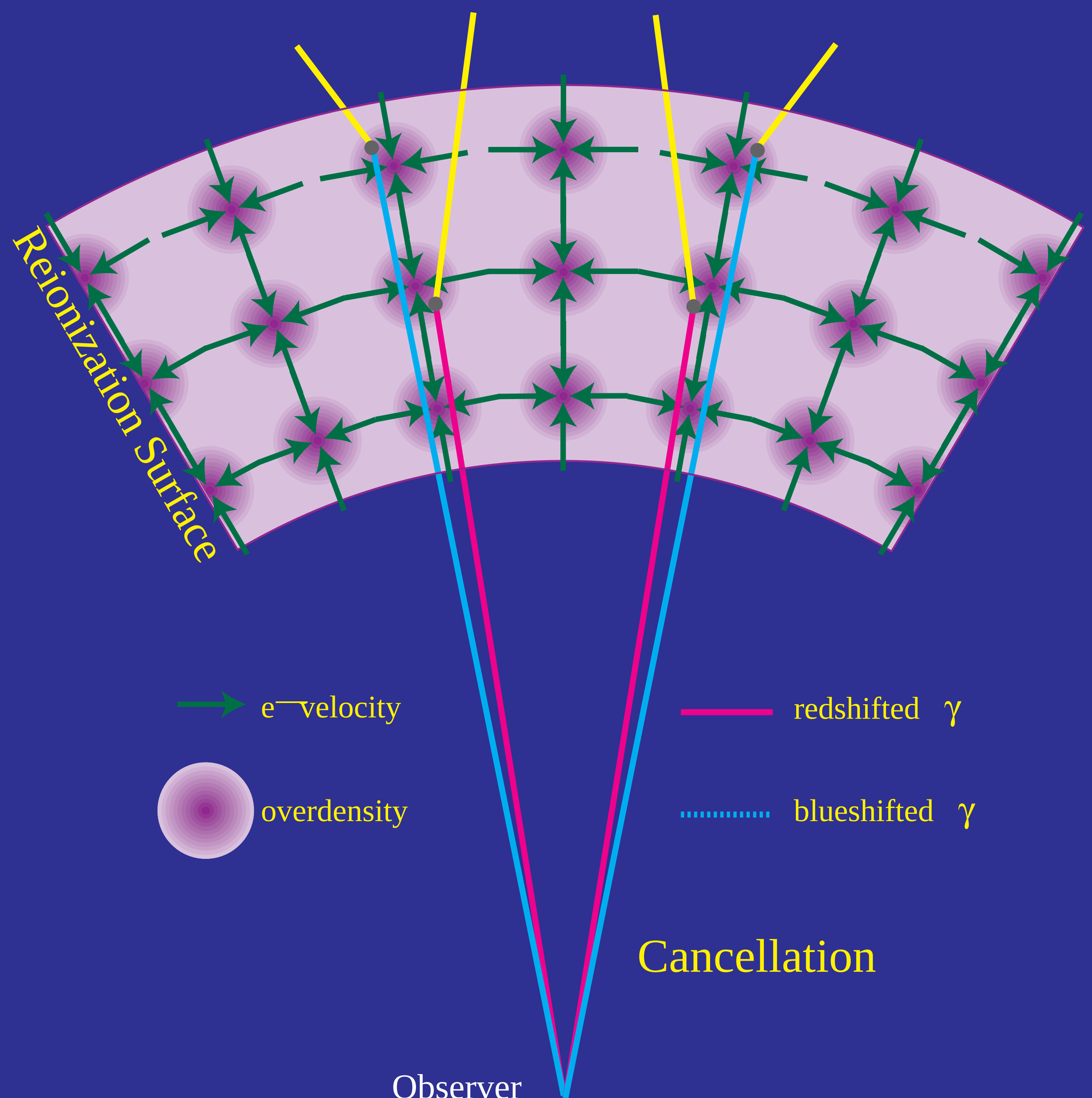

# Modulated Doppler Effect

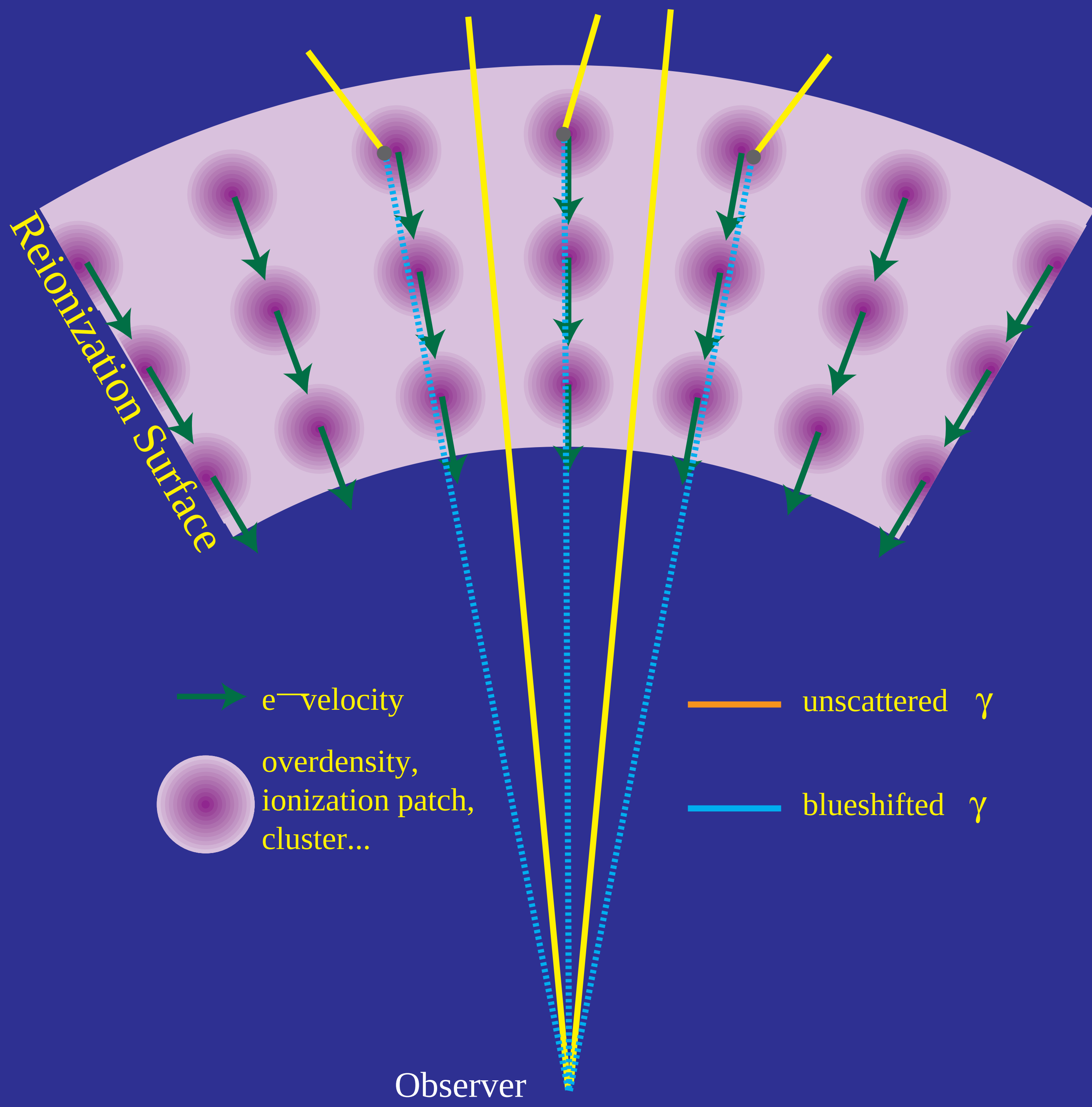

# Ostriker–Vishniac Effect

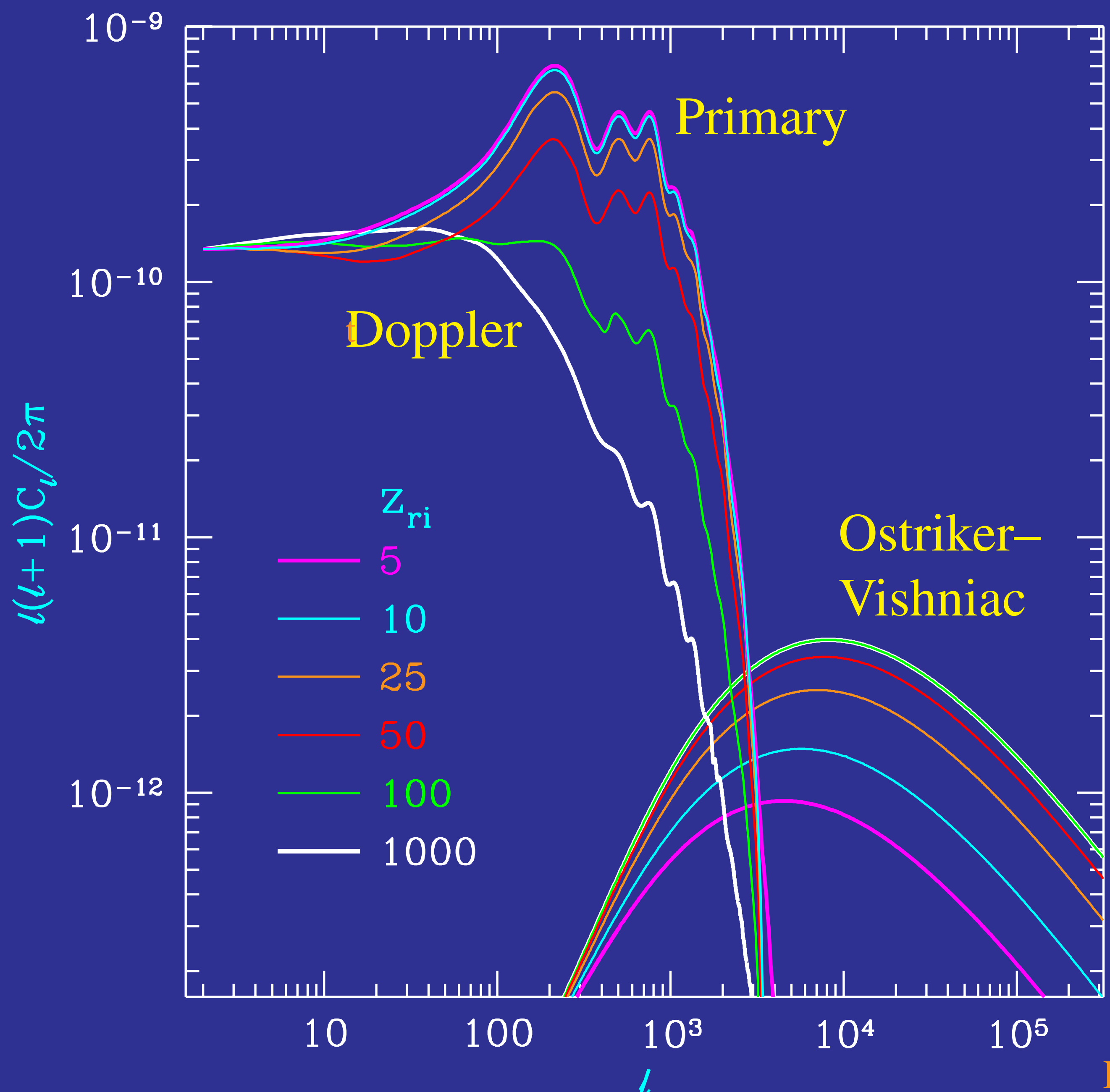


Hu & White (1996)

# Patchy Reionization

# Inhomogeneous Ionization

- As reionization completes, ionization regions grow and fill the space

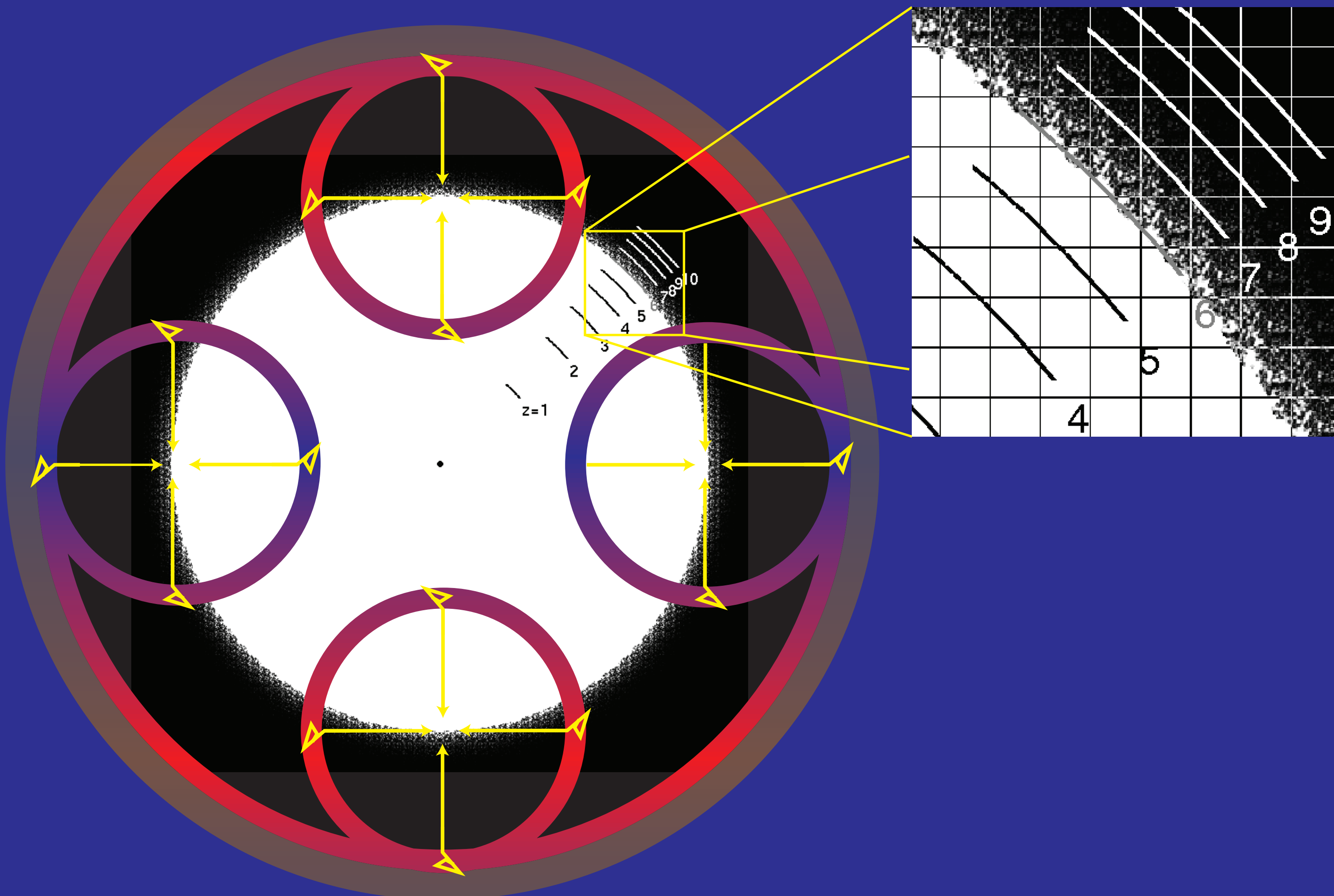


Zahn et al. (2006) [Mortonson et al (2009)]

# Inhomogeneous Ionization

- Provides a source for modulated Doppler effect that appears on the scale of the ionization region

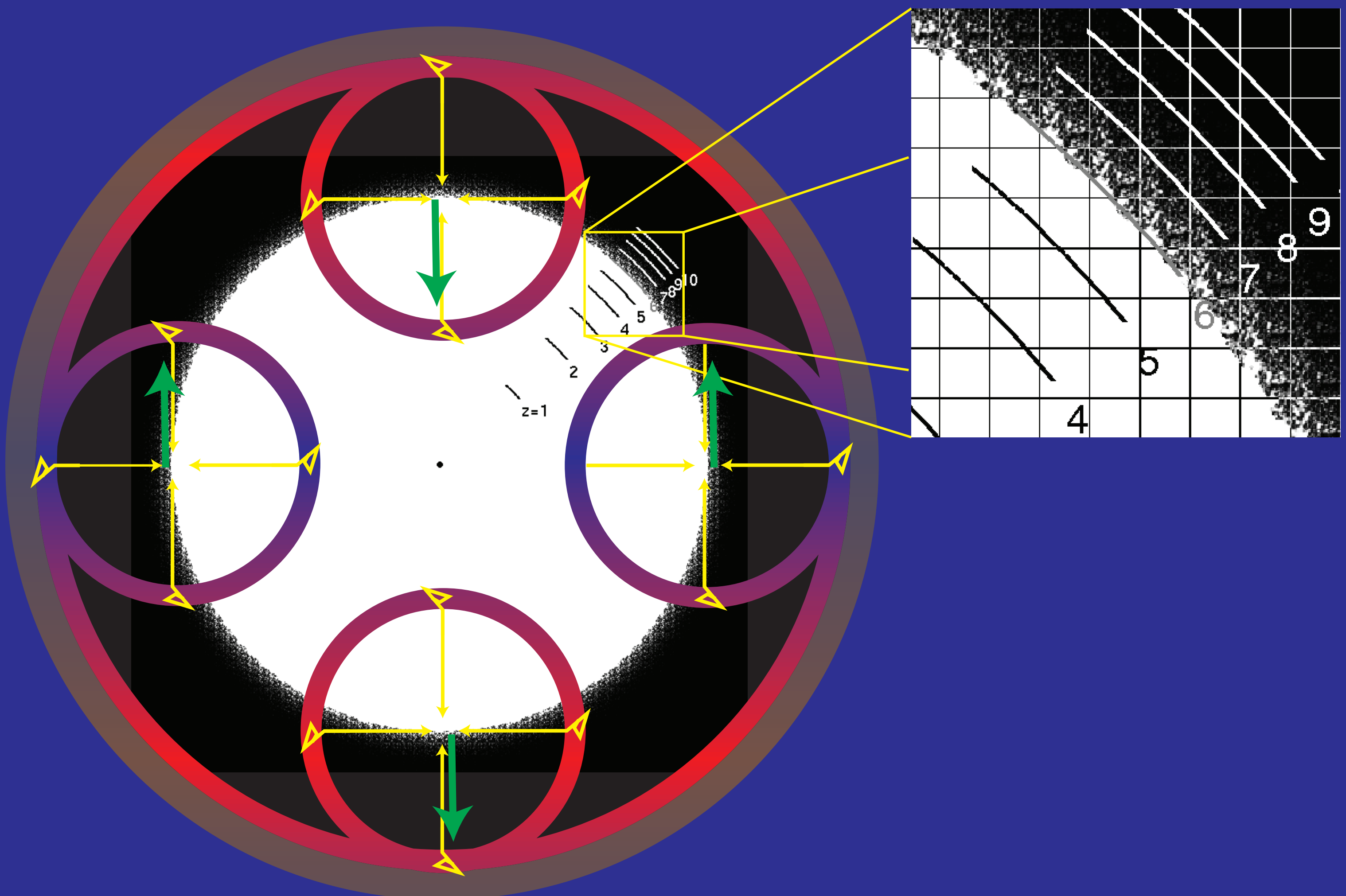

# Patchy Reionization

Aghanim et al (1996)

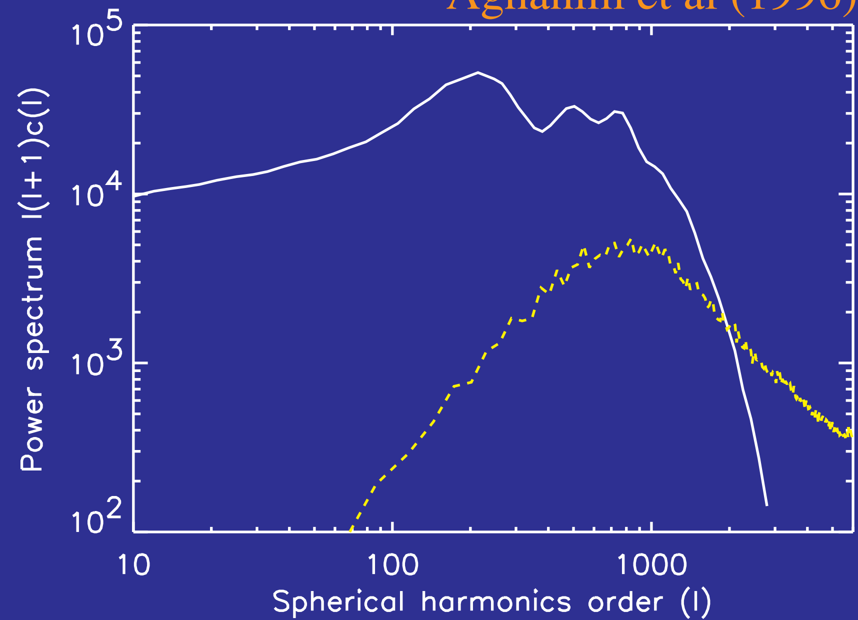


Knox, Scocciomarro & Dodelson (1998)

Gruzinov & Hu (1998)

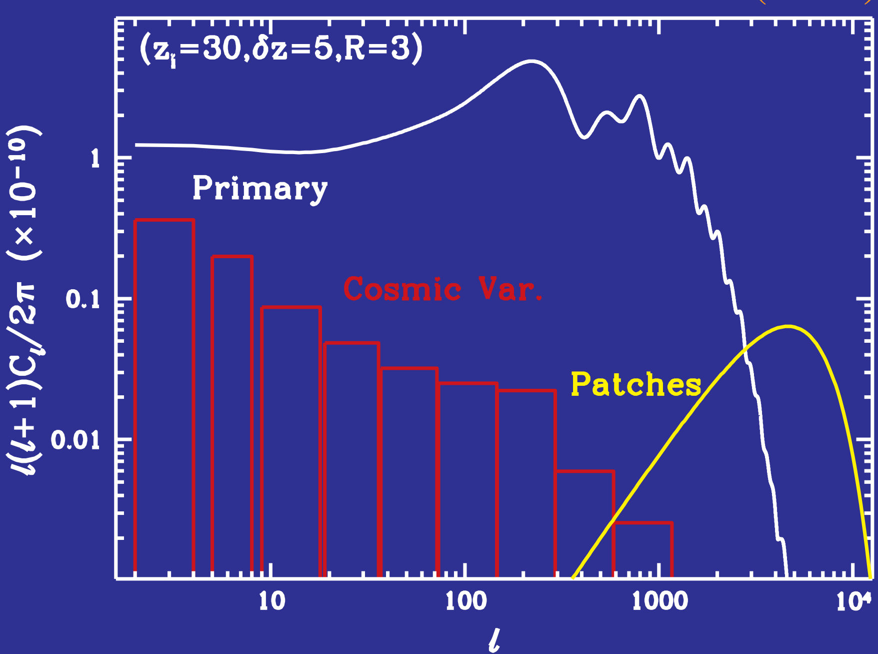


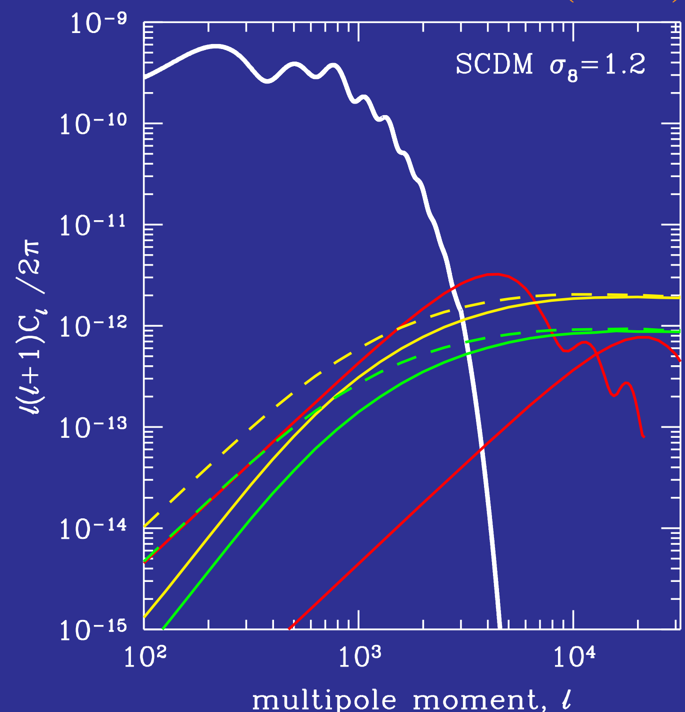

# Observational Constraints

- SPT detection of secondary anisotropy (likely SZ dominated, low level) sets upper limit on modulated Doppler contributions

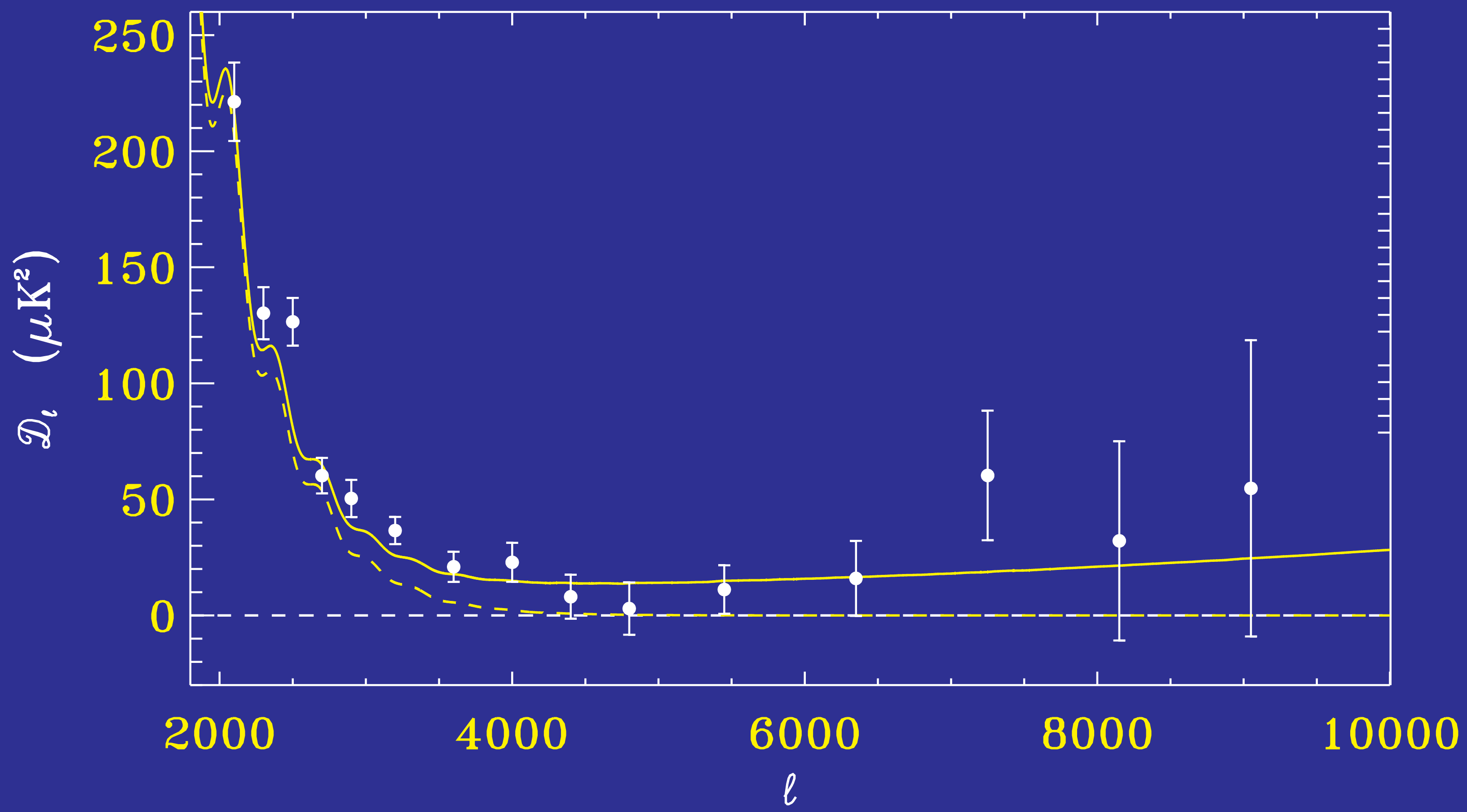


SPT Hall et al - Leuker et al (2010)

# Observational Constraints

- Combined with well-determined velocity, rms optical depth fluctuation at arcmin scale $\delta\tau<0.0036$ (conservative 95% CL)

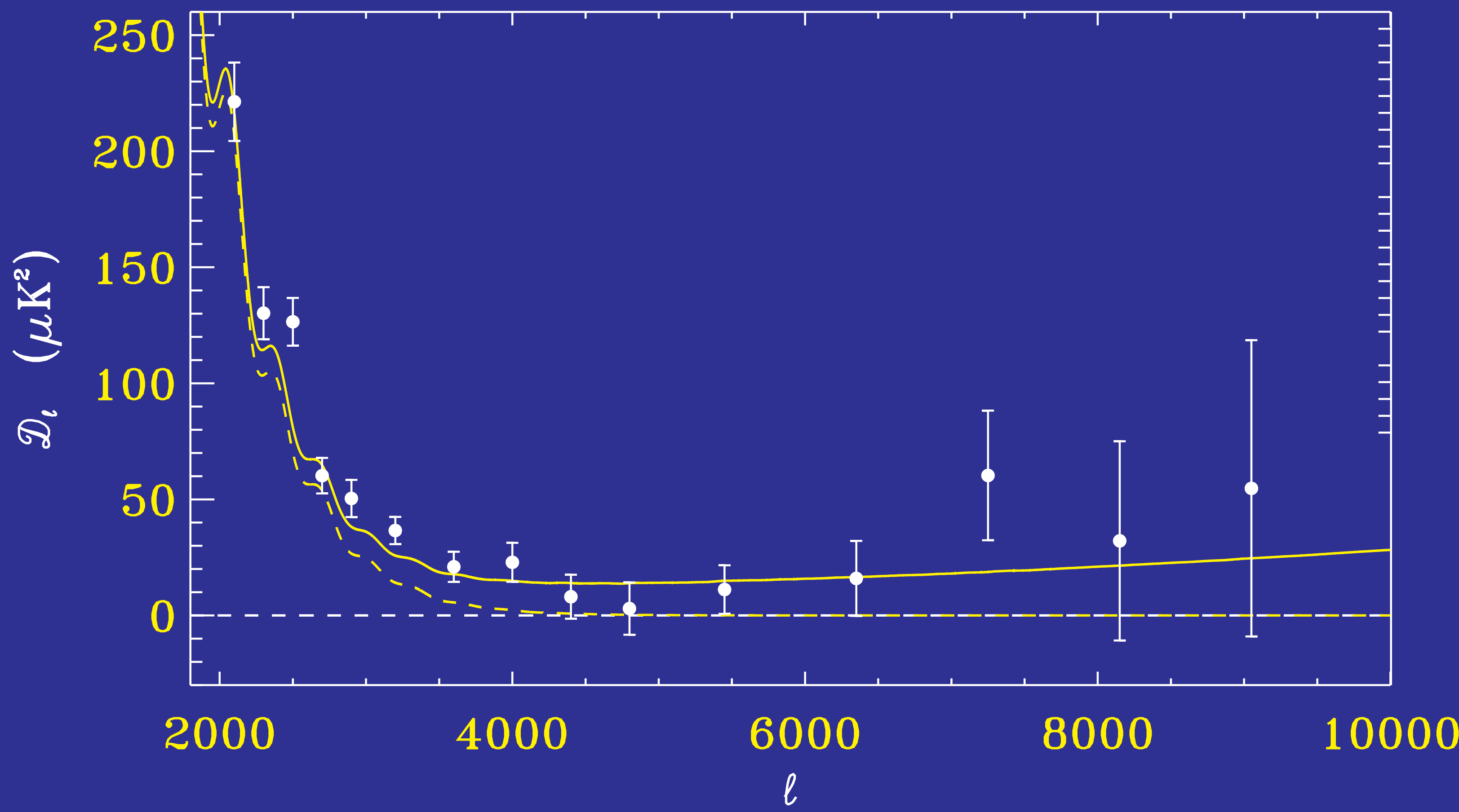


SPT Hall et al - Leuker et al (2010); Mortonson & Hu (2010)

# Secondary Polarization

# WMAP Correlation

- Reionization polarization first detected in WMAP1 through temperature cross correlation at an anomalously high value

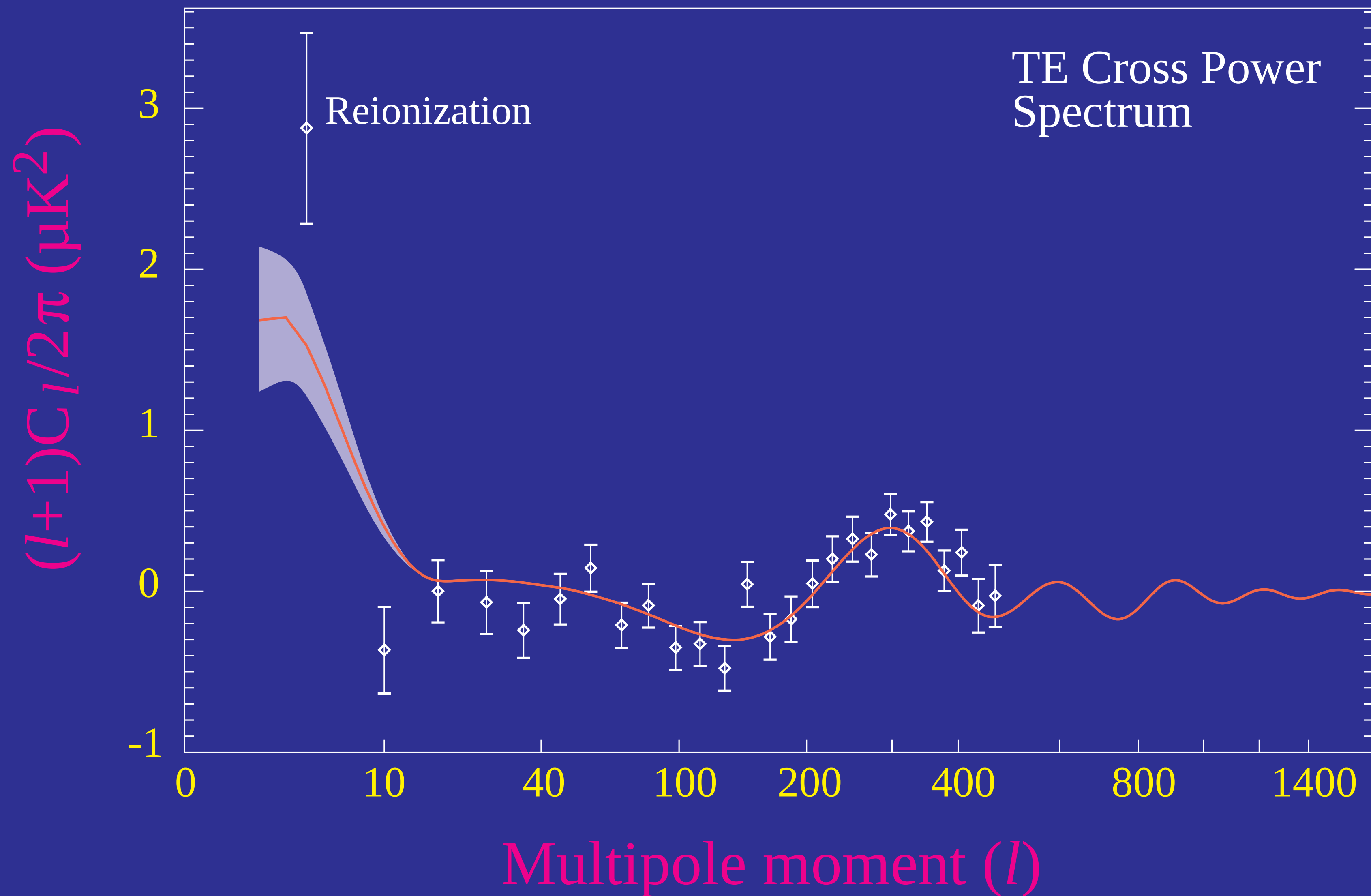

# Polarization from Thomson Scattering

- Differential cross section depends on polarization and angle

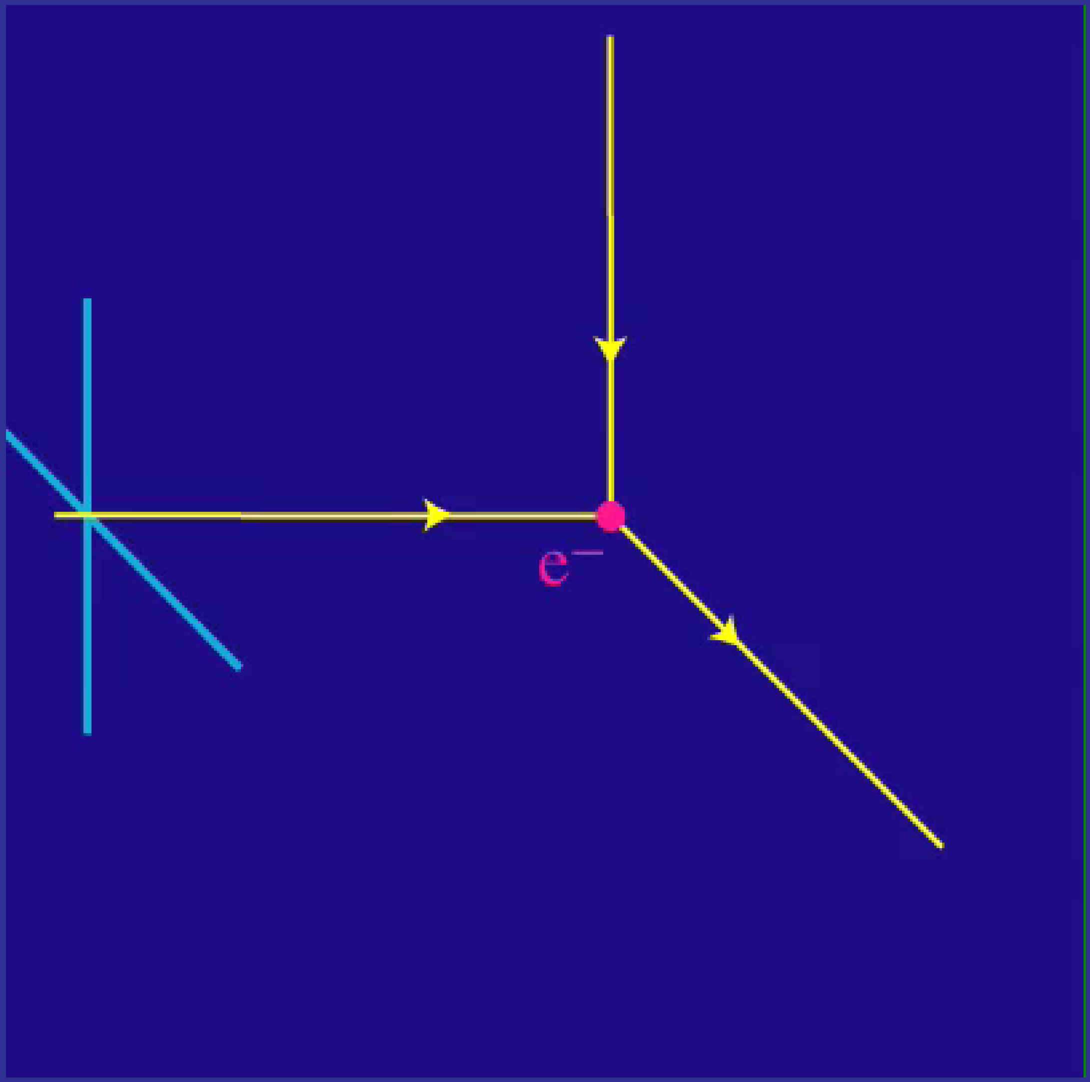


$$\frac{d\sigma}{d\Omega} = \frac{3}{8\pi}|\hat{\varepsilon}' \cdot \hat{\varepsilon}|^2 \sigma_T$$

# Polarization from Thomson Scattering

- Isotropic radiation scatters into unpolarized radiation

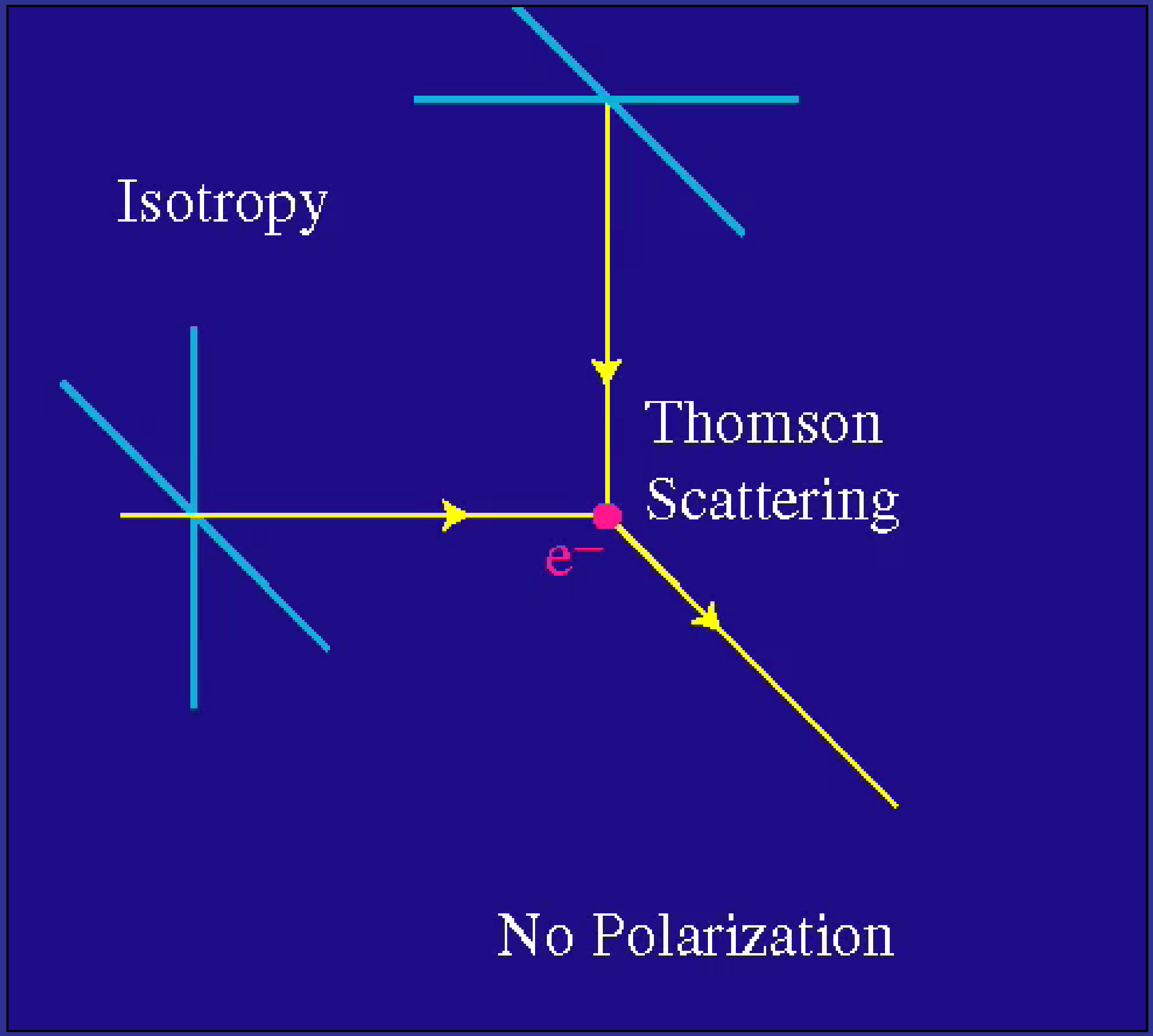

# Polarization from Thomson Scattering

- Quadrupole anisotropies scatter into linear polarization

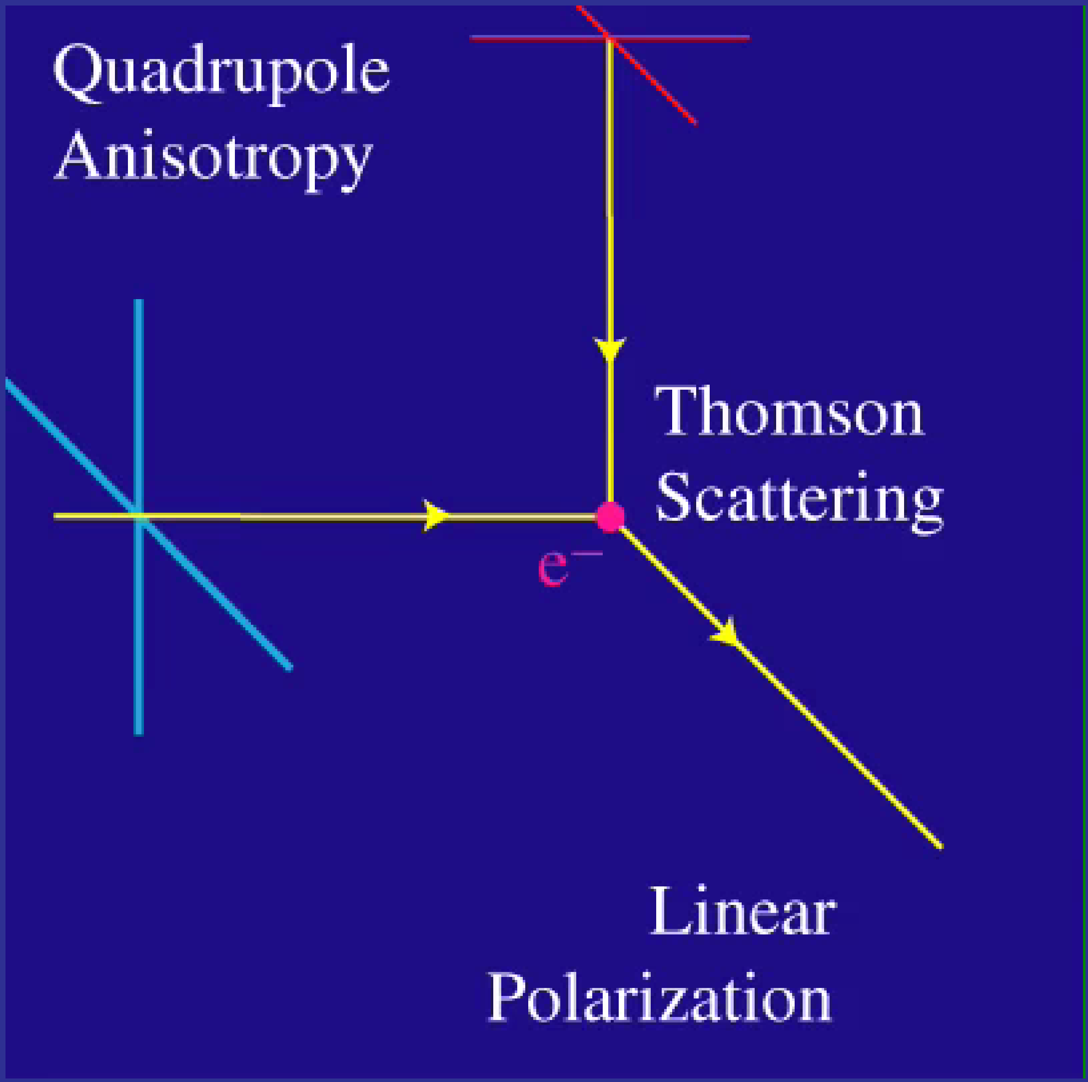


aligned with
cold lobe

# Whence Quadrupoles?

- Temperature inhomogeneities in a medium
- Photons arrive from different regions producing an anisotropy

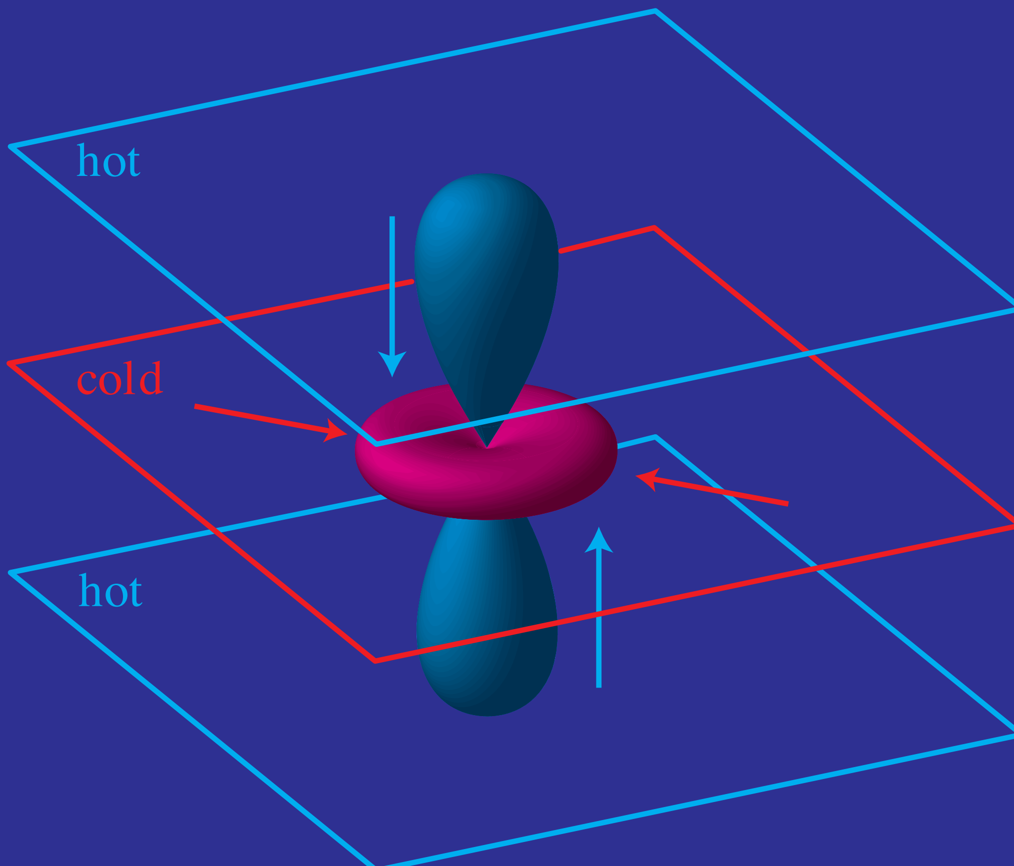


(Scalar) Temperature Inhomogeneity

Hu & White (1997)

# CMB Anisotropy

- WMAP map of the CMB temperature anisotropy

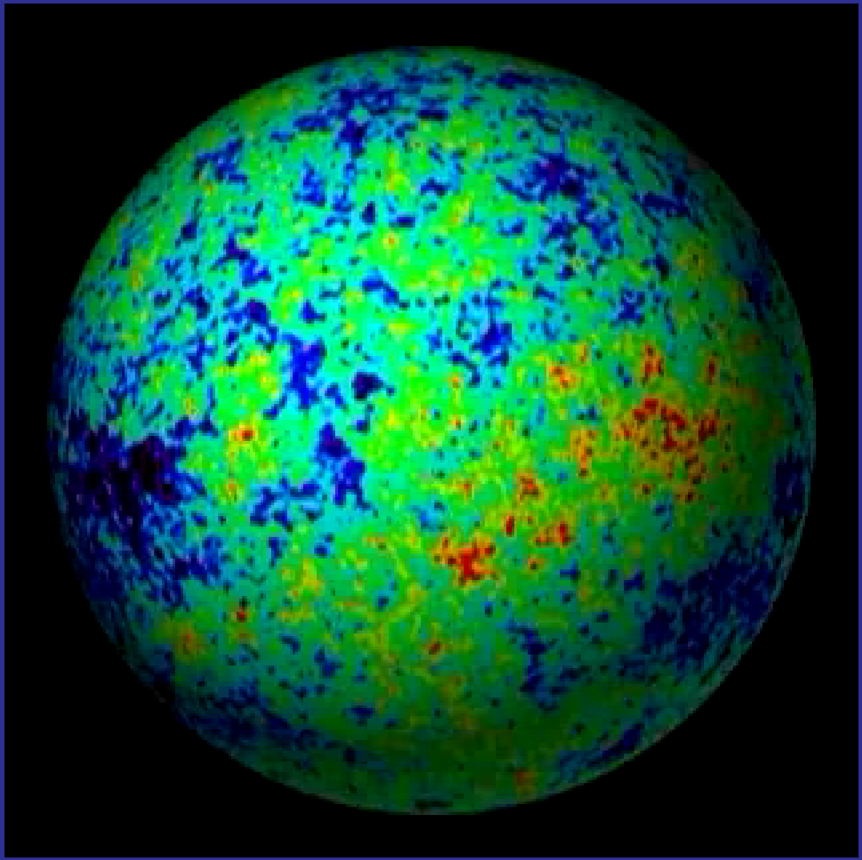

# Whence Polarization Anisotropy?

- Observed photons scatter into the line of sight
- Polarization arises from the projection of the quadrupole on the transverse plane

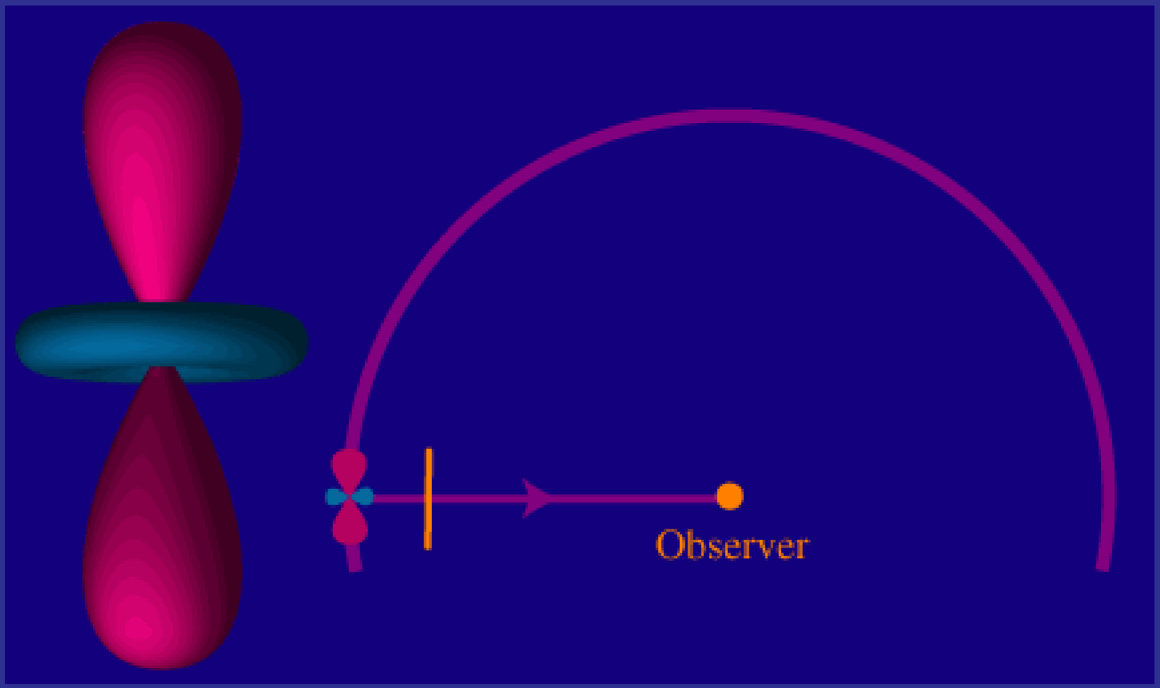

# Polarization Multipoles

- Mathematically pattern is described by the tensor (spin-2) spherical harmonics [eigenfunctions of Laplacian on trace-free 2 tensor]
- Correspondence with scalar spherical harmonics established via Clebsch-Gordan coefficients (spin x orbital)
- Amplitude of the coefficients in the spherical harmonic expansion are the multipole moments; averaged square is the power

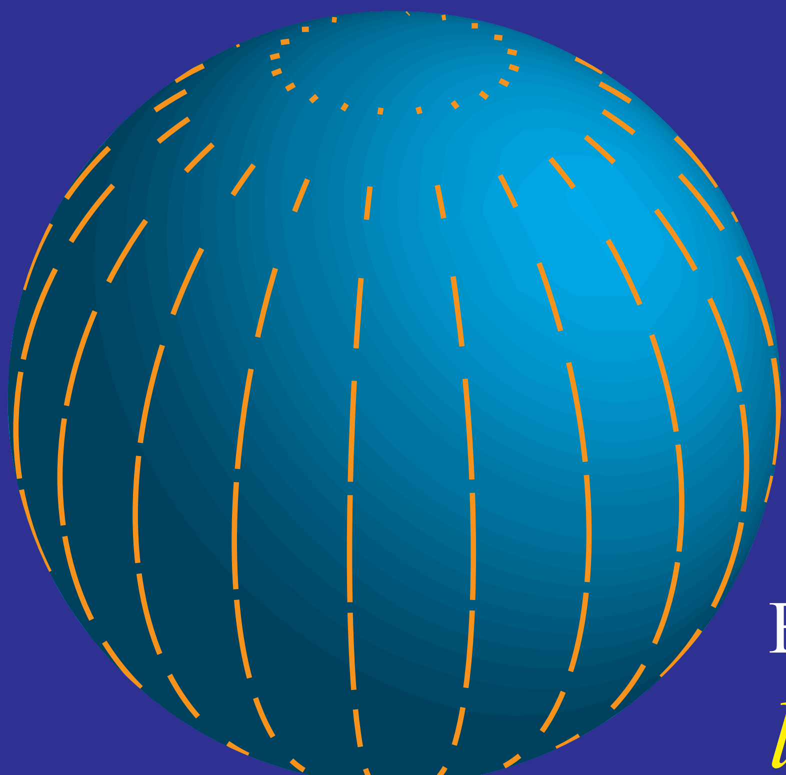

E-tensor harmonic

$l=2, m=0$

# Modulation by Plane Wave

- Amplitude modulated by plane wave → higher multipole moments
- Direction detemined by perturbation type → E-modes

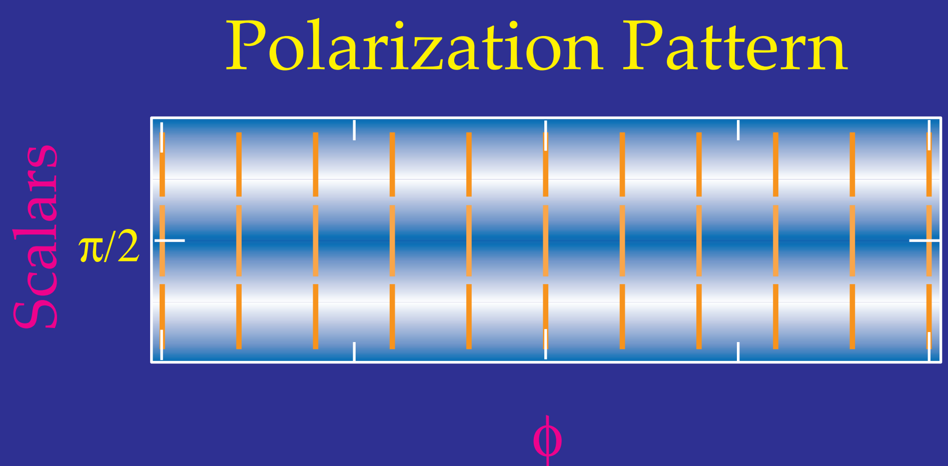


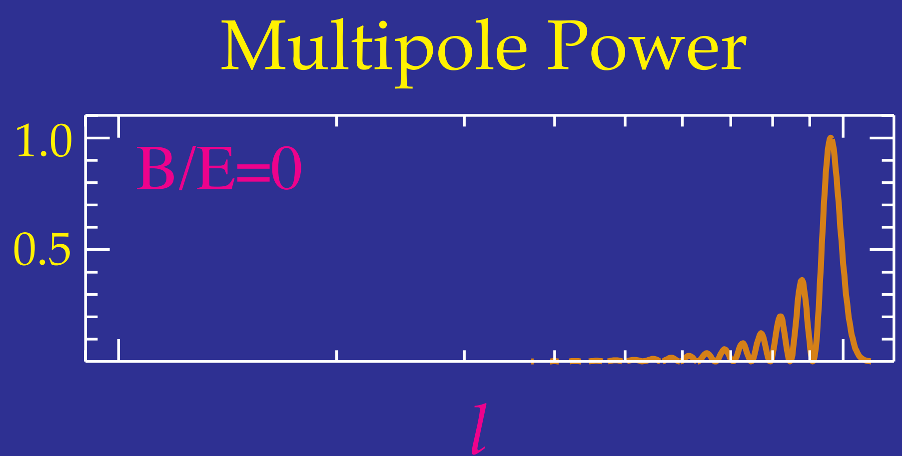

# A Catch-22

- Polarization is generated by scattering of anisotropic radiation
- Scattering isotropizes radiation
- Polarization only arises in optically thin conditions: reionization and end of recombination
- Polarization fraction is at best a small fraction of the $10^{-5}$ anisotropy: $\sim 10^{-6}$ or μK in amplitude

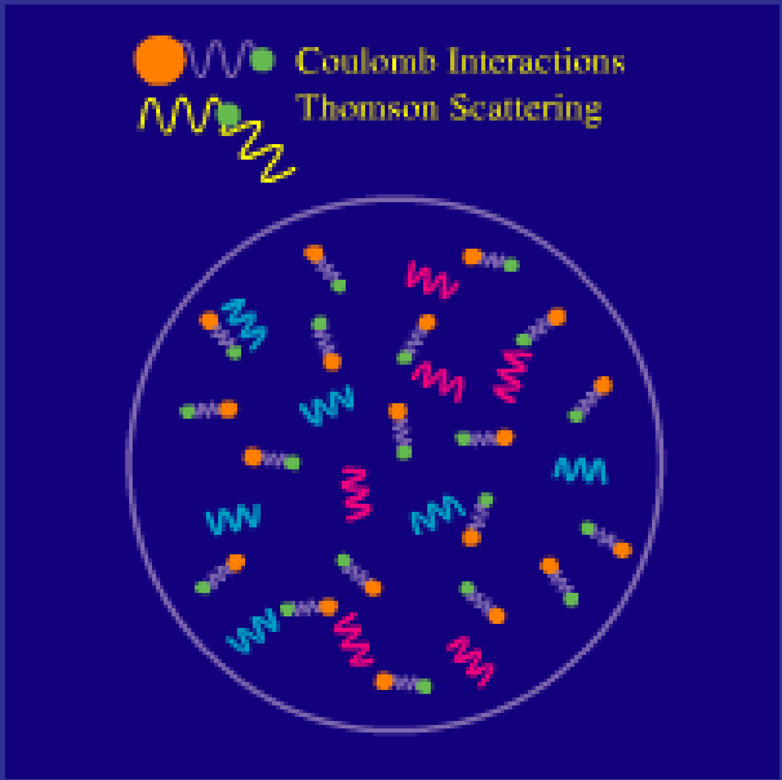

# WMAP 3yr Data

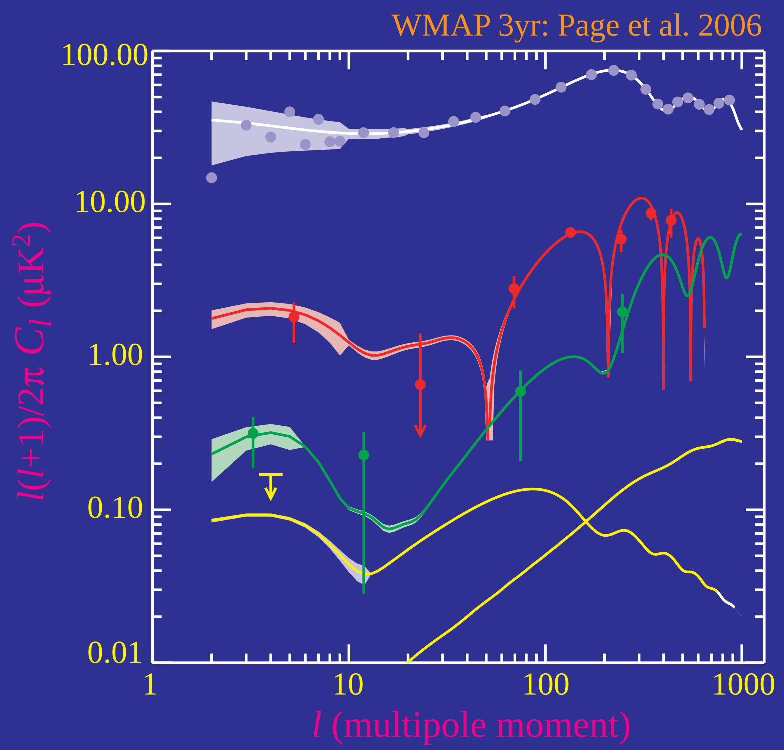


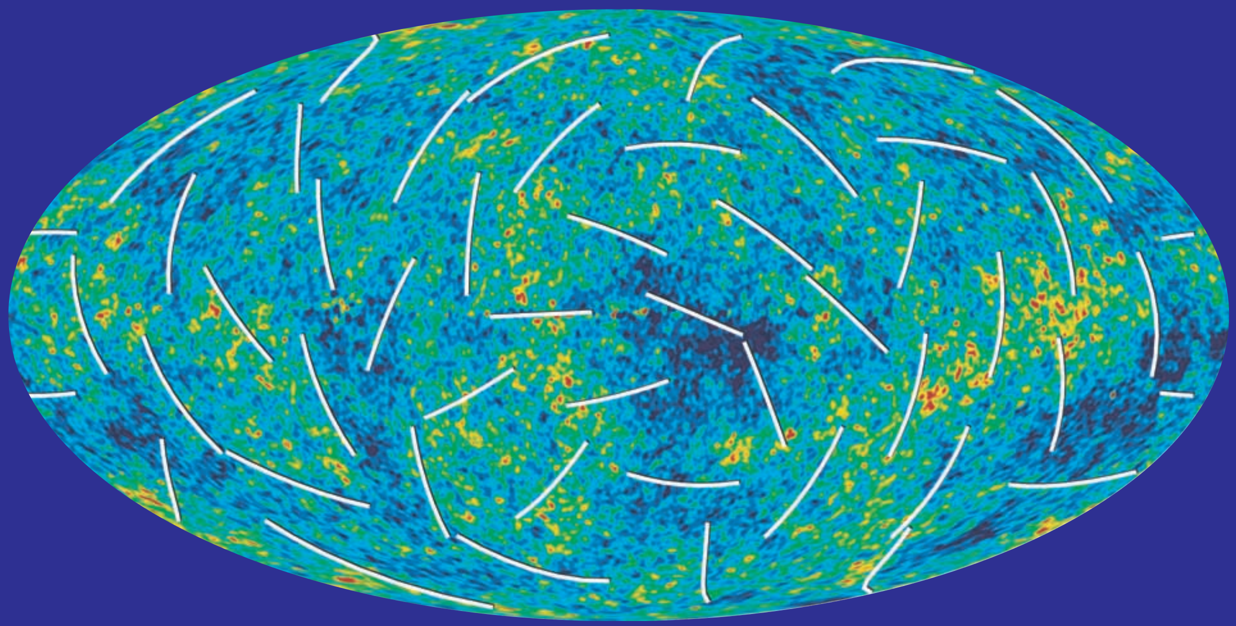

# Temperature Inhomogeneity

- Temperature inhomogeneity reflects initial density perturbation on large scales
- Consider a single Fourier moment:

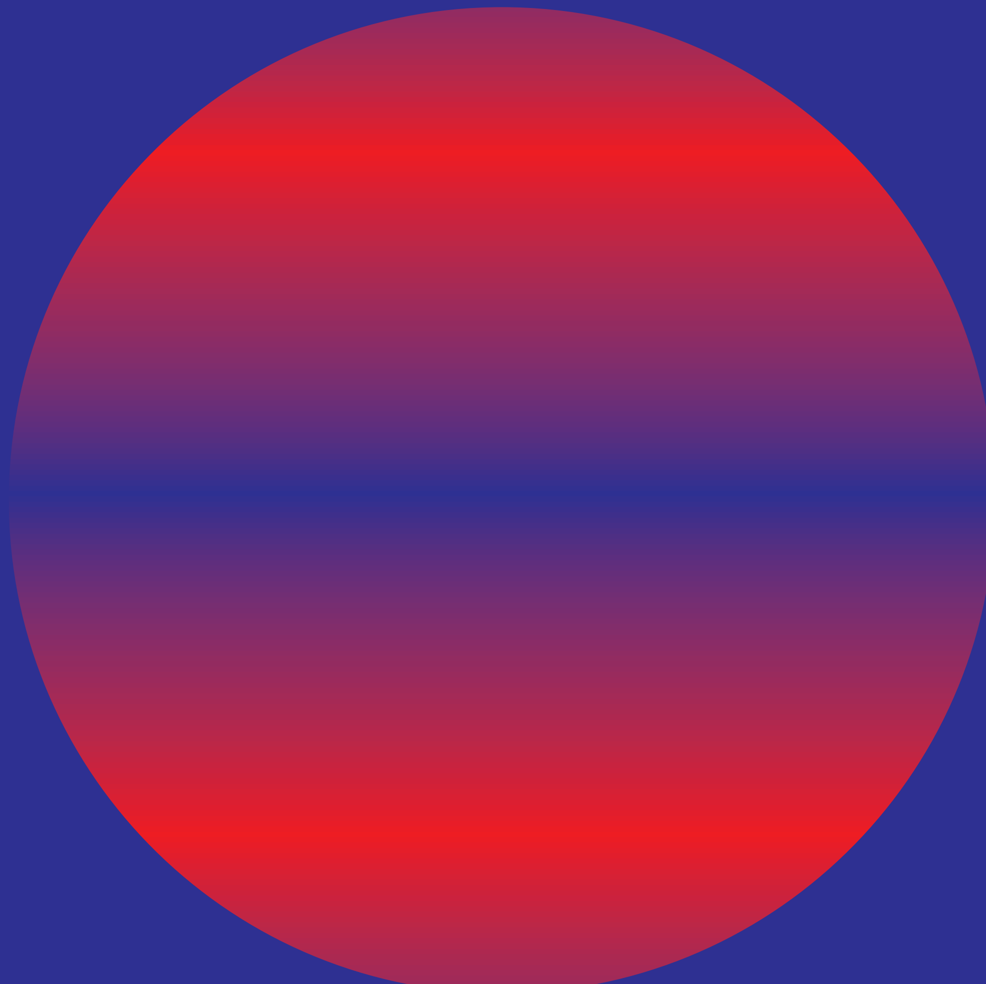

# Locally Transparent

- Presently, the matter density is so low that a typical CMB photon will not scatter in a Hubble time (~age of universe)

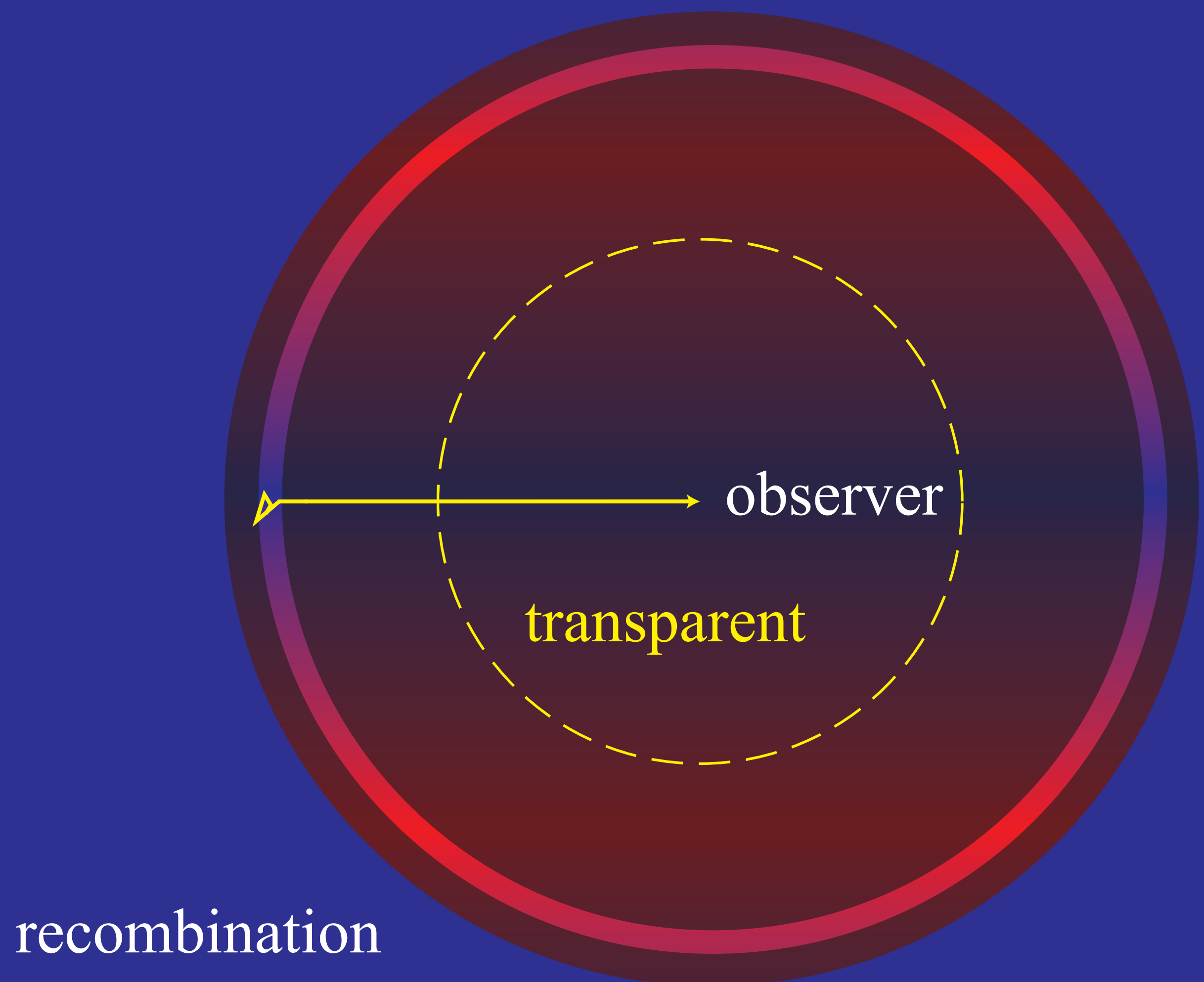

# Reversed Expansion

- Free electron density in an ionized medium increases as scale factor $a^{-3}$; when the universe was a tenth of its current size CMB photons have a finite (~10%) chance to scatter

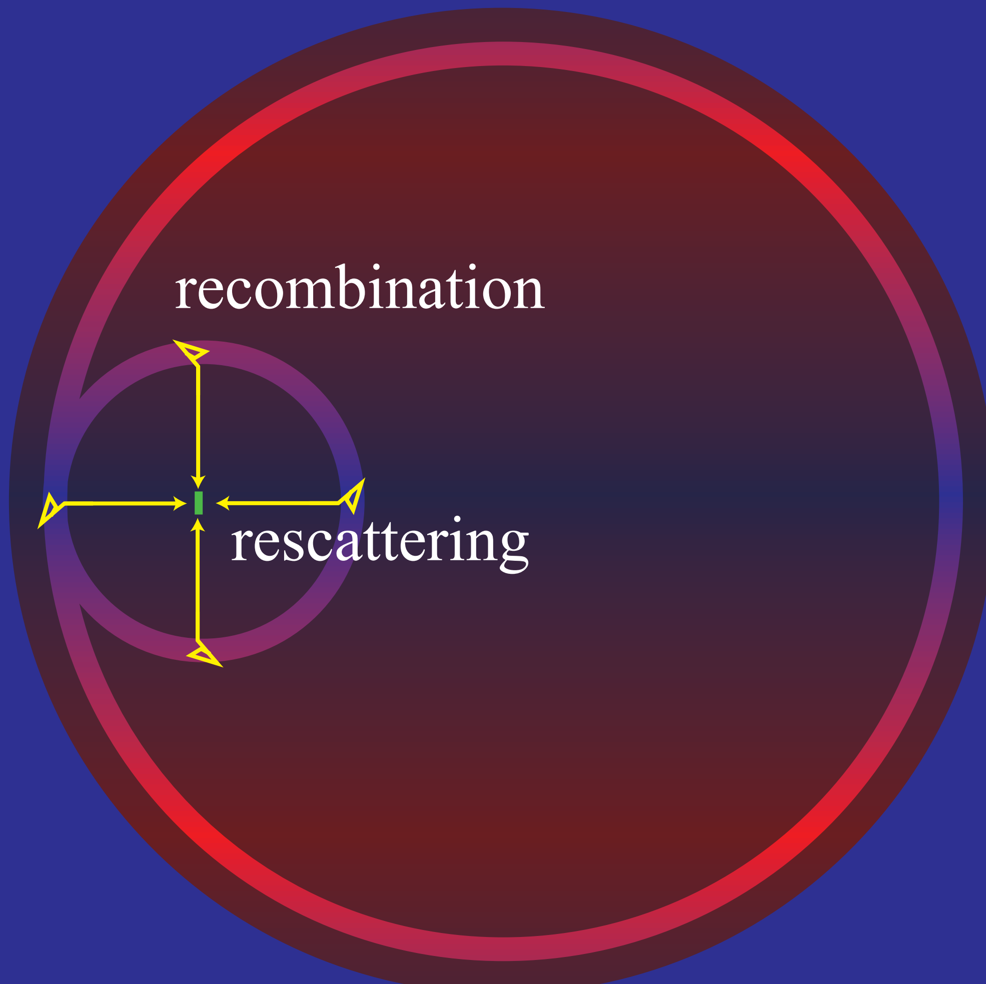

# Polarization Anisotropy

- Electron sees the temperature anisotropy on its recombination surface and scatters it into a polarization

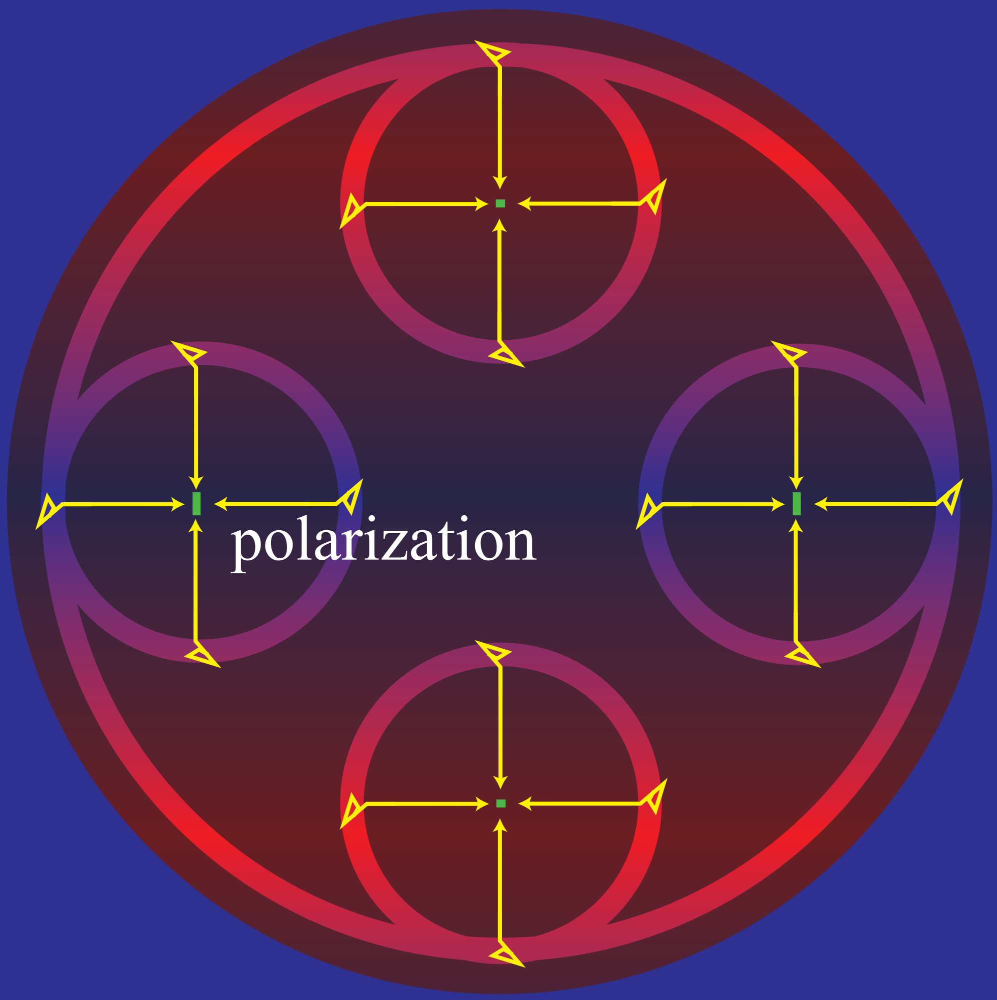

# Temperature Correlation

- Pattern correlated with the temperature anisotropy that generates it; here an $m$=0 quadrupole

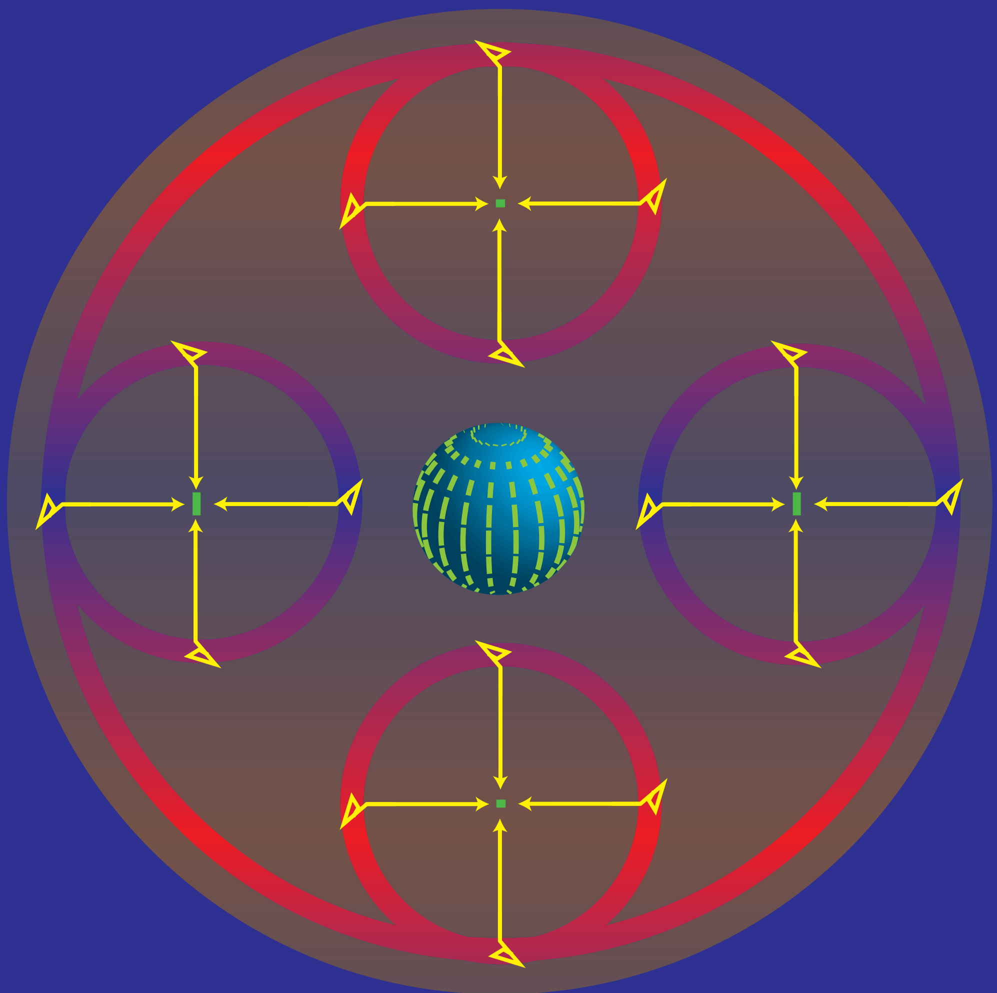

# Instantaneous Reionization

- WMAP data constrains optical depth for instantaneous models of $\tau$=0.087±0.017
- Upper limit on gravitational waves weaker than from temperature

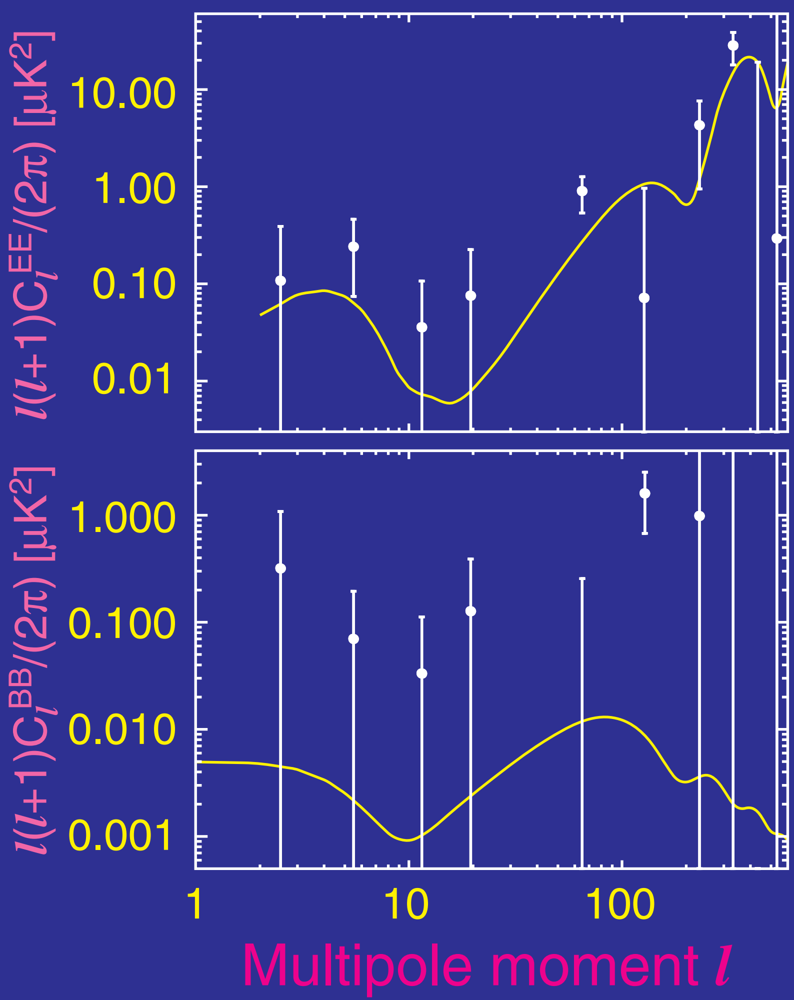

# Why Care?

- Early ionization is puzzling if due to ionizing radiation from normal stars; may indicate more exotic physics is involved

- Reionization screens temperature anisotropy on small scales making the true amplitude of initial fluctuations larger by $e^{\tau}$
- Measuring the growth of fluctuations is one of the best ways of determining the neutrino masses and the dark energy

- Offers an opportunity to study the origin of the low multipole statistical anomalies
- Presents a second, and statistically cleaner, window on gravitational waves from the early universe

# Distance Predicts Growth

- With smooth dark energy, distance predicts scale-invariant growth to a few percent - a falsifiable prediction

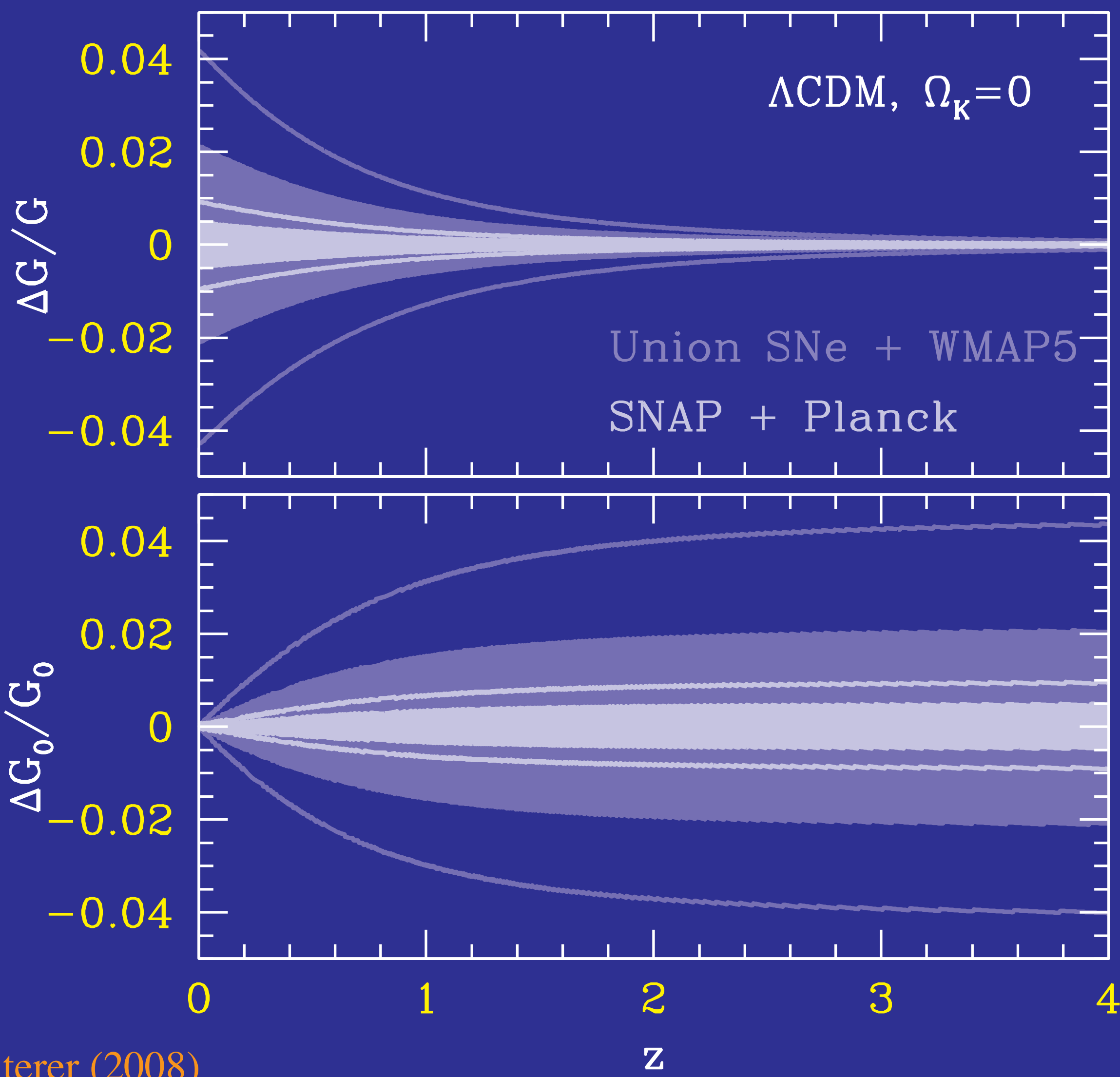


Mortonson, Hu, Huterer (2008)

# Ionization History

- Two models with same optical depth τ but different ionization history

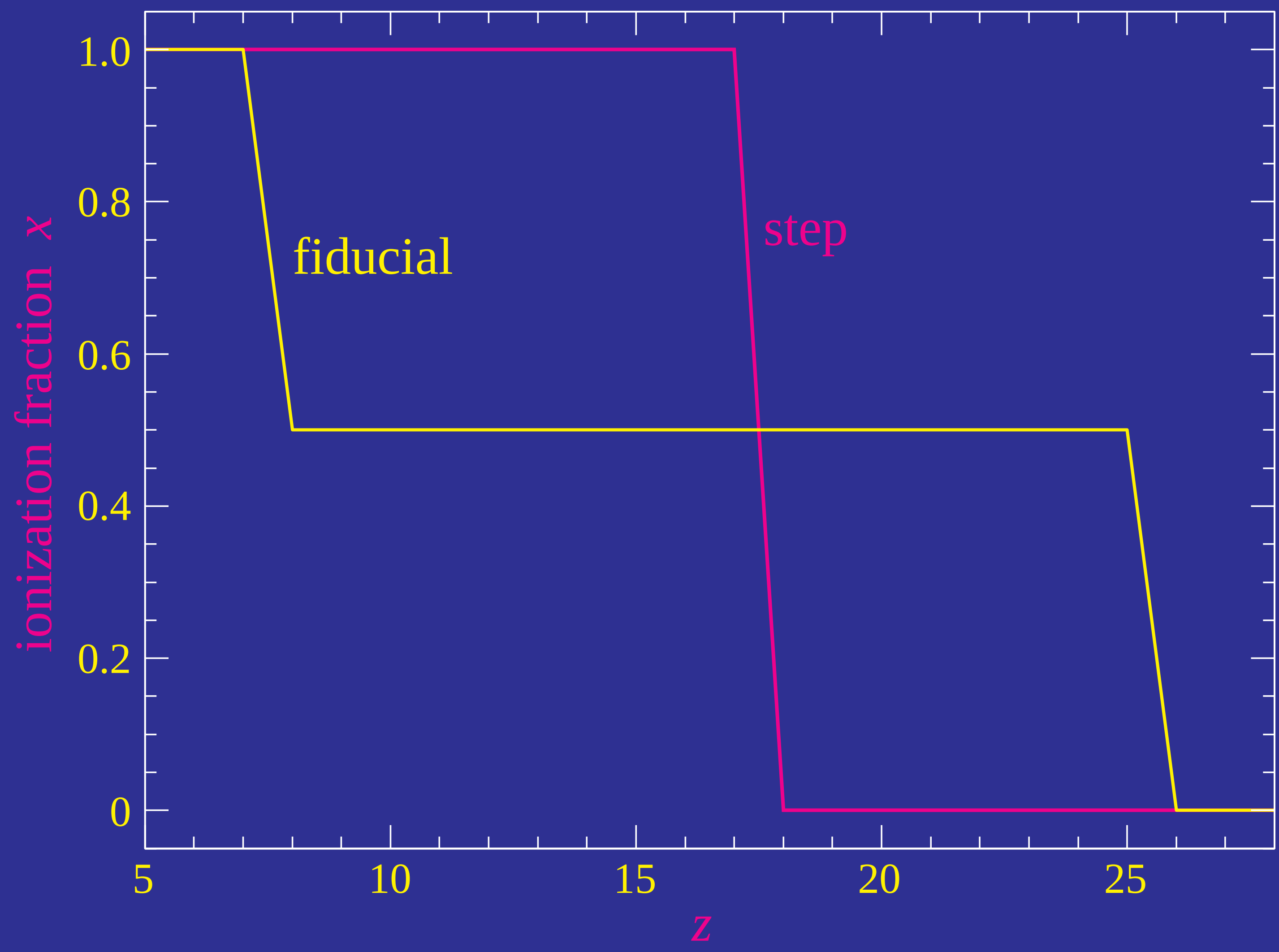


Kaplinghat et al. (2002); Hu & Holder (2003)

# Distinguishable History

- Same optical depth, but different coherence - horizon scale during scattering epoch

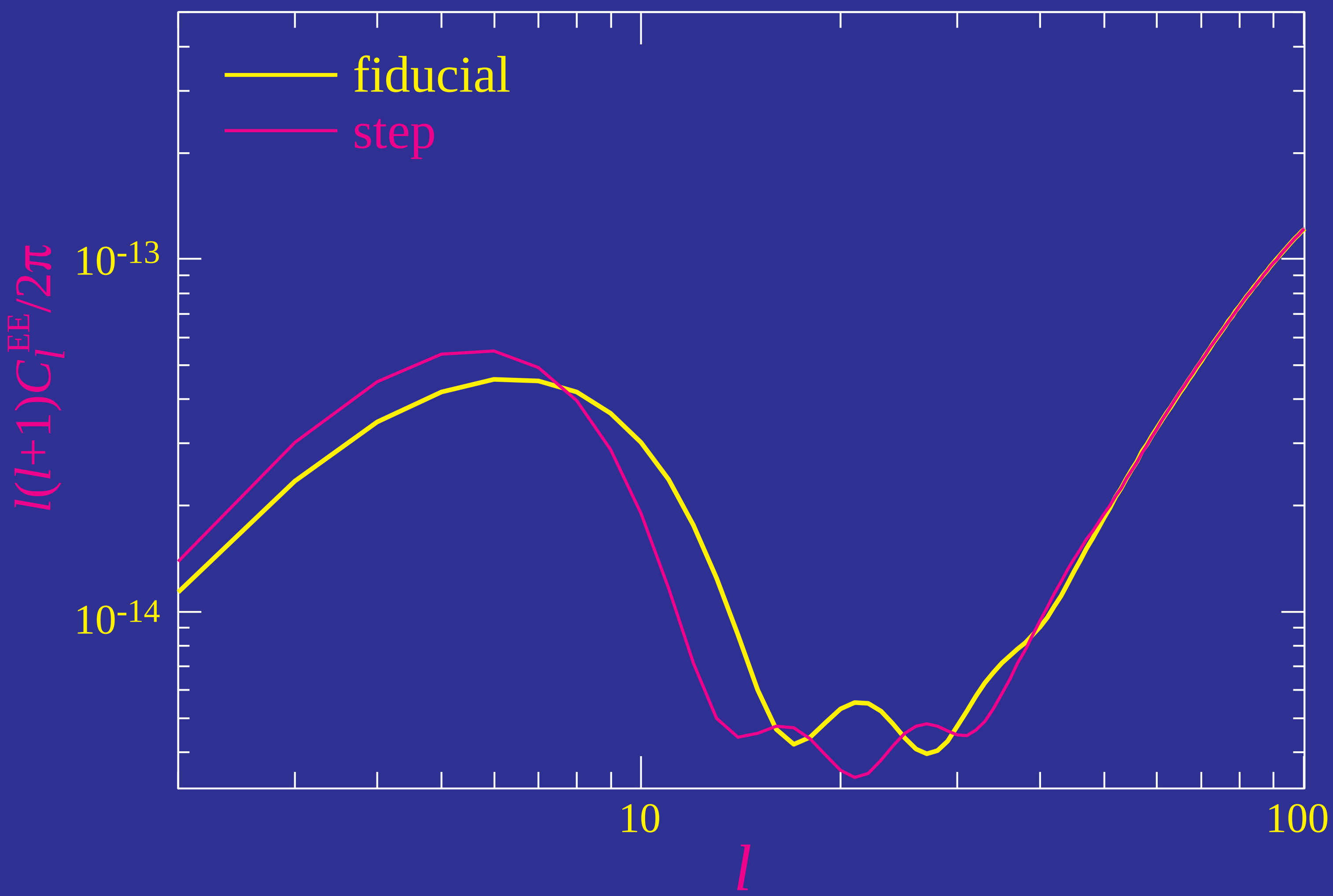


Kaplinghat et al. (2002); Hu & Holder (2003)

# Principal Components

- Eigenvectors of the Fisher Matrix

$$F_{ij} \equiv \sum_{\ell} (\ell + 1/2) T_{\ell i} T_{\ell j} = \sum_{\mu} S_{i\mu} \sigma_{\mu}^{-2} S_{j\mu}$$

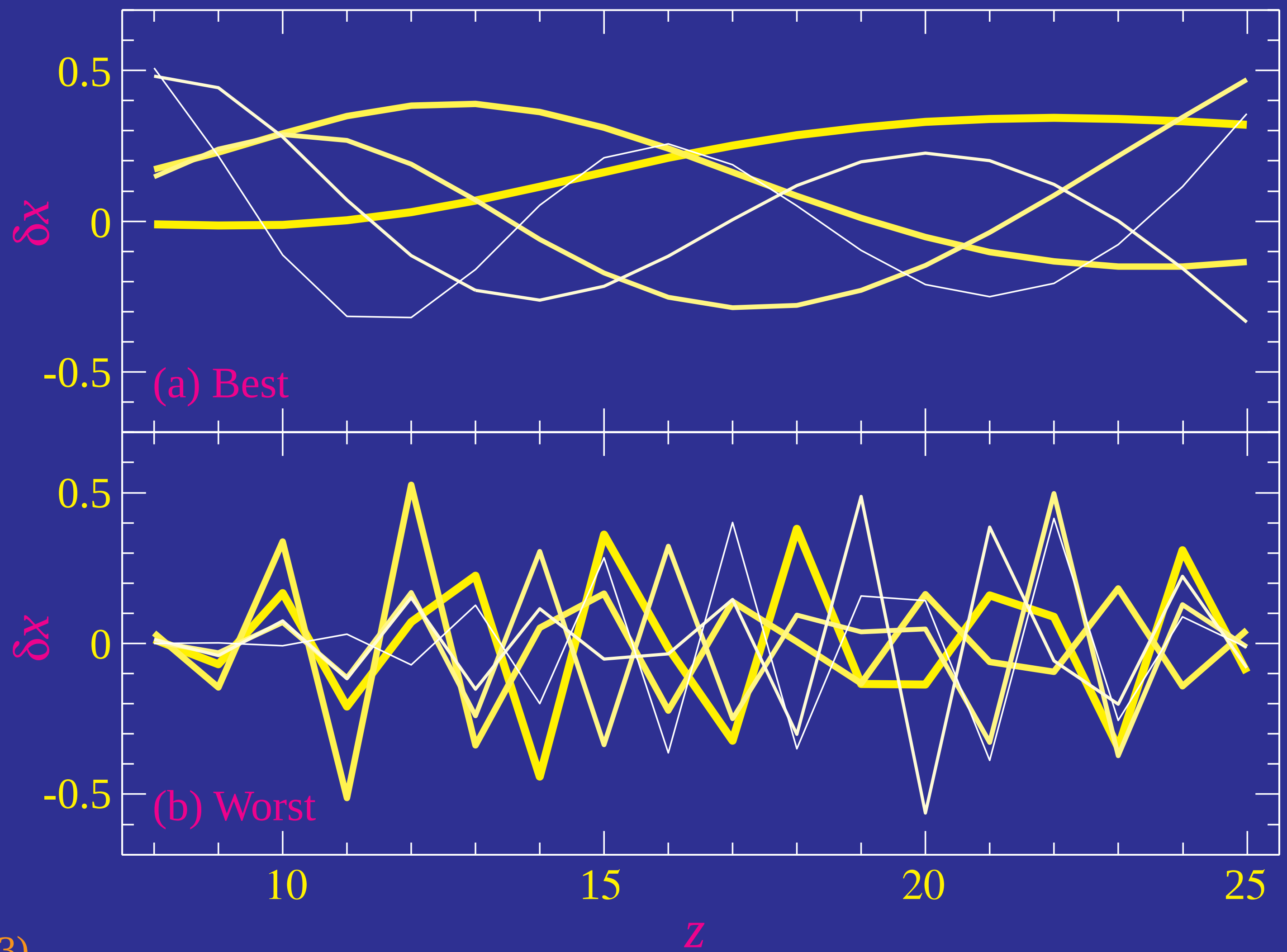


Hu & Holder (2003)

# Capturing the Observables

- First 5 modes have the information content and most of optical depth

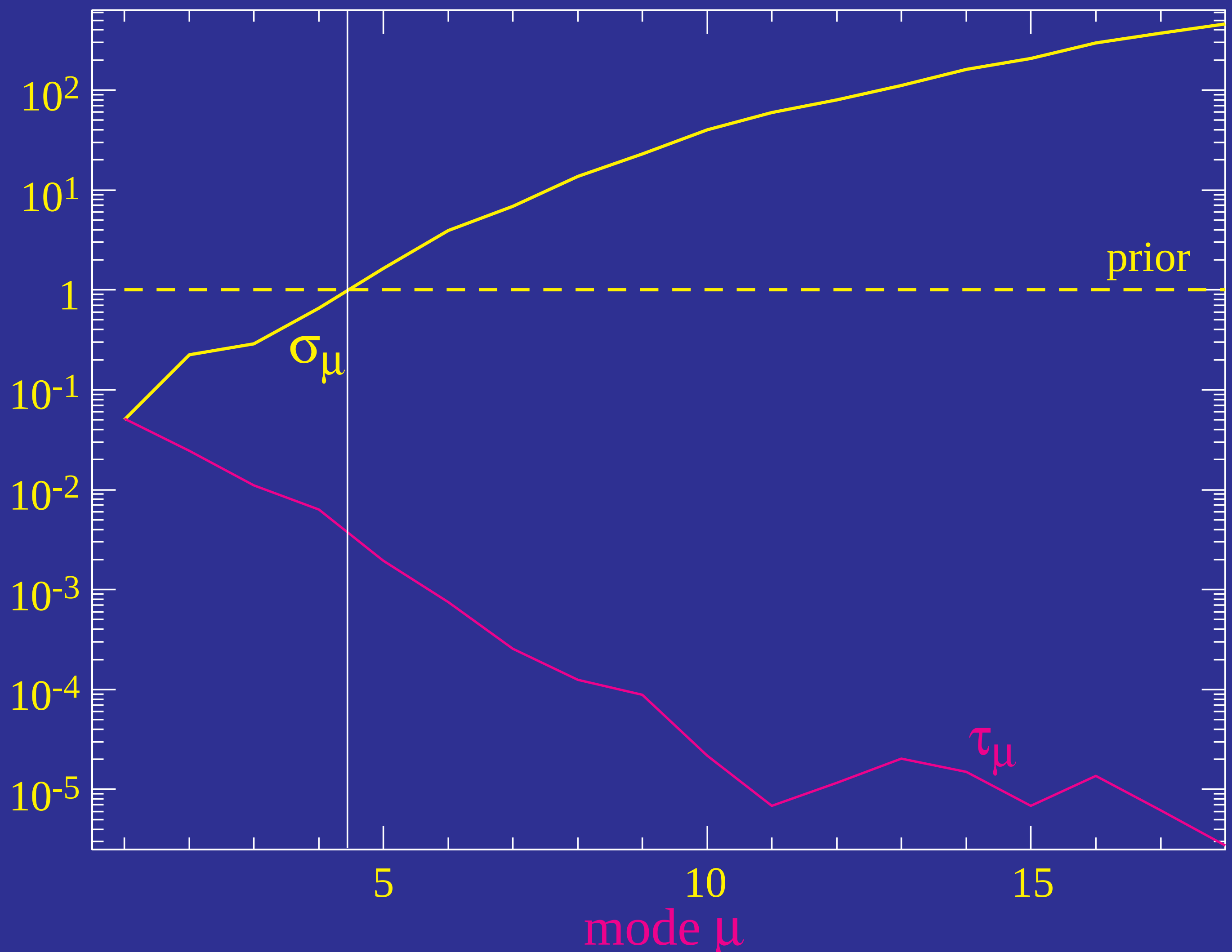


Hu & Holder (2003)

# Representation in Modes

- Truncation at 5 modes leaves a low pass filtered of ionization history
- Ionization fraction allowed to go negative (Boltzmann code has negative sources)

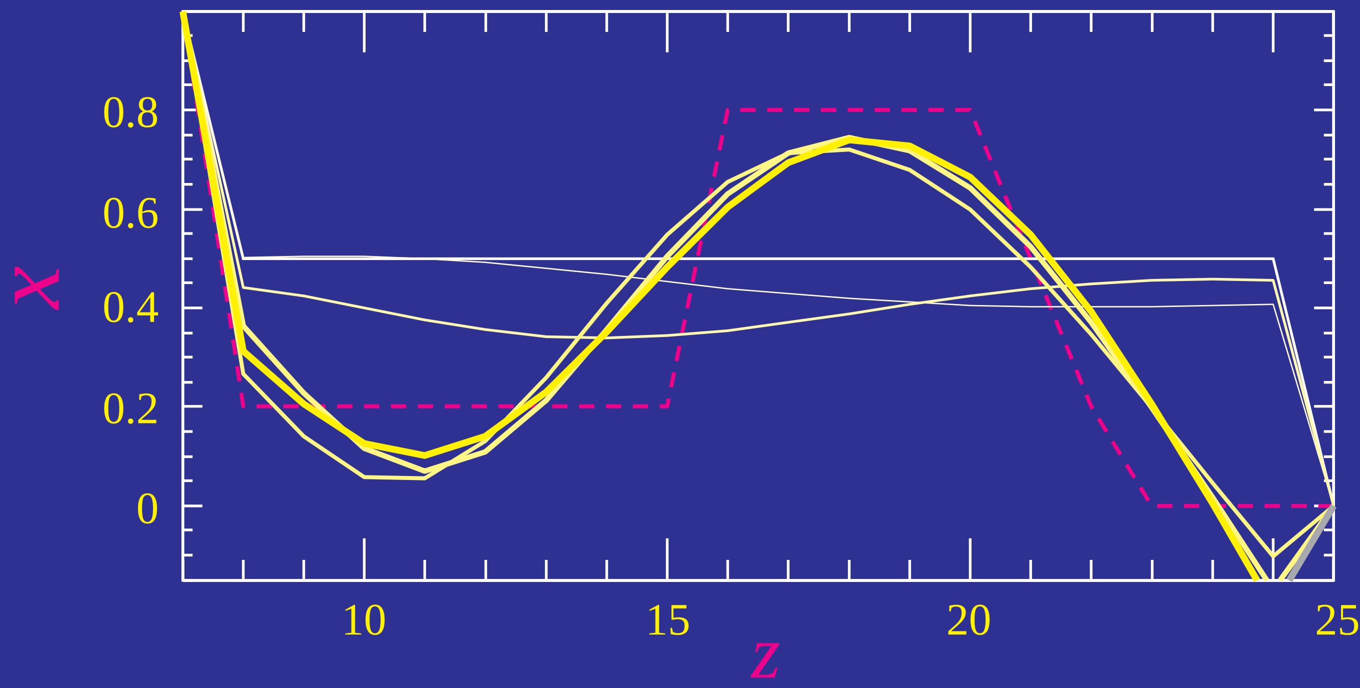


Hu & Holder (2003)

# Representation in Modes

- Reproduces the power spectrum with sum over >3 modes
  more generally 5 modes suffices: e.g. total $\tau$=0.1375 vs 0.1377

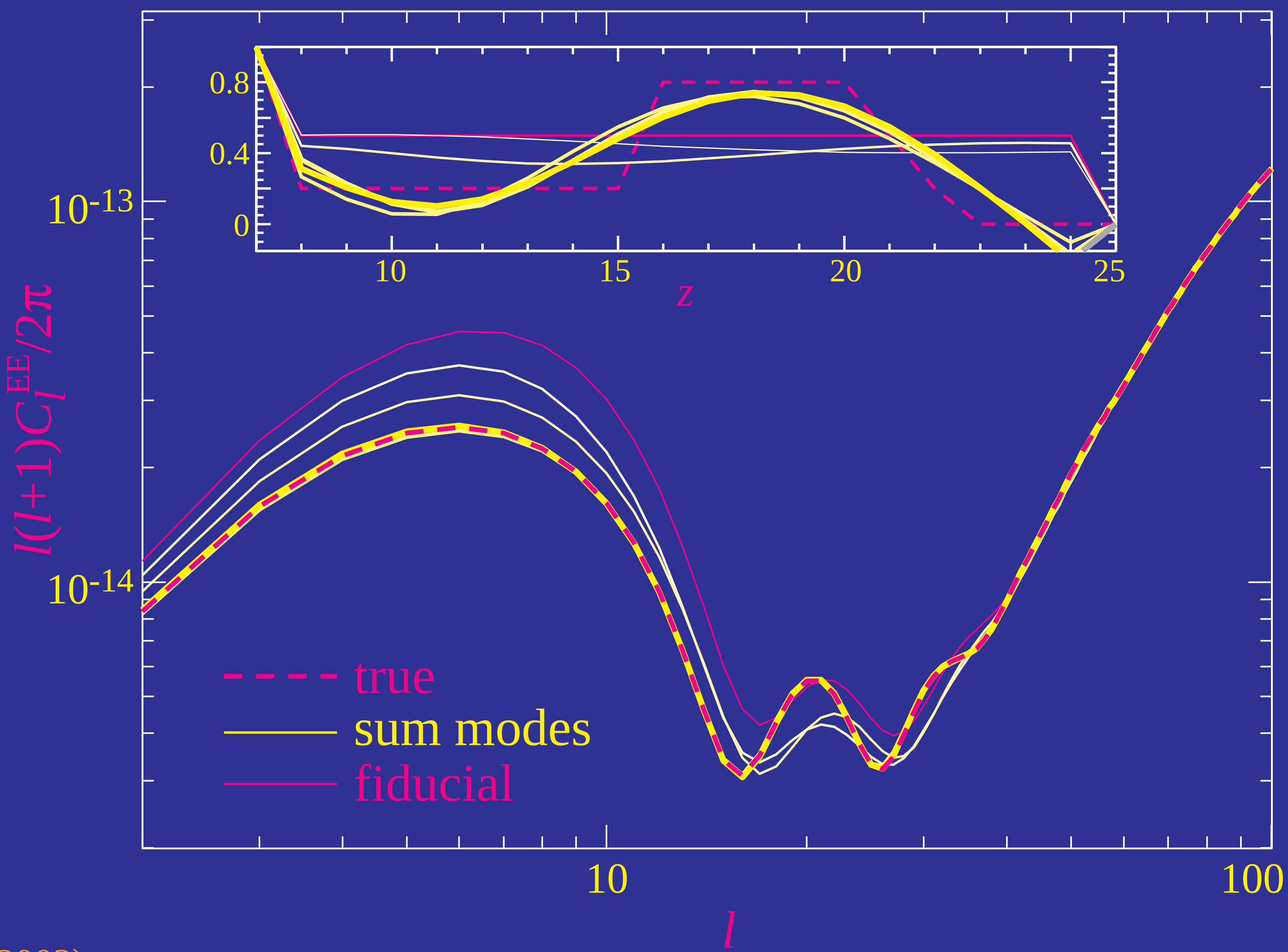


Hu & Holder (2003)

# Total Optical Depth

- Optical depth measurement unbiased
- Ultimate errors set by cosmic variance here 0.01
- Equivalently 1% measure of initial amplitude, impt for dark energy

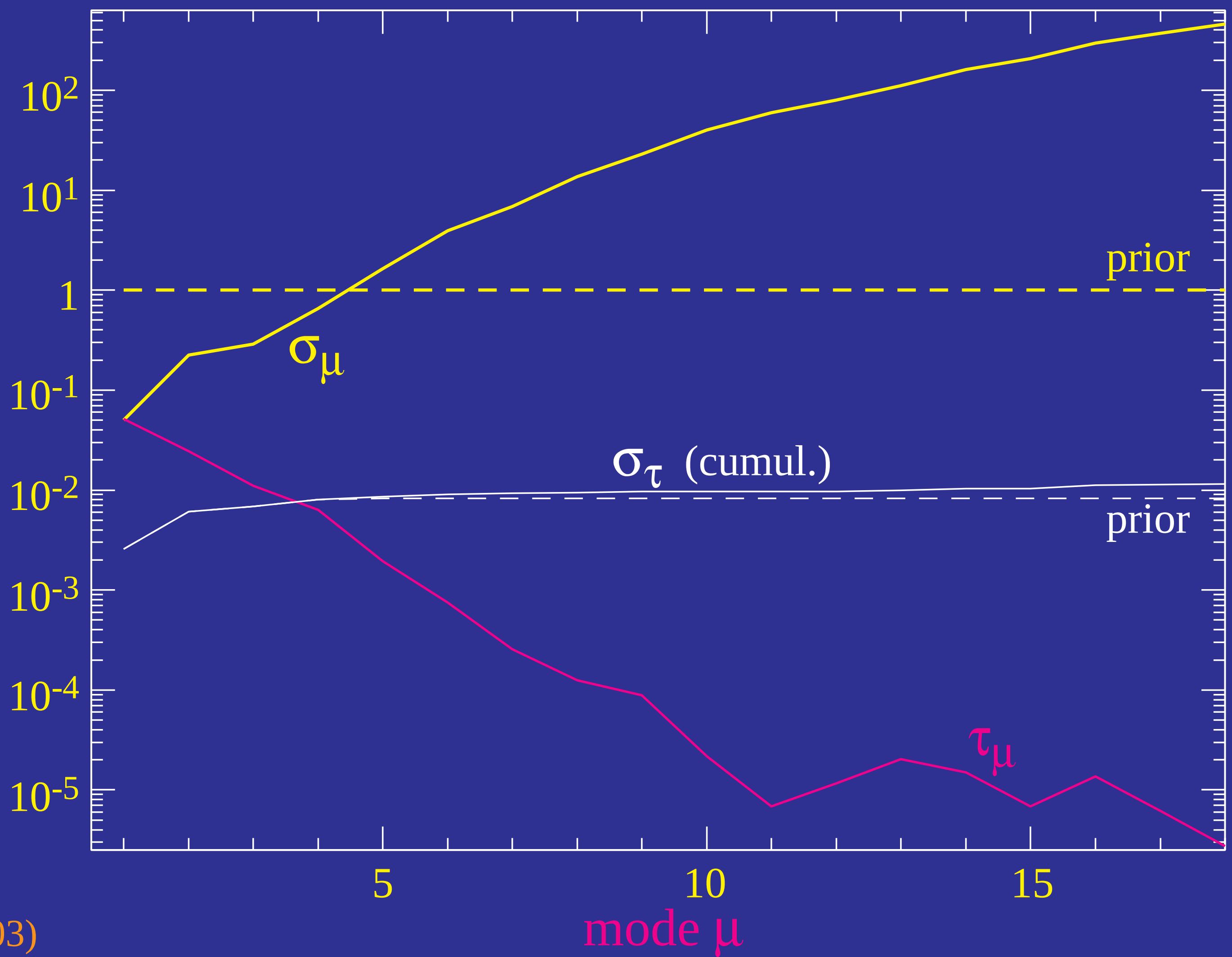


Hu & Holder (2003)

# WMAP5 Ionization PCs

- Only first two modes constrained, $\tau$=0.101±0.017

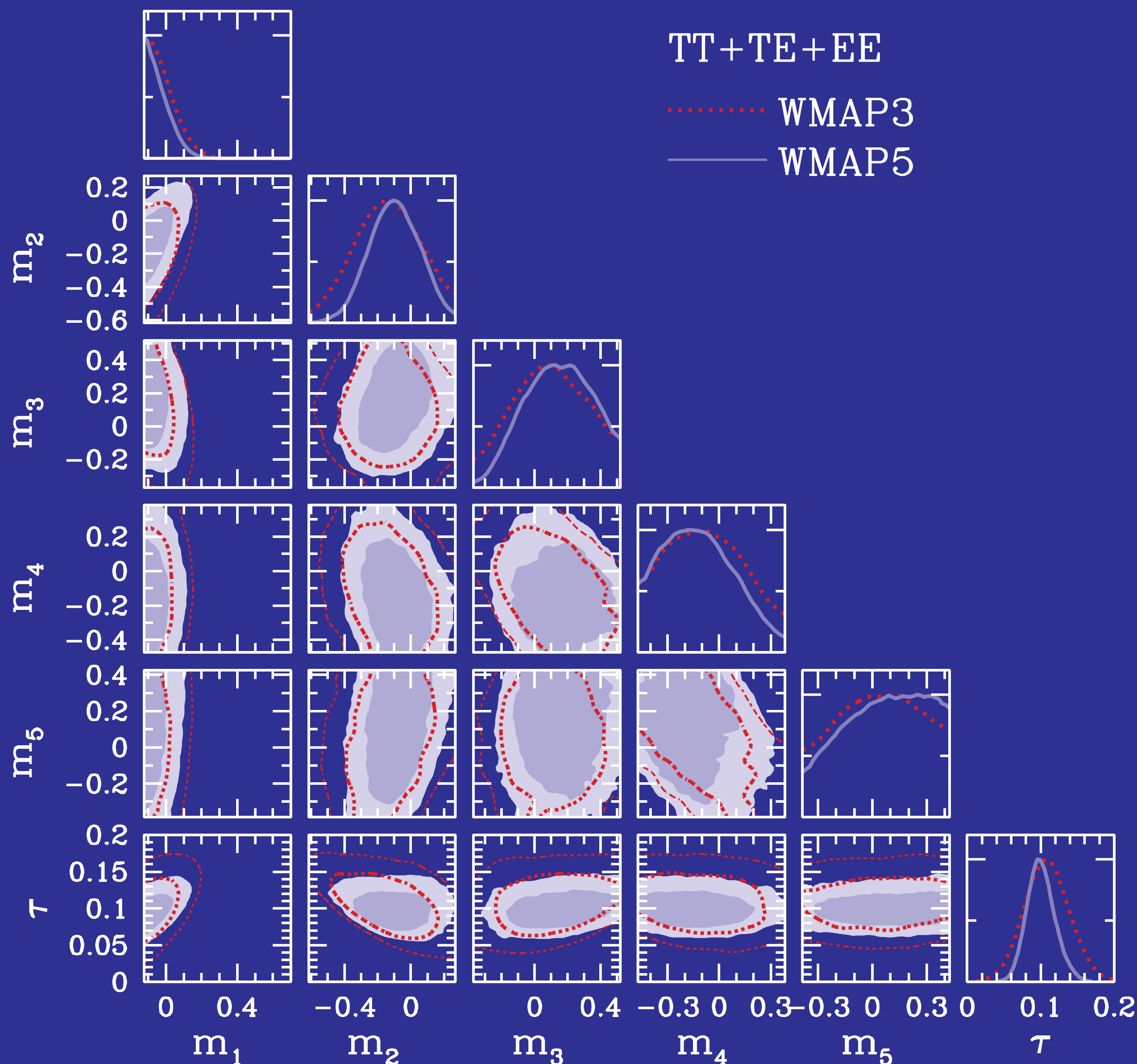


Mortonson & Hu (2008)

# Model-Independent Reionization

- All possible ionization histories at $z<30$
- Detections at $20<l<30$ required to further constrain general ionization which widens the $\tau$-$n_s$ degeneracy allowing $n_s=1$
- Quadrupole & octopole predicted to better than cosmic variance test ΛCDM for anomalies

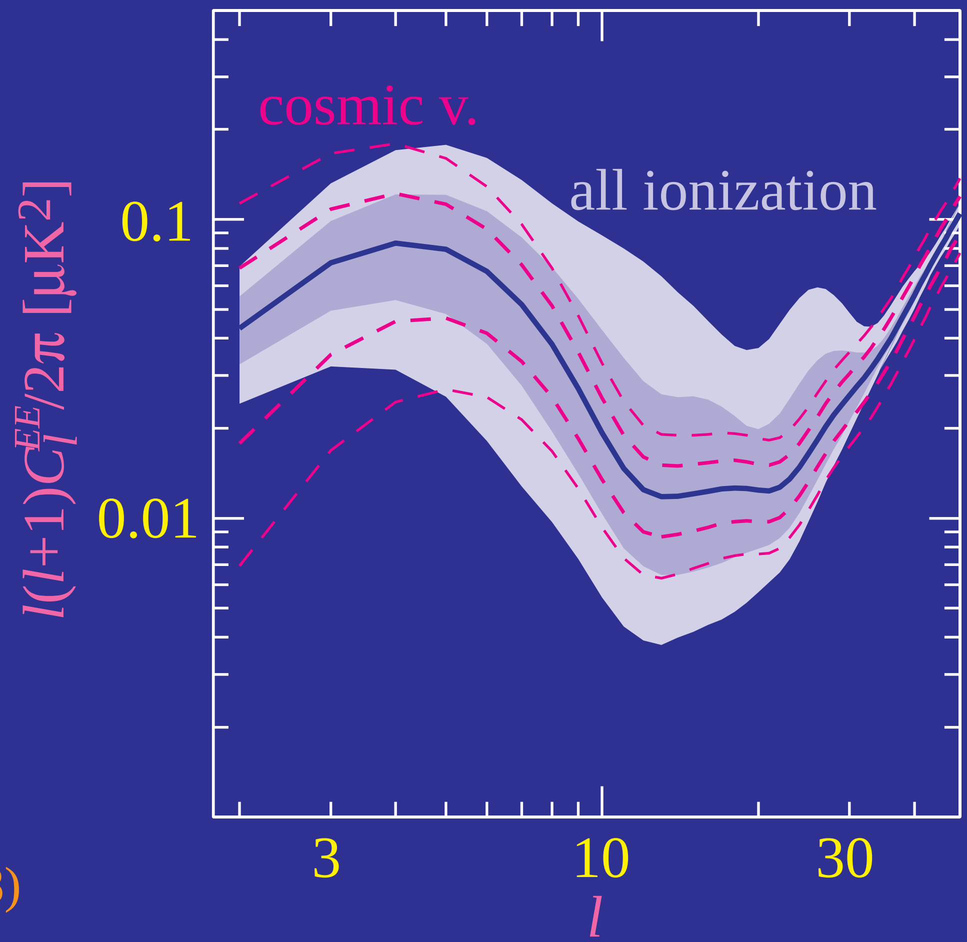


Mortonson & Hu (2008)

# Gravitational Secondaries

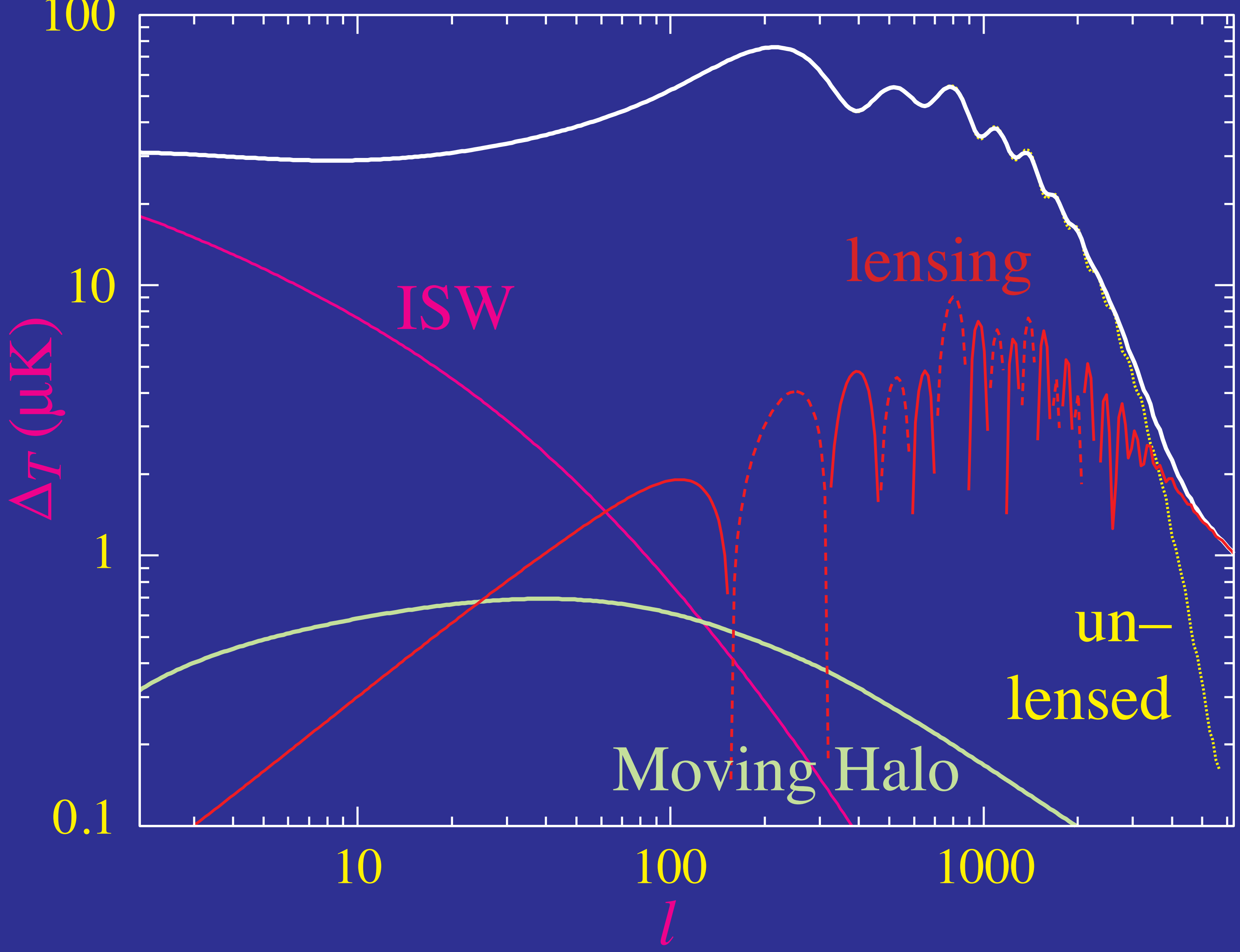

# Integrated Sachs-Wolfe Effect

# Scattering Secondaries

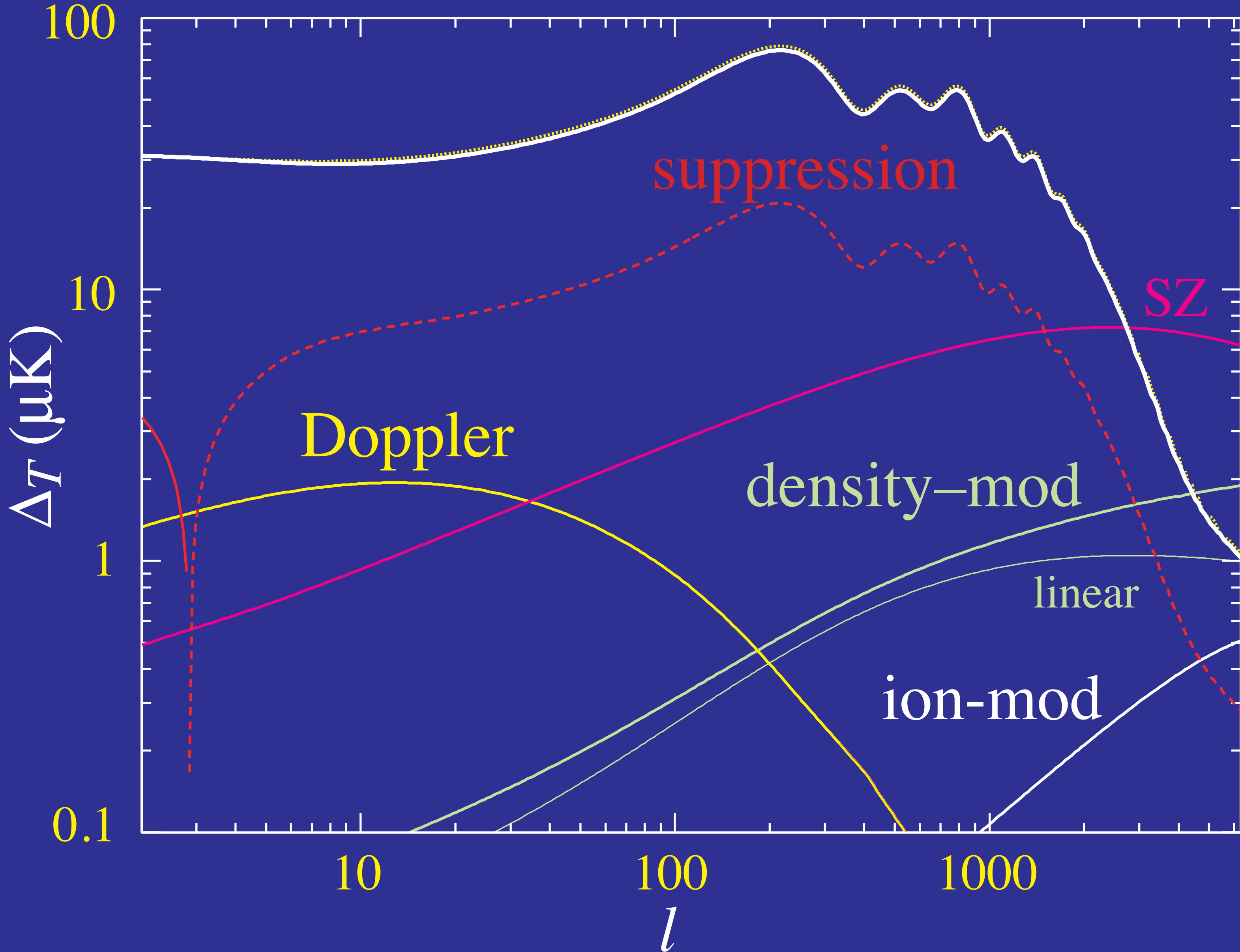

# Gravitational Secondaries

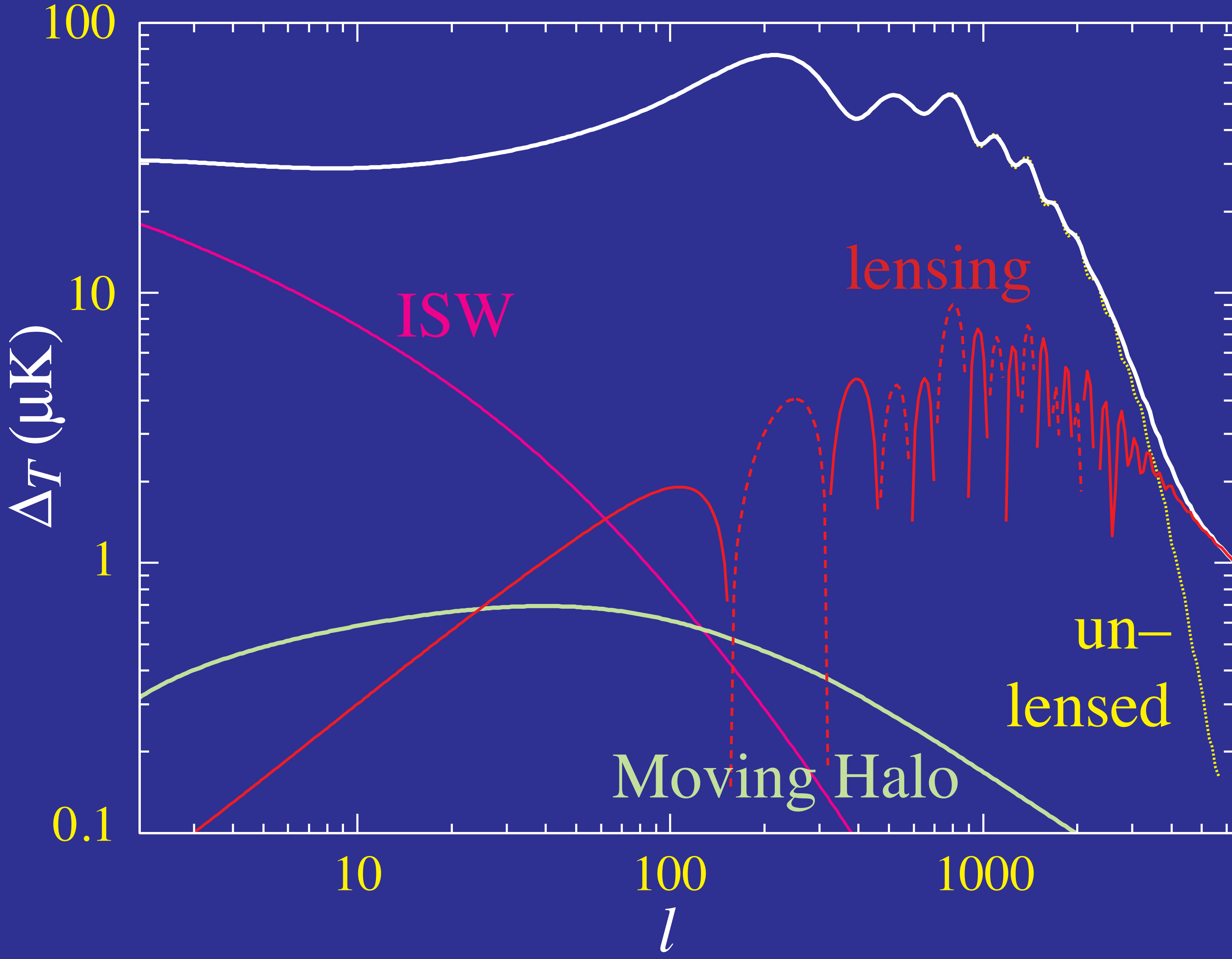

# ISW Effect

- Gravitational blueshift on infall does not cancel redshift on climbing out
- Contraction of spatial metric doubles the effect: $\Delta T/T = 2\Delta\Phi$
- Effect from potential hills and wells cancel on small scales

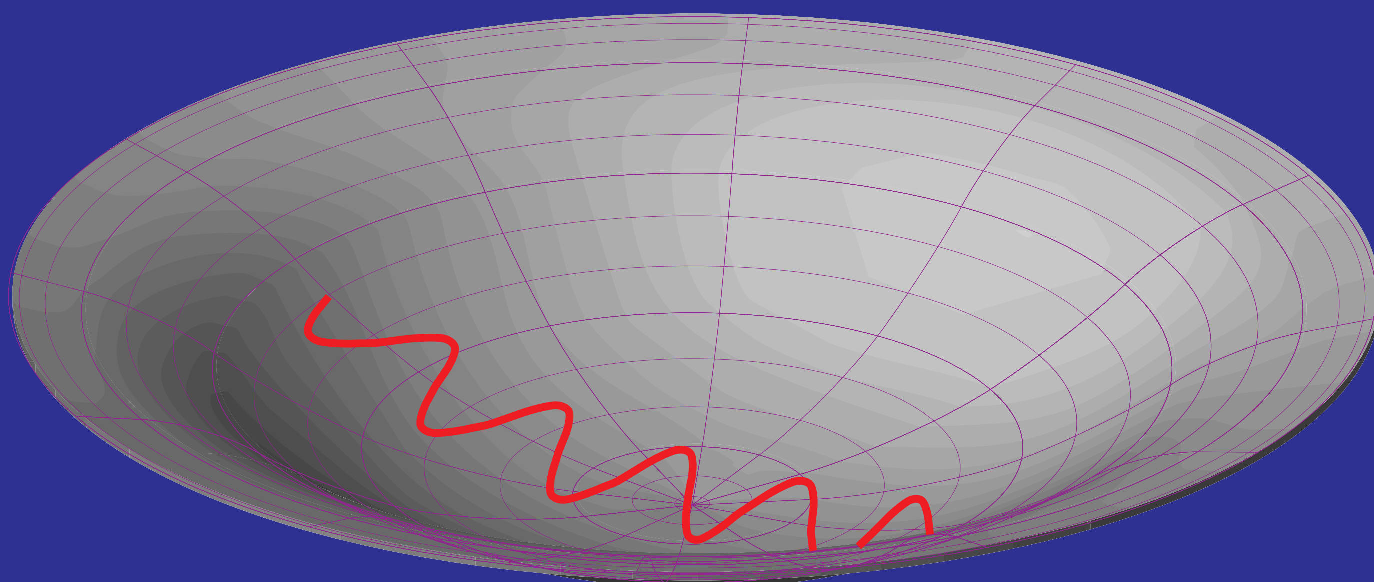

# ISW Effect

- Gravitational blueshift on infall does not cancel redshift on climbing out
- Contraction of spatial metric doubles the effect: $\Delta T/T = 2\Delta\Phi$
- Effect from potential hills and wells cancel on small scales

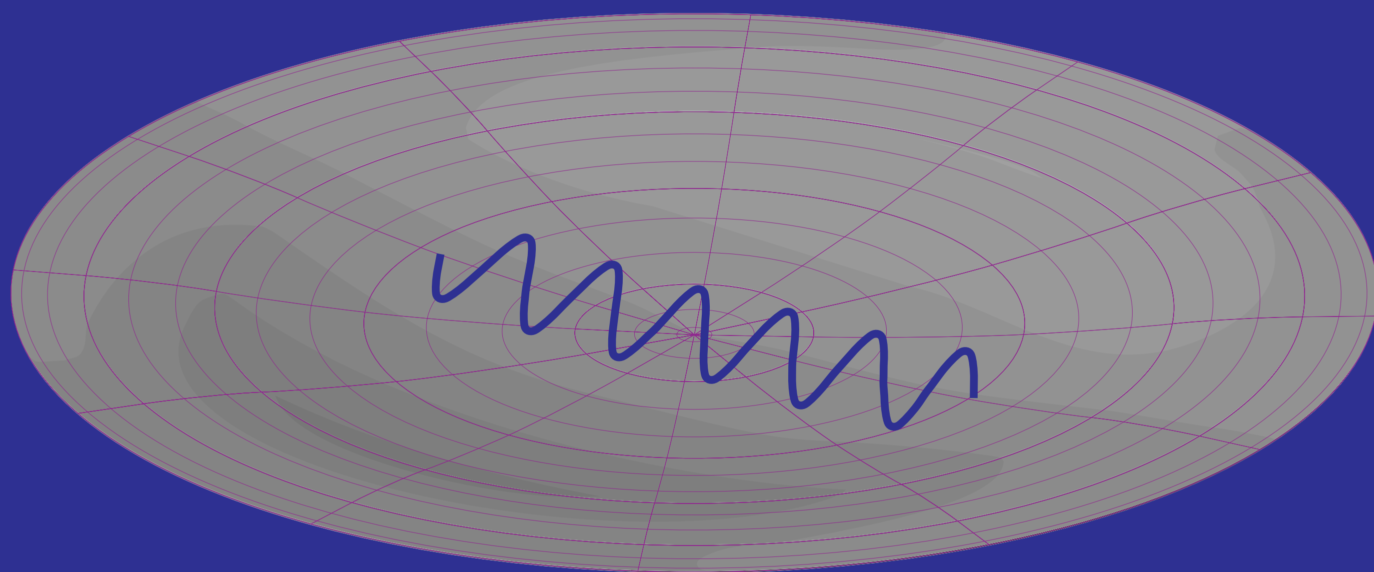

# Smooth Energy Density & Potential Decay

- Regardless of the equation of state an energy component that clusters preserves an approximately constant gravitational potential (formally Bardeen curvature $\zeta$)

# Smooth Energy Density & Potential Decay

- Regardless of the equation of state an energy component that clusters preserves an approximately constant gravitational potential (formally Bardeen curvature $\zeta$)
- A smooth component contributes

  density $\rho$ to the expansion

  but not

  density fluctuation $\delta\rho$ to the Poisson equation
- Imbalance causes potential to decay once smooth component dominates the expansion

# ISW Spatial Modes

- ISW effect comes from nearby acceleration regime
- Shorter wavelengths project onto same angle
- Broad source kernel: Limber cancellation out to quadrupole

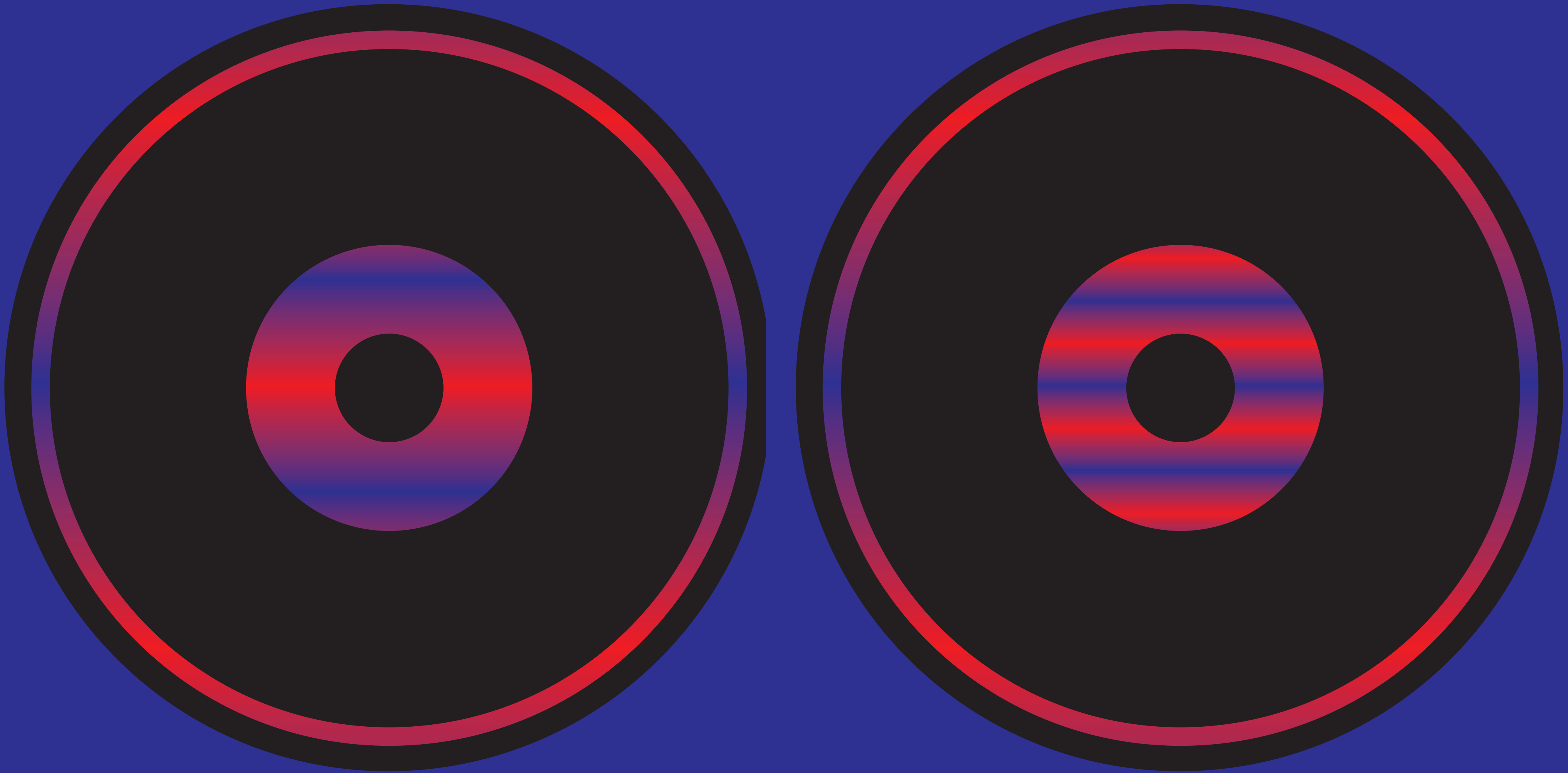

# Quadrupole Origins

- Transfer function for the quadrupole

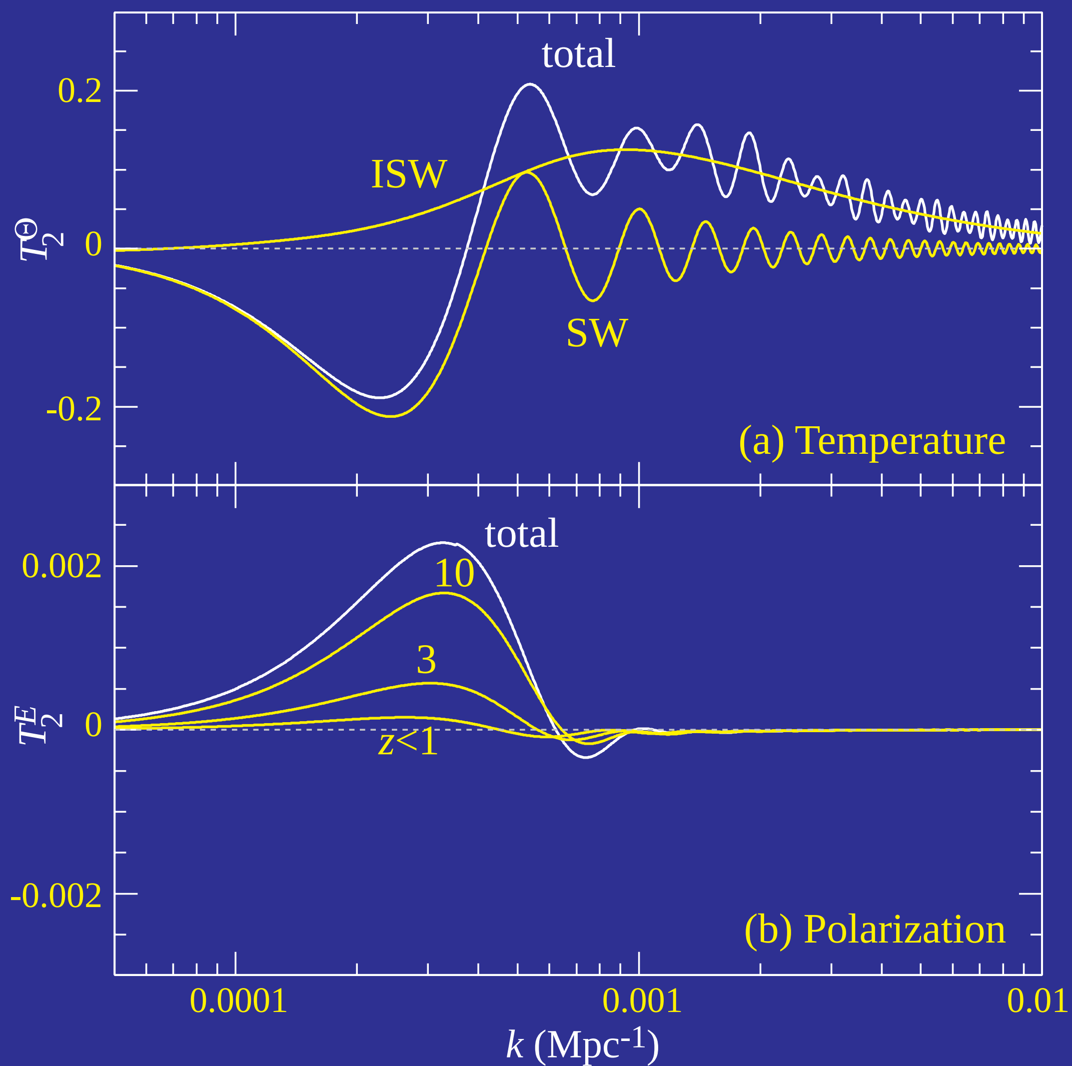


Gordon & Hu (2004)

# Smooth Energy Density & Potential Decay

- Regardless of the equation of state an energy component that clusters preserves an approximately constant gravitational potential (formally Bardeen curvature $\zeta$)
- A smooth component contributes

  density $\rho$ to the expansion

  but not

  density fluctuation $\delta\rho$ to the Poisson equation
- Imbalance causes potential to decay once smooth component dominates the expansion
- Scalar field dark energy (quintessence) is smooth out to the horizon scale (sound speed $c_s=1$)
- Potential decay measures the clustering properties and hence the particle properties of the dark energy

# ISW & Dark Energy

# Dark Energy

- Peaks measure distance to recombination
- ISW effect constrains dynamics of acceleration

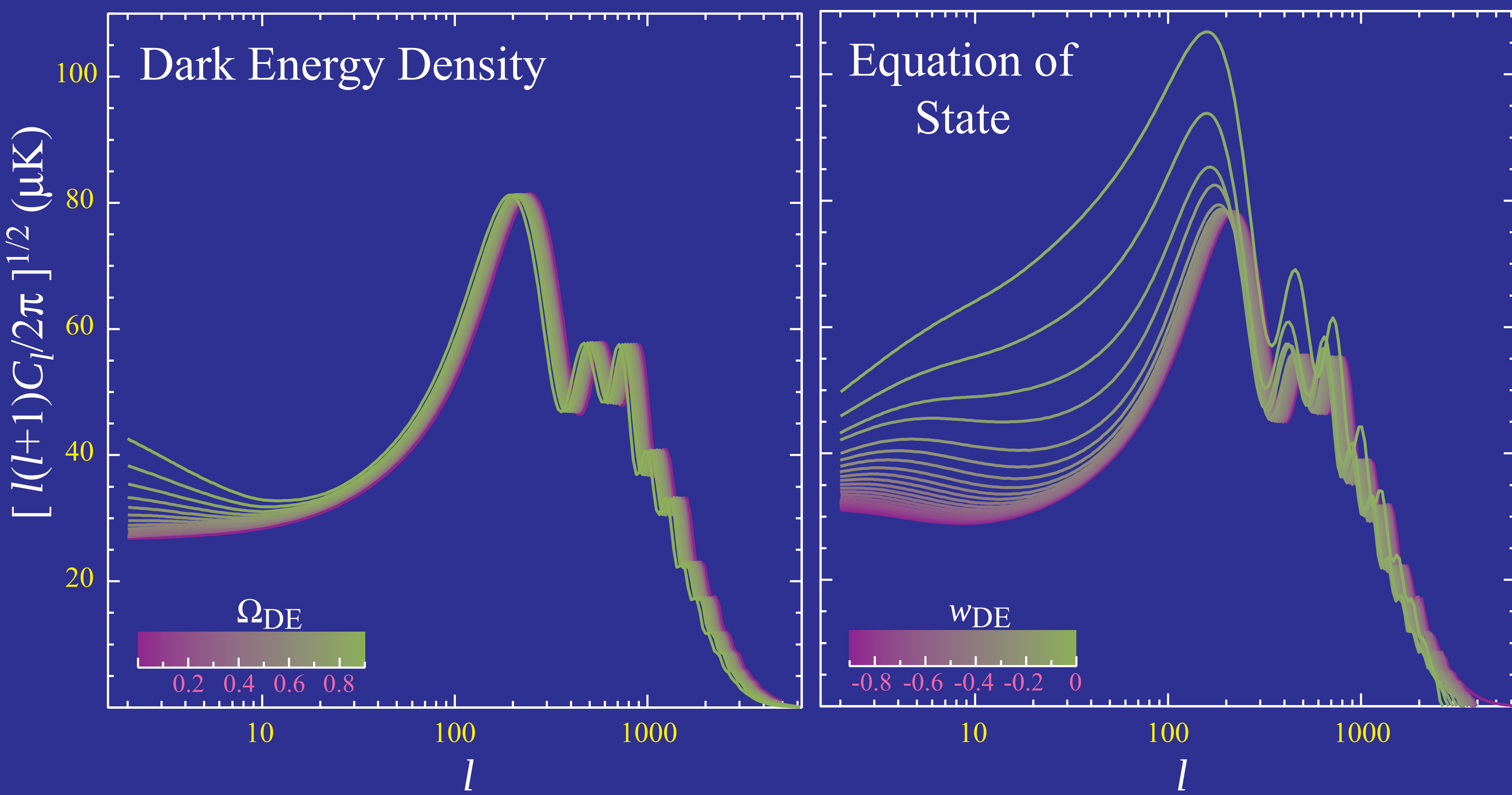

# Dark Energy Sound Speed

- Smooth and clustered regimes separated by sound horizon
- Covariant definition: $c_e^2 = \delta p / \delta\rho$ where momentum flux vanishes
- For scalar field dark energy uniquely defined by kinetic term

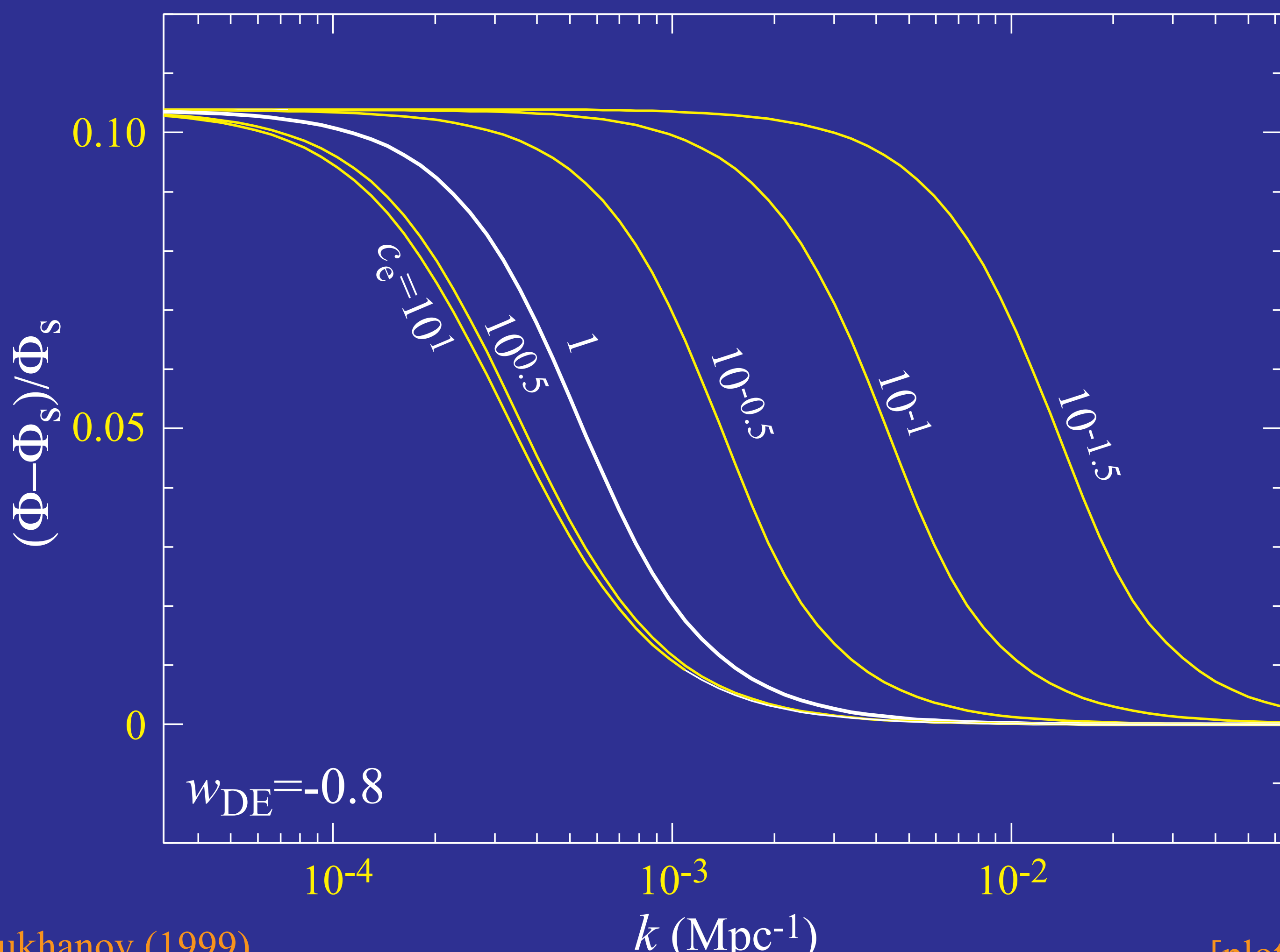


Hu (1998)
Garriga & Mukhanov (1999)

[plot: Hu & Scranton (2004)]

# Dark Energy Clustering

- ISW effect intrinsically sensitive to dark energy smoothness
- Large angle contributions reduced if clustered

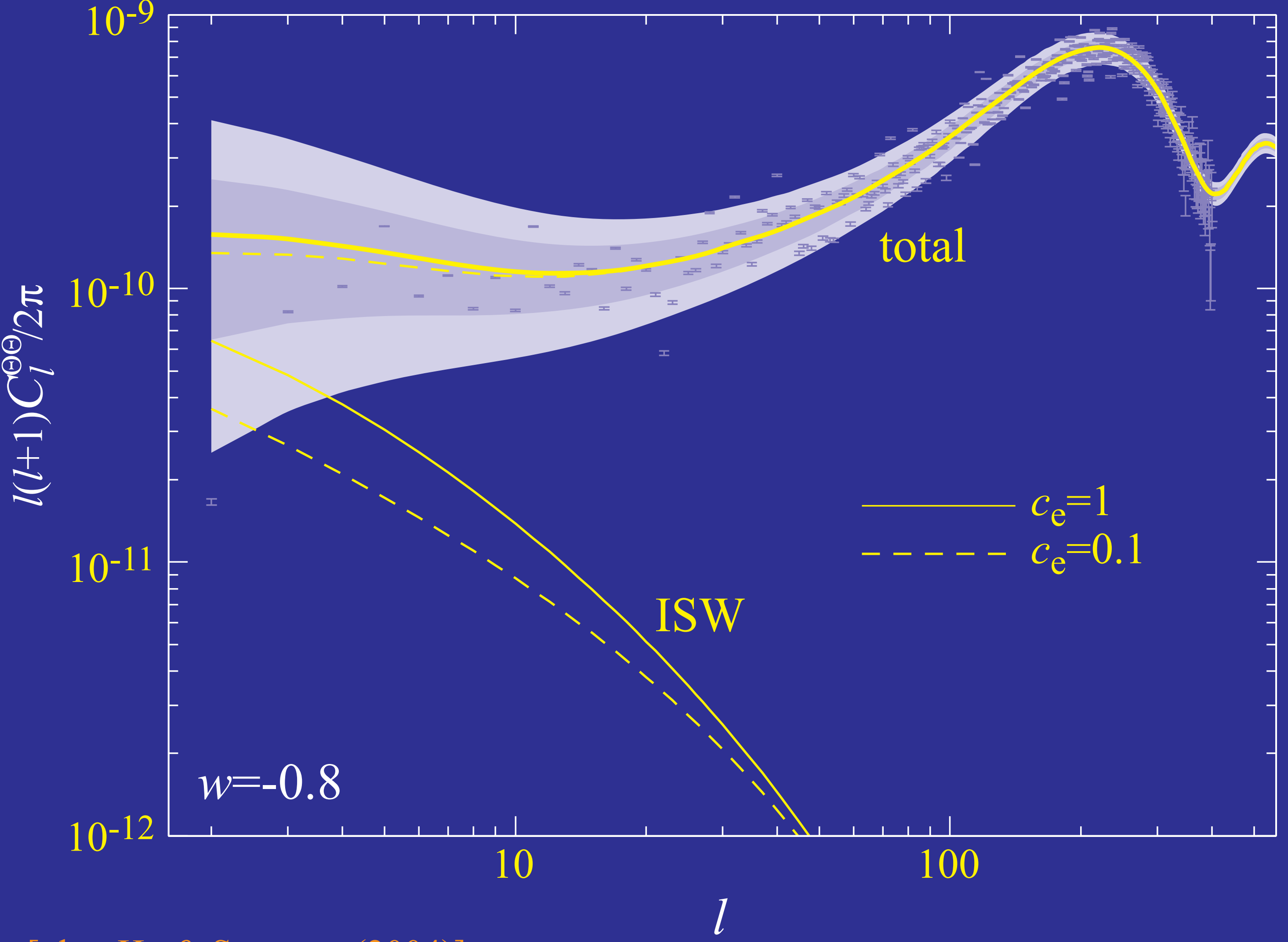


Hu (1998); [plot: Hu & Scranton (2004)]

# DGP CMB Large-Angle Excess

- Extra dimension modify gravity on large scales
- 4D universe bending into extra dimension alters gravitational redshifts in cosmic microwave background

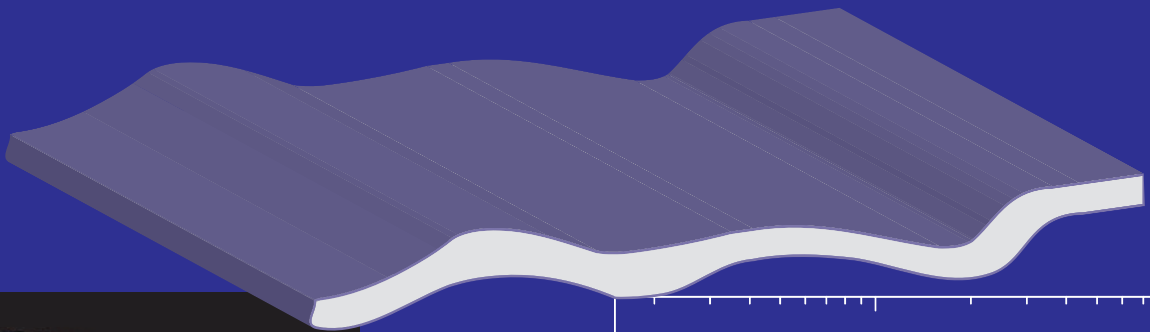

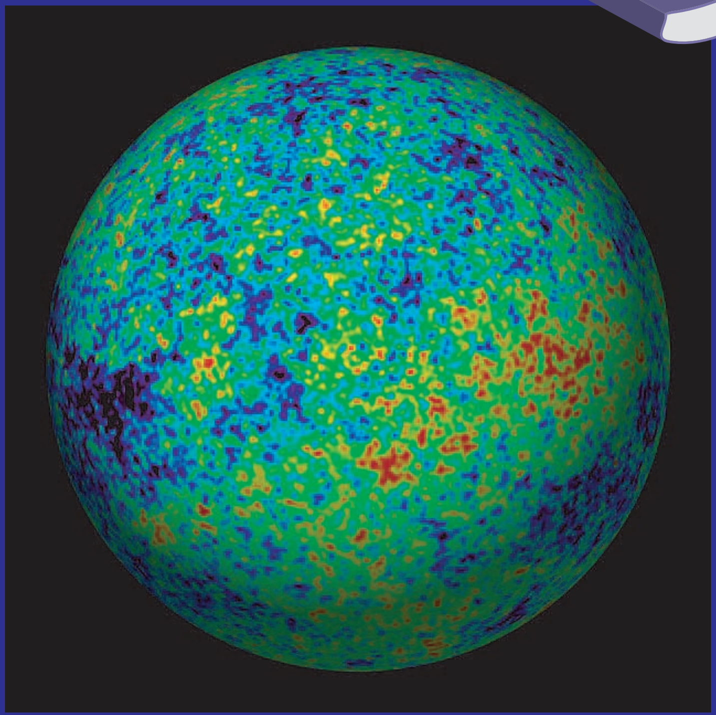

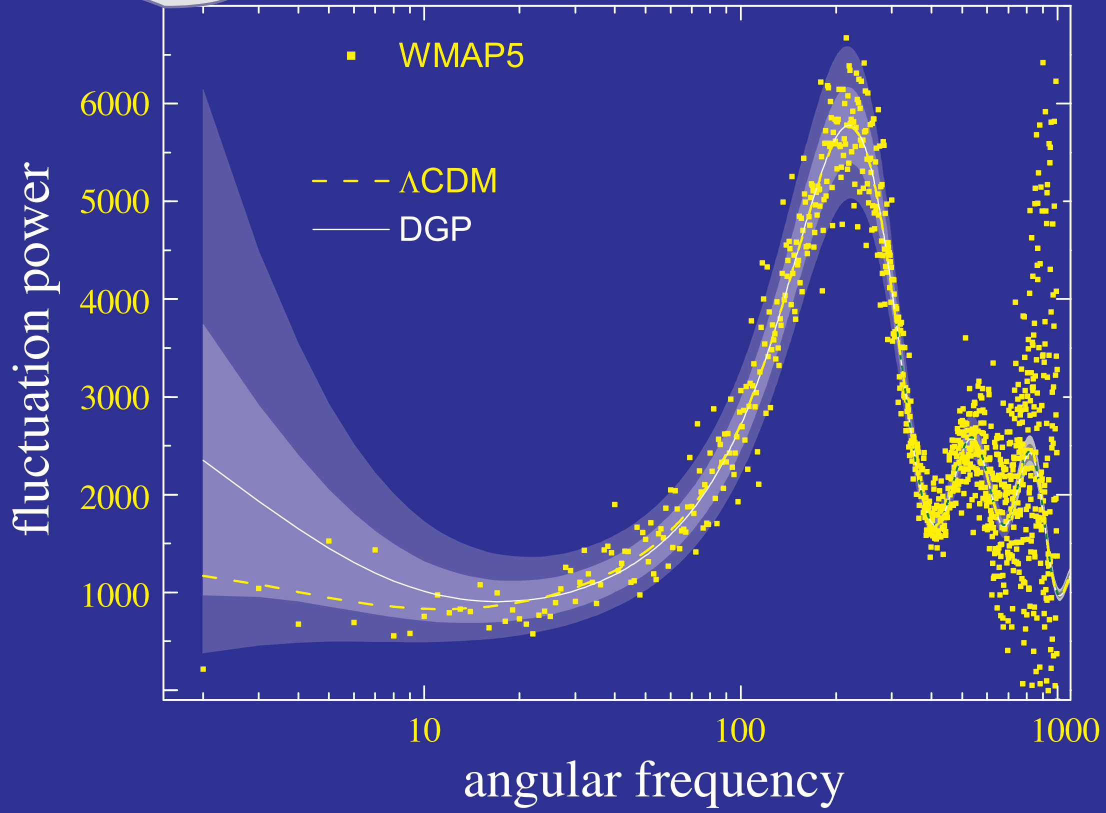

# Lensing of CMB Fields

# Gravitational Lensing

- Lensing is a surface brightness conserving remapping of source to image planes by the gradient of the projected potential

$$\phi(\hat{\mathbf{n}}) = 2\int \frac{dz}{H(z)} \frac{D_A(D_s - D)}{D_A(D)\, D_A(D_s)} \Phi(D_A\hat{\mathbf{n}}, D)\,,$$

  such that the fields are remapped as

$$x(\hat{\mathbf{n}}) \to x(\hat{\mathbf{n}} + \nabla\phi)\,,$$

  where $x \in \{T, Q, U\}$ temperature and polarization.

- Taylor expansion leads to product of fields and Fourier mode-coupling
- Appears in the power spectrum as a convolution kernel for $T$ and $E$ and an $E \to B$.

# Lensing of a Gaussian Random Field

- CMB temperature and polarization anisotropies are Gaussian random fields – unlike galaxy weak lensing
- Average over many noisy images – like galaxy weak lensing

# Gravitational Lensing

- Gravitational lensing by large scale structure distorts the observed temperature and polarization fields
- Exaggerated example for the temperature

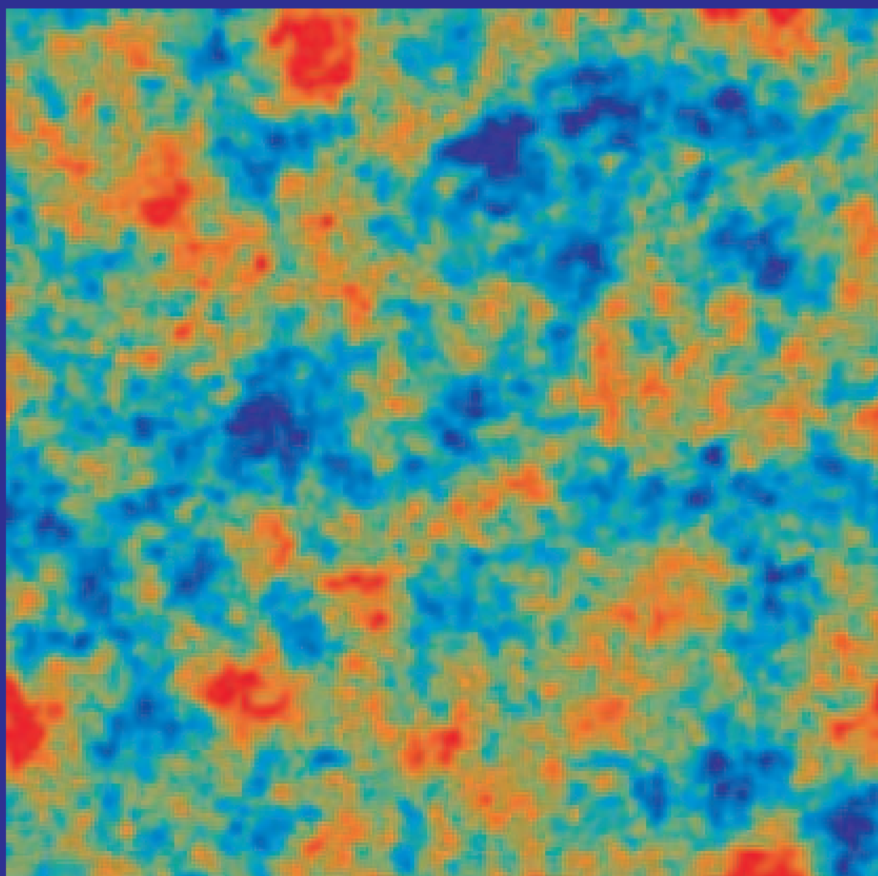

Original

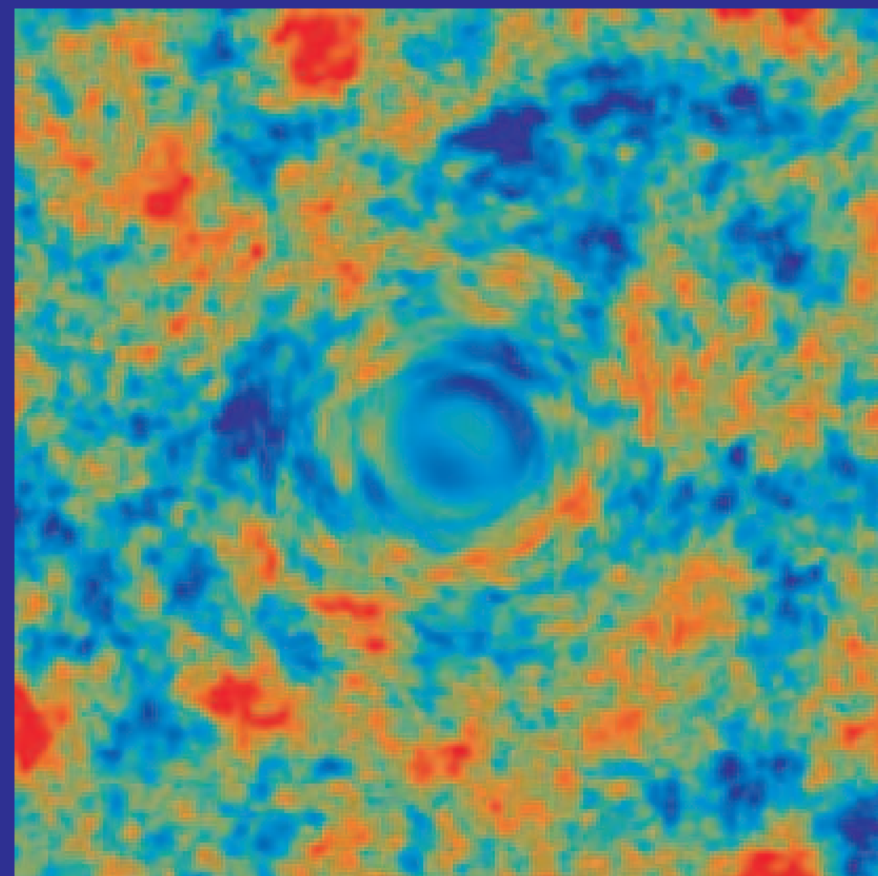

Lensed

# Polarization Lensing

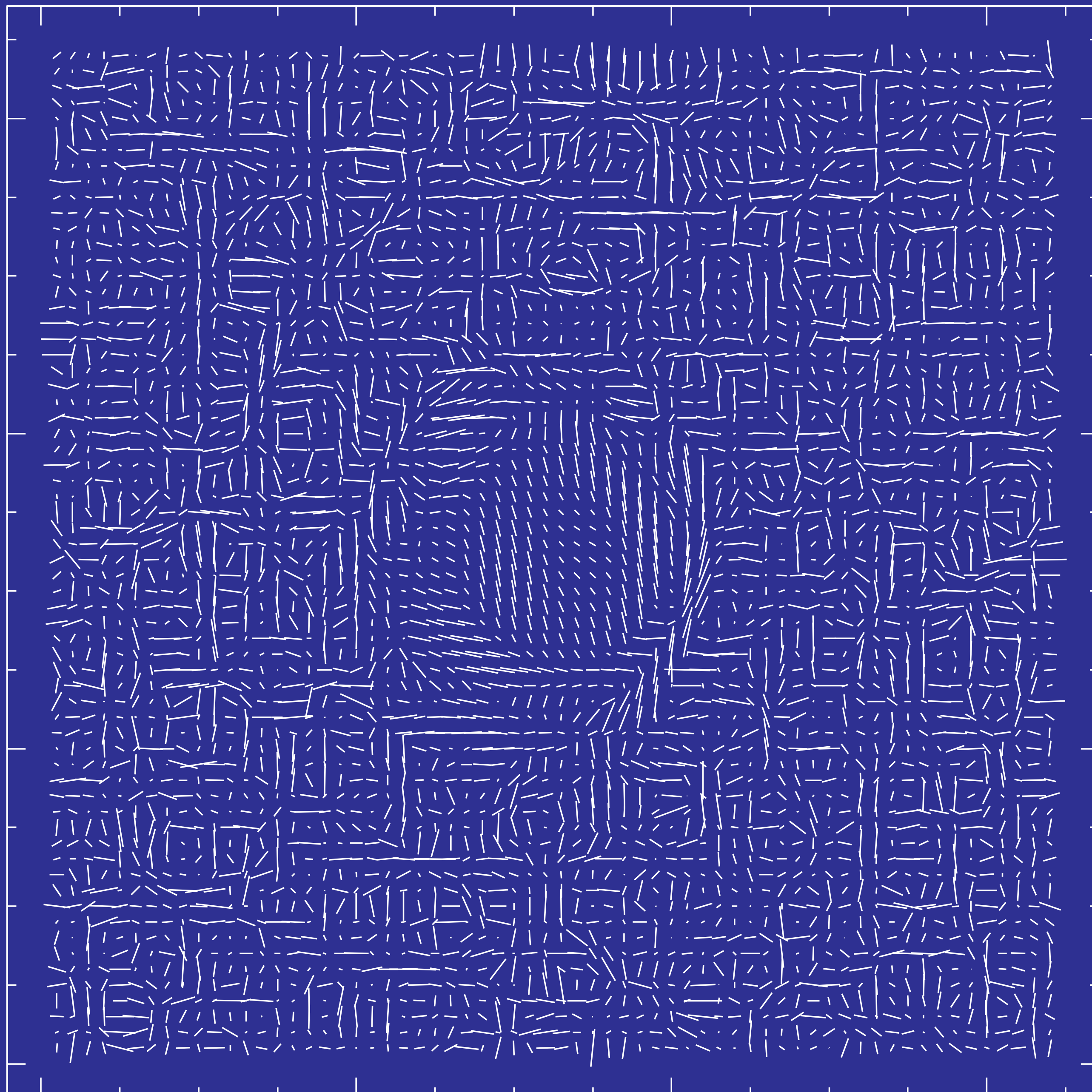

# Electric & Magnetic Polarization

(a.k.a. gradient & curl)

- Alignment of principal vs polarization axes
  (curvature matrix vs polarization direction)

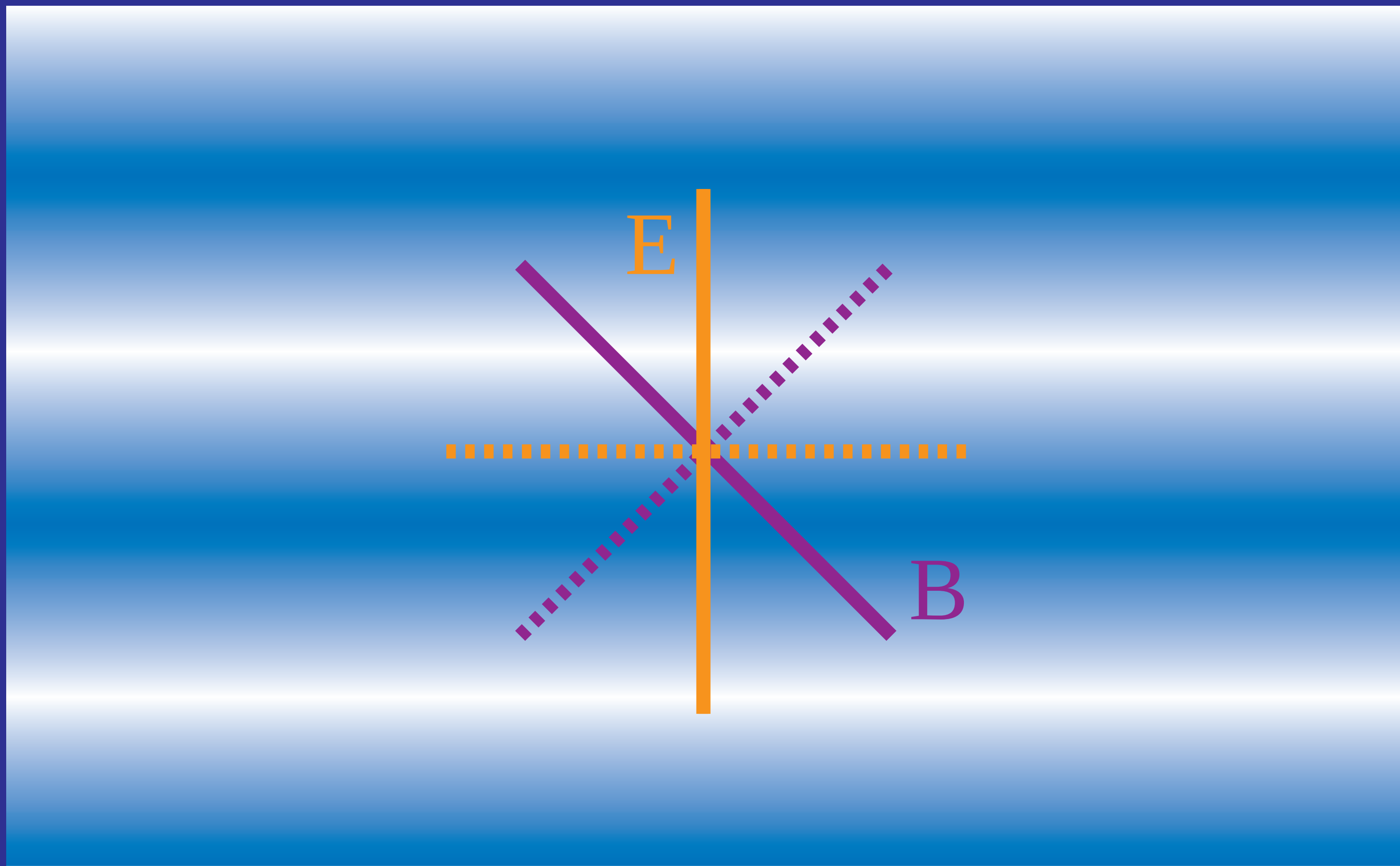


Kamionkowski, Kosowsky, Stebbins (1997)
Zaldarriaga & Seljak (1997)

# Temperature & Polarization

- Warping of the polarization field generates B-modes from E-modes at recombination (100 sq deg.)

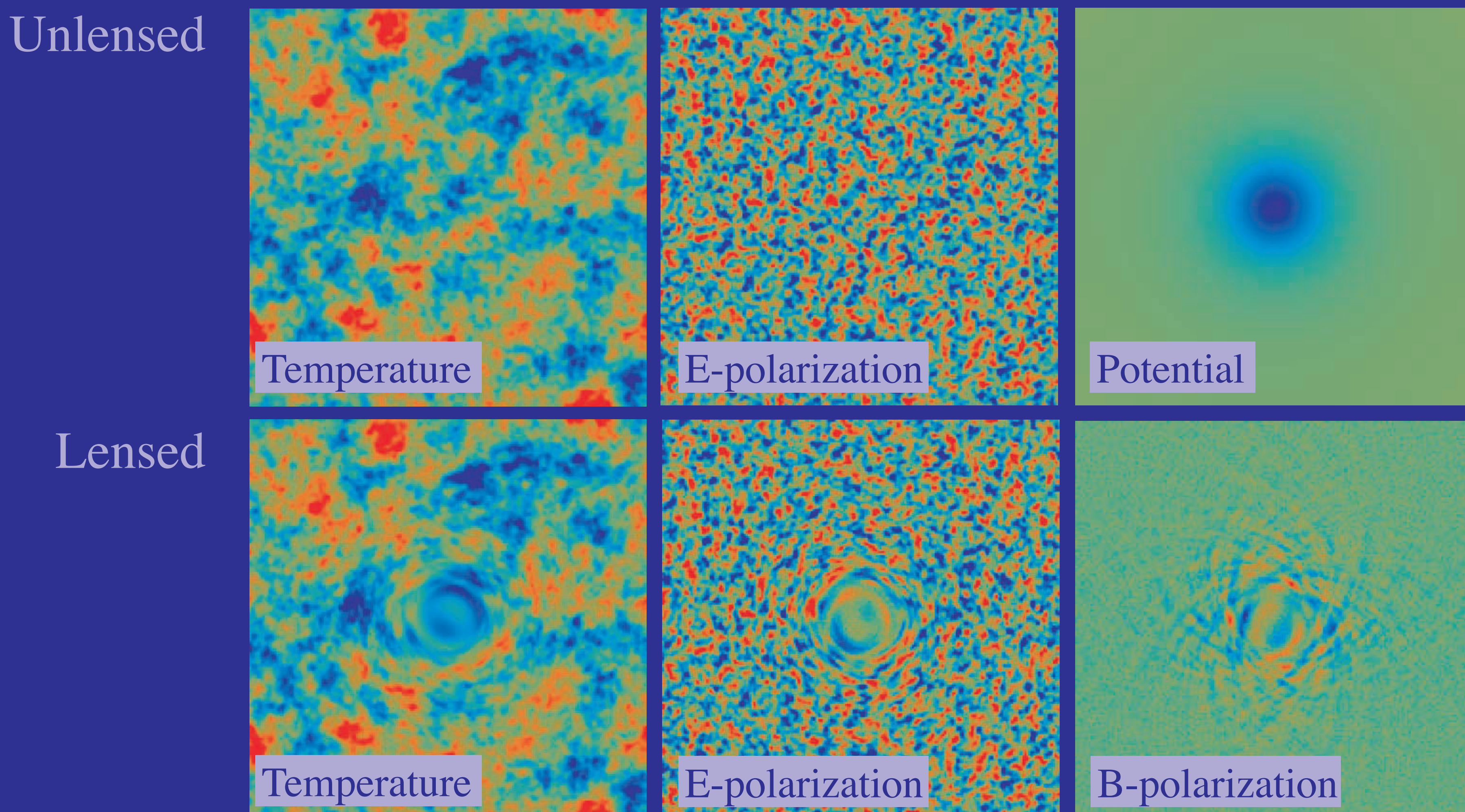


Zaldarriaga & Seljak (1999) [figure from Hu & Okamoto (2001)]

# Lensing by a Gaussian Random Field

- Mass distribution at large angles and high redshift in in the linear regime
- Projected mass distribution (low pass filtered reflecting deflection angles): 1000 sq. deg

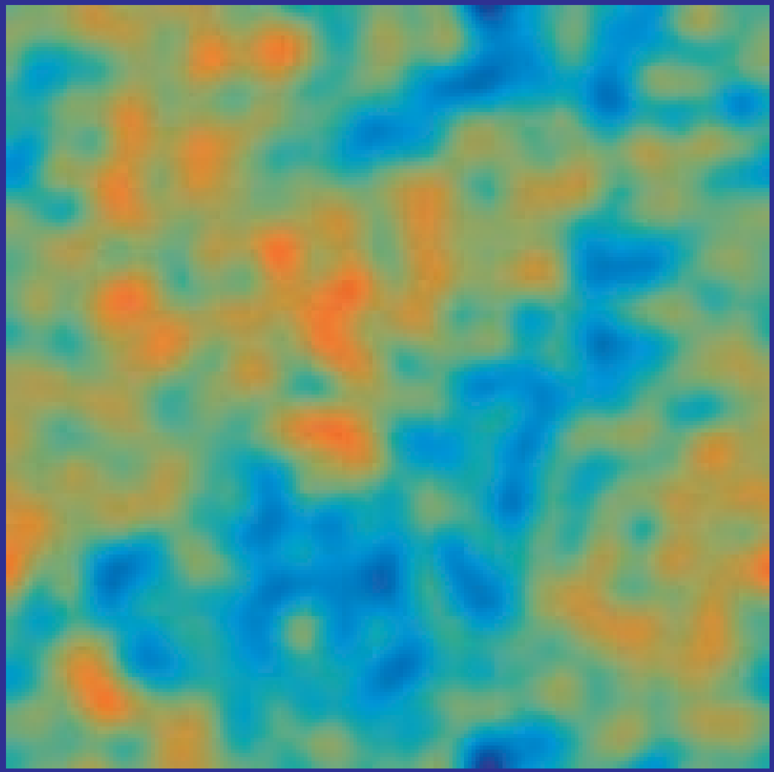

rms deflection

2.6'

deflection coherence

10°

# Deflection Power Spectrum

- Fundamental observable is deflection power spectrum (or convergence / $l^2$ )
- Nearly entirely in linear regime

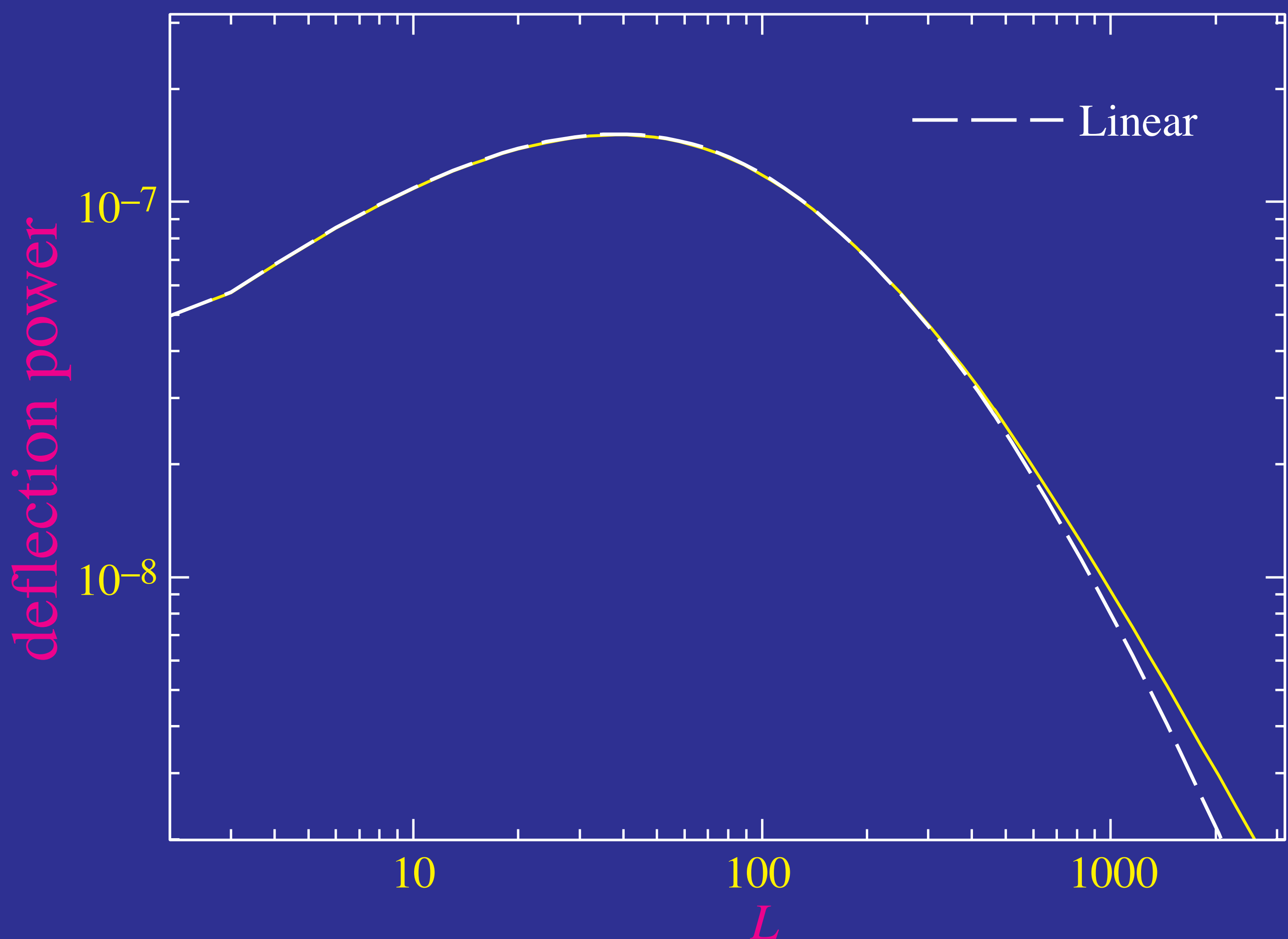

# Power Spectrum Observables

# Gravitational Lensing

- Lensing is a surface brightness conserving remapping of source to image planes by the gradient of the projected potential

$$\phi(\hat{\mathbf{n}}) = 2 \int_{\eta_*}^{\eta_0} d\eta \, \frac{(D_* - D)}{D \, D_*} \Phi(D\hat{\mathbf{n}}, \eta) \, .$$

  such that the fields are remapped as

$$x(\hat{\mathbf{n}}) \to x(\hat{\mathbf{n}} + \nabla\phi) \, ,$$

  where $x \in \{\Theta, Q, U\}$ temperature and polarization.

- Taylor expansion leads to product of fields and Fourier mode-coupling

# Flat-sky Treatment

- Taylor expand

$$\Theta(\hat{\mathbf{n}}) = \tilde{\Theta}(\hat{\mathbf{n}} + \nabla\phi)$$
$$= \tilde{\Theta}(\hat{\mathbf{n}}) + \nabla_i\phi(\hat{\mathbf{n}})\nabla^i\tilde{\Theta}(\hat{\mathbf{n}}) + \frac{1}{2}\nabla_i\phi(\hat{\mathbf{n}})\nabla_j\phi(\hat{\mathbf{n}})\nabla^i\nabla^j\tilde{\Theta}(\hat{\mathbf{n}}) + \ldots$$

- Fourier decomposition

$$\phi(\hat{\mathbf{n}}) = \int \frac{d^2l}{(2\pi)^2}\phi(\mathbf{l})e^{i\mathbf{l}\cdot\hat{\mathbf{n}}}$$
$$\tilde{\Theta}(\hat{\mathbf{n}}) = \int \frac{d^2l}{(2\pi)^2}\tilde{\Theta}(\mathbf{l})e^{i\mathbf{l}\cdot\hat{\mathbf{n}}}$$

# Flat-sky Treatment

- Mode coupling of harmonics

$$\Theta(\mathbf{l}) = \int d\hat{\mathbf{n}}\, \Theta(\hat{\mathbf{n}}) e^{-il\cdot\hat{\mathbf{n}}}$$
$$= \tilde{\Theta}(\mathbf{l}) - \int \frac{d^2\mathbf{l}_1}{(2\pi)^2} \tilde{\Theta}(\mathbf{l}_1) L(\mathbf{l}, \mathbf{l}_1)\,,$$

where

$$L(\mathbf{l}, \mathbf{l}_1) = \phi(\mathbf{l} - \mathbf{l}_1)\,(\mathbf{l} - \mathbf{l}_1) \cdot \mathbf{l}_1$$
$$+ \frac{1}{2} \int \frac{d^2\mathbf{l}_2}{(2\pi)^2} \phi(\mathbf{l}_2) \phi^*(\mathbf{l}_2 + \mathbf{l}_1 - \mathbf{l})\,(\mathbf{l}_2 \cdot \mathbf{l}_1)(\mathbf{l}_2 + \mathbf{l}_1 - \mathbf{l}) \cdot \mathbf{l}_1\,.$$

- Represents a coupling of harmonics separated by $L \approx 60$ peak of deflection power

# Power Spectrum

- Power spectra

$$\langle \Theta^*(\mathbf{l})\Theta(\mathbf{l}')\rangle = (2\pi)^2\delta(\mathbf{l}-\mathbf{l}')\; C_l^{\Theta\Theta}\,,$$
$$\langle \phi^*(\mathbf{l})\phi(\mathbf{l}')\rangle = (2\pi)^2\delta(\mathbf{l}-\mathbf{l}')\; C_l^{\phi\phi}\,,$$

becomes

$$C_l^{\Theta\Theta} = \left(1 - l^2 R\right)\tilde{C}_l^{\Theta\Theta} + \int \frac{d^2\mathbf{l}_1}{(2\pi)^2}\tilde{C}_{|\mathbf{l}-\mathbf{l}_1|}^{\Theta\Theta} C_{l_1}^{\phi\phi}[(\mathbf{l}-\mathbf{l}_1)\cdot\mathbf{l}_1]^2\,,$$

where

$$R = \frac{1}{4\pi}\int \frac{dl}{l}\, l^4 C_l^{\phi\phi}\,.$$

# Smoothing Power Spectrum

- If $\tilde{C}_l^{\Theta\Theta}$ slowly varying then two term cancel

$$\tilde{C}_l^{\Theta\Theta} \int \frac{d^2\mathbf{l}_1}{(2\pi)^2} C_l^{\phi\phi} (\mathbf{l} \cdot \mathbf{l}_1)^2 \approx l^2 R \tilde{C}_l^{\Theta\Theta} \, .$$

- So lensing acts to smooth features in the power spectrum. Smoothing kernel is $\Delta L \sim 60$ the peak of deflection power spectrum
- Because acoustic feature appear on a scale $l_A \sim 300$, smoothing is a subtle effect in the power spectrum.
- Lensing generates power below the damping scale which directly reflect power in deflections on the same scale

# Lensing in the Power Spectrum

- Lensing smooths the power spectrum with a width $\Delta l \sim 60$
- Convolution with specific kernel: higher order correlations between multipole moments – not apparent in power

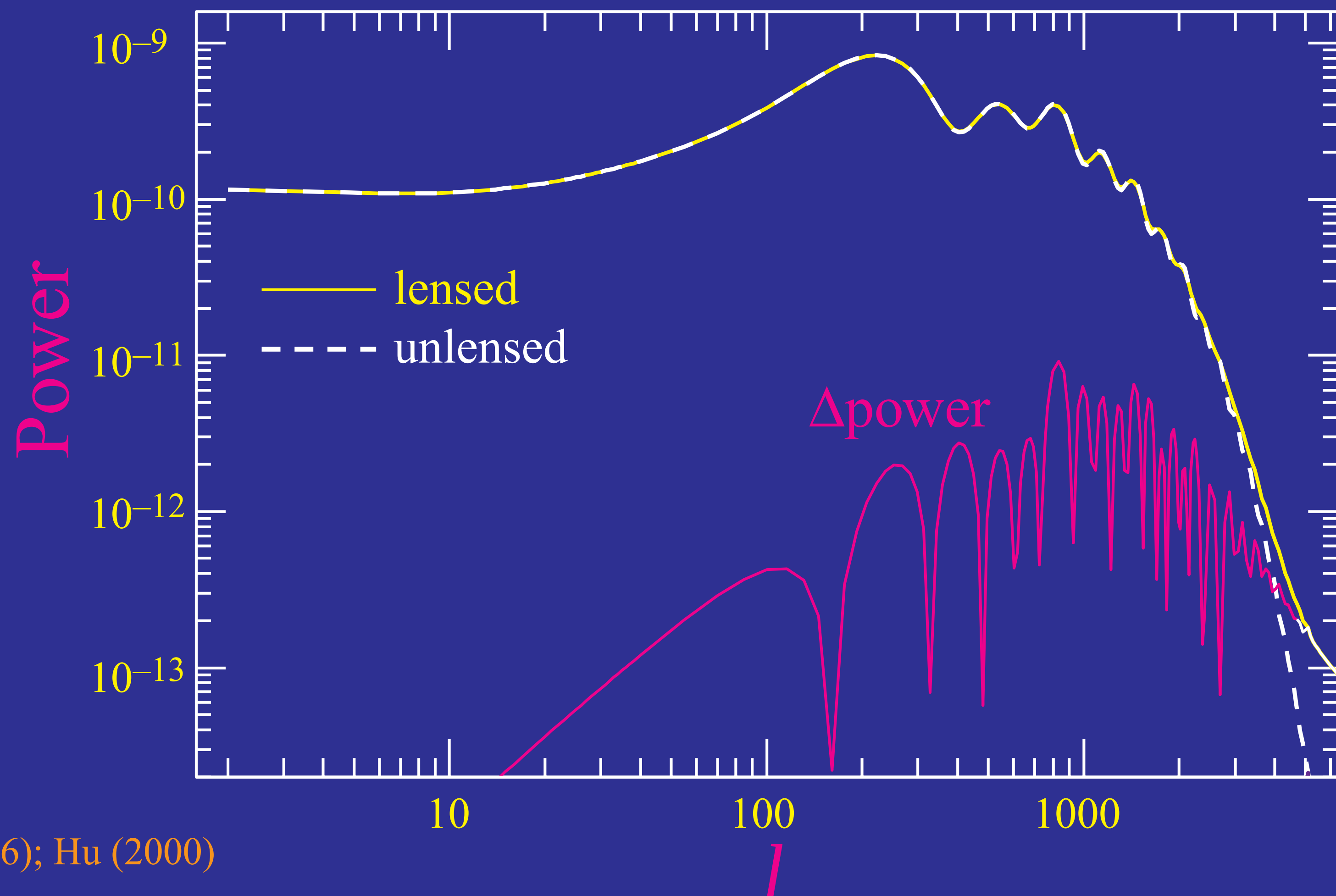


Seljak (1996); Hu (2000)

# Generation of Power

- On scales below the damping scale, primary CMB looks like a smooth gradient
- Lensing effects modulate the gradient ($l_1 \ll l$):

$$C_l^{\Theta\Theta} \approx \int \frac{d^2\mathbf{l}_1}{(2\pi)^2} \tilde{C}_{l_1}^{\Theta\Theta} C_{|\mathbf{l}-\mathbf{l}_1|}^{\phi\phi} [(\mathbf{l}-\mathbf{l}_1)\cdot\mathbf{l}_1]^2$$

$$\approx \frac{1}{2} l^2 C_l^{\phi\phi} \int \frac{d^2\mathbf{l}_1}{(2\pi)^2} l_1^2 \tilde{C}_{l_1}^{\Theta\Theta}$$

and produce power on the same scale from power in the primary gradient (Zaldarriaga 2000)

# Lensing in the Power Spectrum

- Small scale lenses modulate the large scale temperature field
- Generates power below damping scale from gradient power

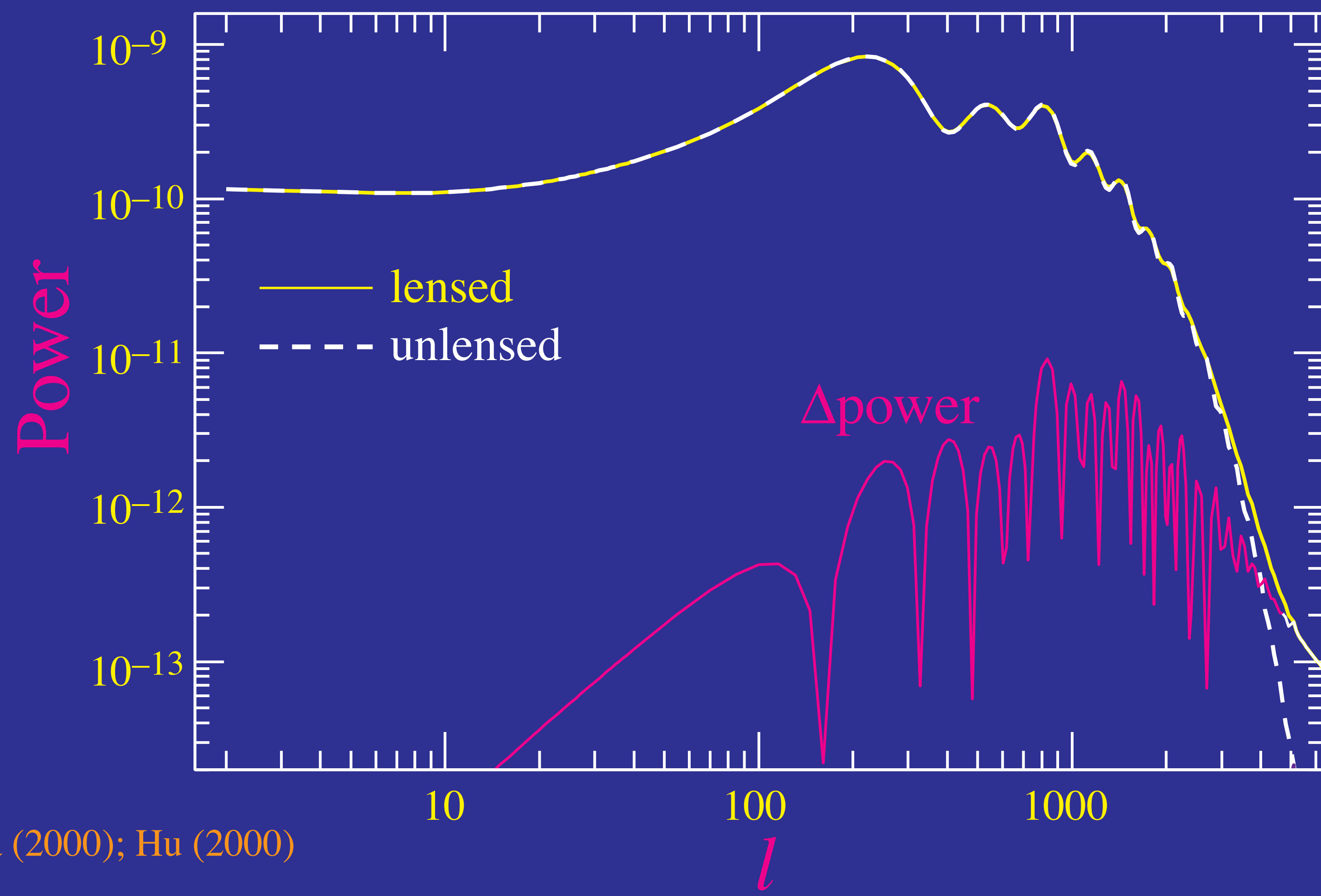


Zaldarriaga (2000); Hu (2000)

# Temperature Power Spectrum

- Lensing acts to smooth the temperature (and E polarization peaks)
- Subtle effect reaches 10% deep in the damping tail
- Statistically detectable at high significance with Planck in the absence of other secondaries and foregrounds

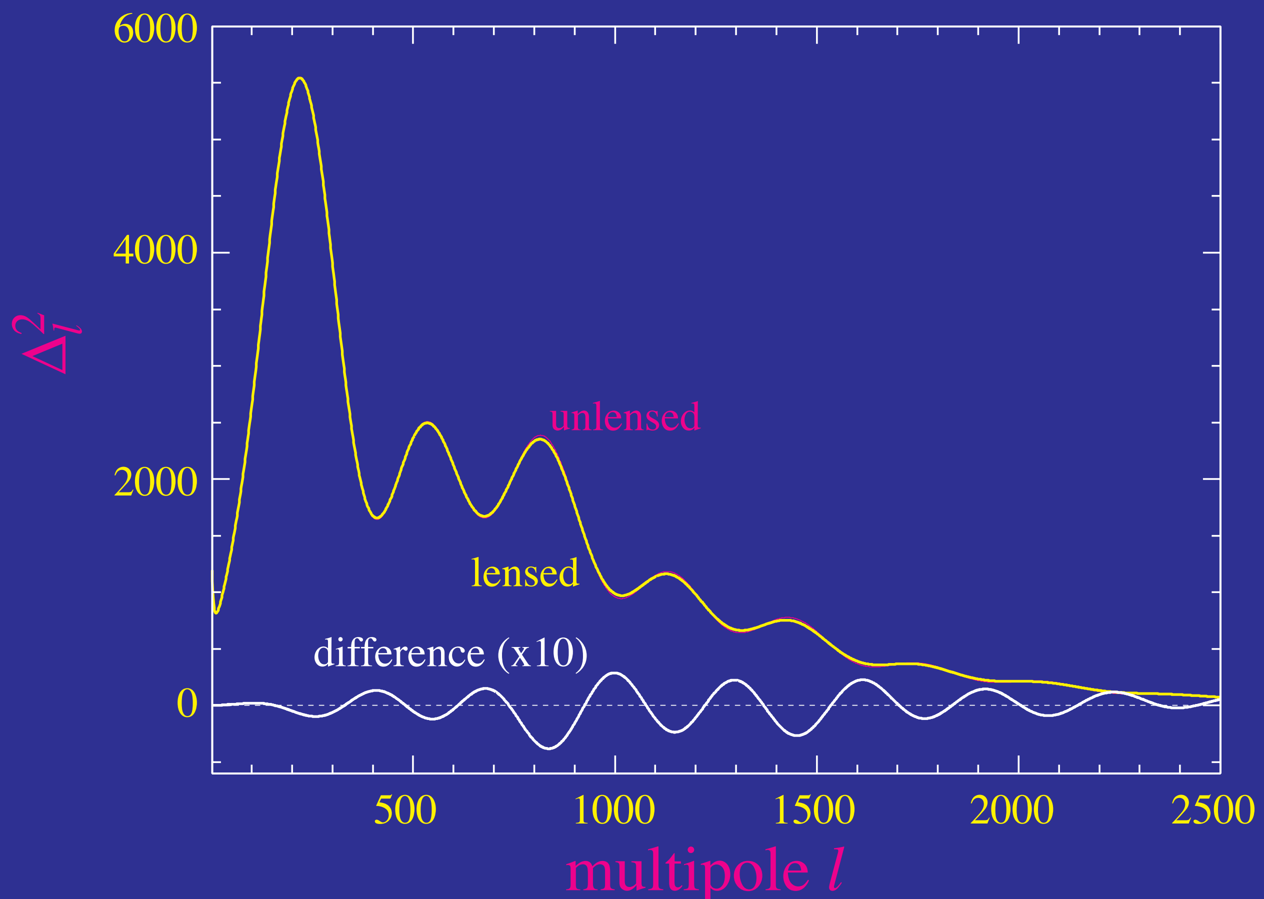


Seljak (1996) [see Challinor & Lewis (2006) for refinements]

# Polarization Lensing

- Polarization field harmonics lensed similarly

$$[Q \pm iU](\hat{\mathbf{n}}) = -\int \frac{d^2l}{(2\pi)^2}[E \pm iB](\mathbf{l})e^{\pm 2i\phi_{\mathbf{l}}}e^{\mathbf{l}\cdot\hat{\mathbf{n}}}$$

so that

$$\begin{aligned}
[Q \pm iU](\hat{\mathbf{n}}) &= [\tilde{Q} \pm i\tilde{U}](\hat{\mathbf{n}} + \nabla\phi) \\
&\approx [\tilde{Q} \pm i\tilde{U}](\hat{\mathbf{n}}) + \nabla_i\phi(\hat{\mathbf{n}})\nabla^i[\tilde{Q} \pm i\tilde{U}](\hat{\mathbf{n}}) \\
&\quad + \frac{1}{2}\nabla_i\phi(\hat{\mathbf{n}})\nabla_j\phi(\hat{\mathbf{n}})\nabla^i\nabla^j[\tilde{Q} \pm i\tilde{U}](\hat{\mathbf{n}})
\end{aligned}$$

# Polarization Power Spectra

- Carrying through the algebra to the power spectrum

$$
\begin{aligned}
C_l^{EE} &= \left(1 - l^2 R\right) \tilde{C}_l^{EE} + \frac{1}{2} \int \frac{d^2\mathbf{l}_1}{(2\pi)^2} [(\mathbf{l} - \mathbf{l}_1) \cdot \mathbf{l}_1]^2 C^{\phi\phi}_{|\mathbf{l}-\mathbf{l}_1|} \\
&\quad \times [(\tilde{C}_{l_1}^{EE} + \tilde{C}_{l_1}^{BB}) + \cos(4\varphi_{l_1})(\tilde{C}_{l_1}^{EE} - \tilde{C}_{l_1}^{BB})] \,, \\
C_l^{BB} &= \left(1 - l^2 R\right) \tilde{C}_l^{BB} + \frac{1}{2} \int \frac{d^2\mathbf{l}_1}{(2\pi)^2} [(\mathbf{l} - \mathbf{l}_1) \cdot \mathbf{l}_1]^2 C^{\phi\phi}_{|\mathbf{l}-\mathbf{l}_1|} \\
&\quad \times [(\tilde{C}_{l_1}^{EE} + \tilde{C}_{l_1}^{BB}) - \cos(4\varphi_{l_1})(\tilde{C}_{l_1}^{EE} - \tilde{C}_{l_1}^{BB})] \,, \\
C_l^{\Theta E} &= \left(1 - l^2 R\right) \tilde{C}_l^{\Theta E} + \int \frac{d^2\mathbf{l}_1}{(2\pi)^2} [(\mathbf{l} - \mathbf{l}_1) \cdot \mathbf{l}_1]^2 C^{\phi\phi}_{|\mathbf{l}-\mathbf{l}_1|} \\
&\quad \times \tilde{C}_{l_1}^{\Theta E} \cos(2\varphi_{l_1}) \,,
\end{aligned}
$$

- Lensing generates $B$-modes out of the acoustic polaraization $E$-modes contaminates gravitational wave signature if $E_i < 10^{16}$GeV.

# Temperature and Polarization Spectra

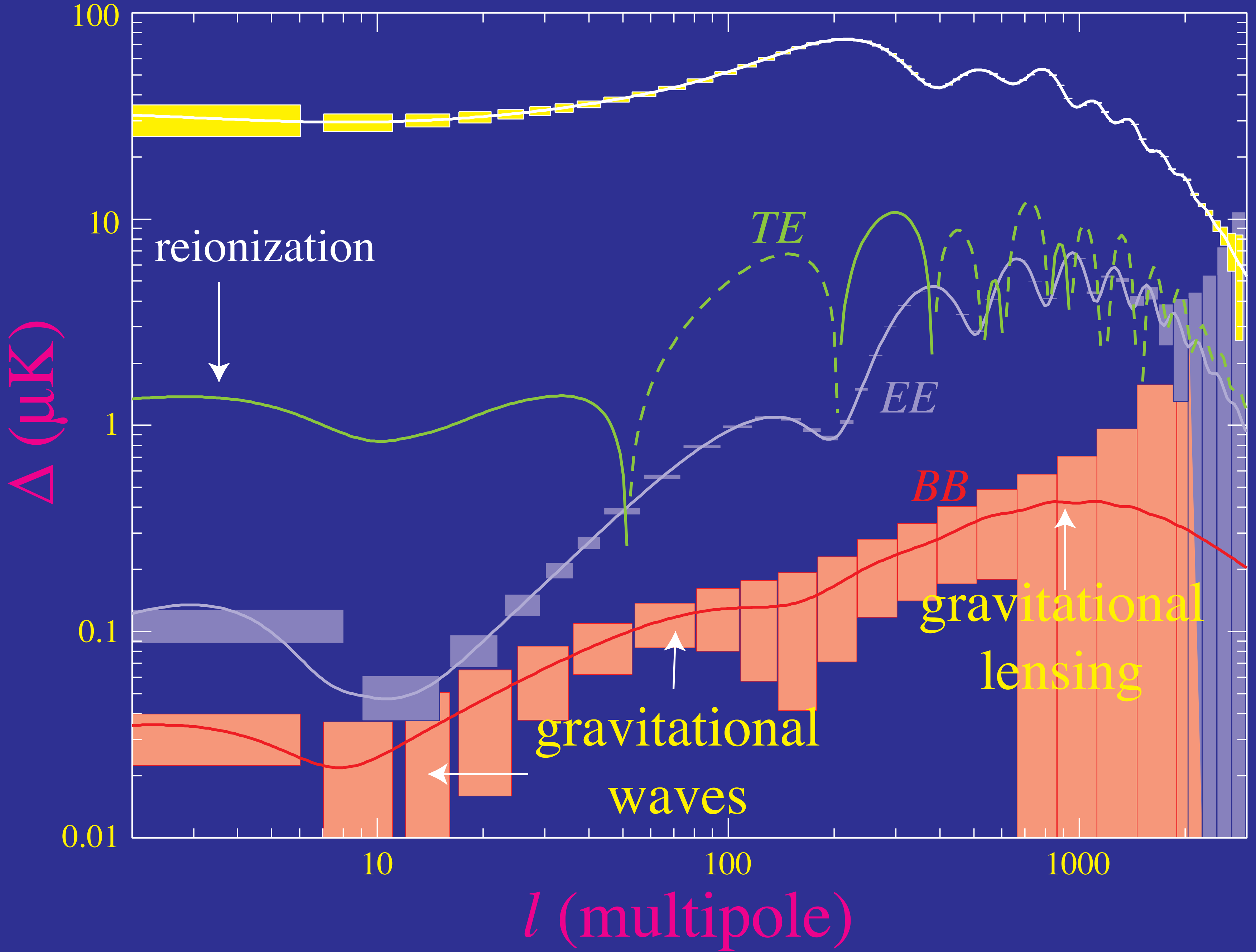

# Power Spectrum Measurements

- Lensed field is non-Gaussian in that a single degree scale lens controls the polarization at arcminutes
- Increased variance and covariance implies that 10x as much sky needed compared with Gaussian fields

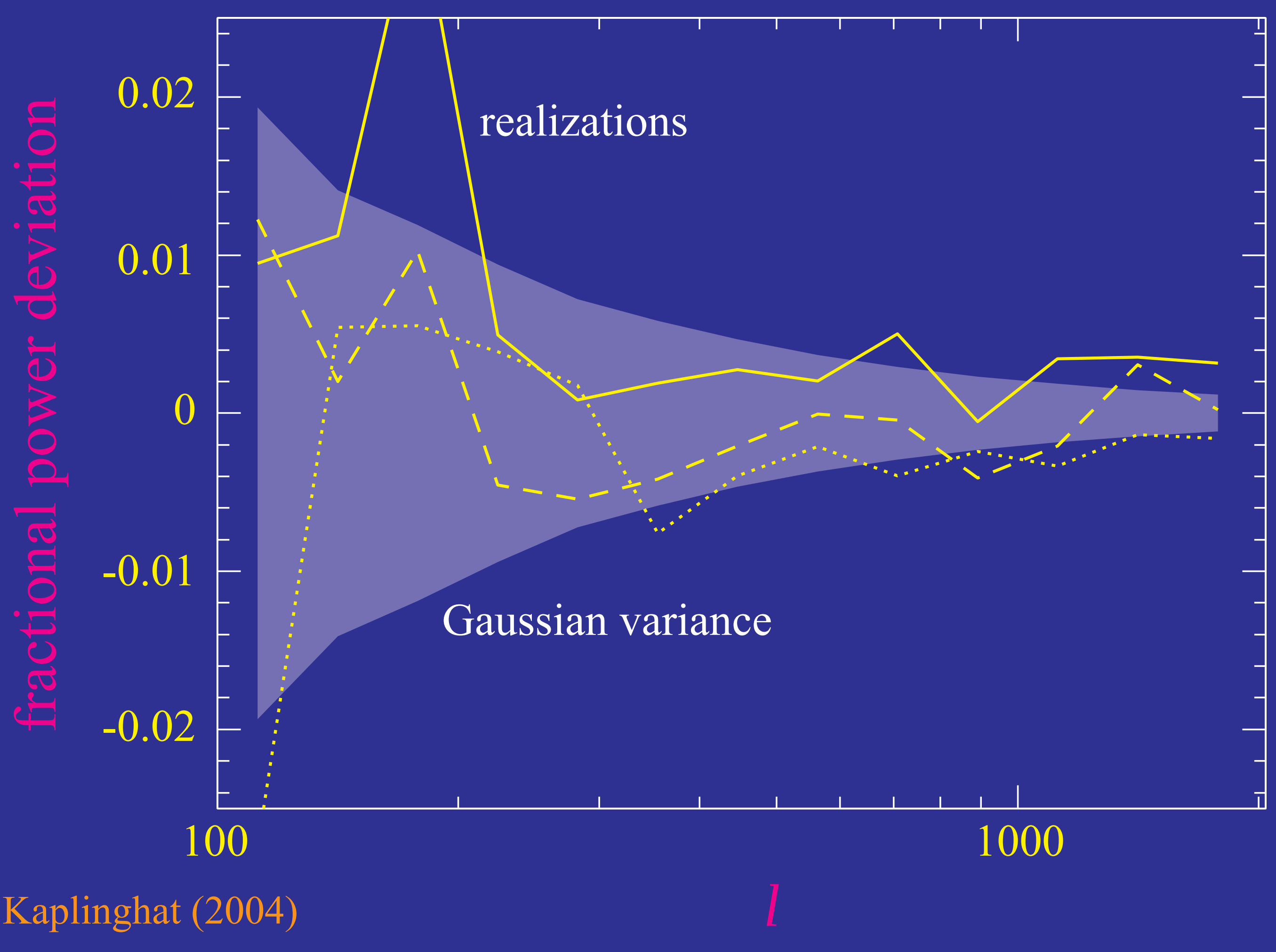


Smith, Hu & Kaplinghat (2004)

# Lensed Power Spectrum Observables

- Principal components show two observables in lensed power spectra
- Temperature and E-polarization: deflection power at $l$~100
  B-polarization: deflection power at $l$~500
- Normalized so that observables error = fractional lens power error

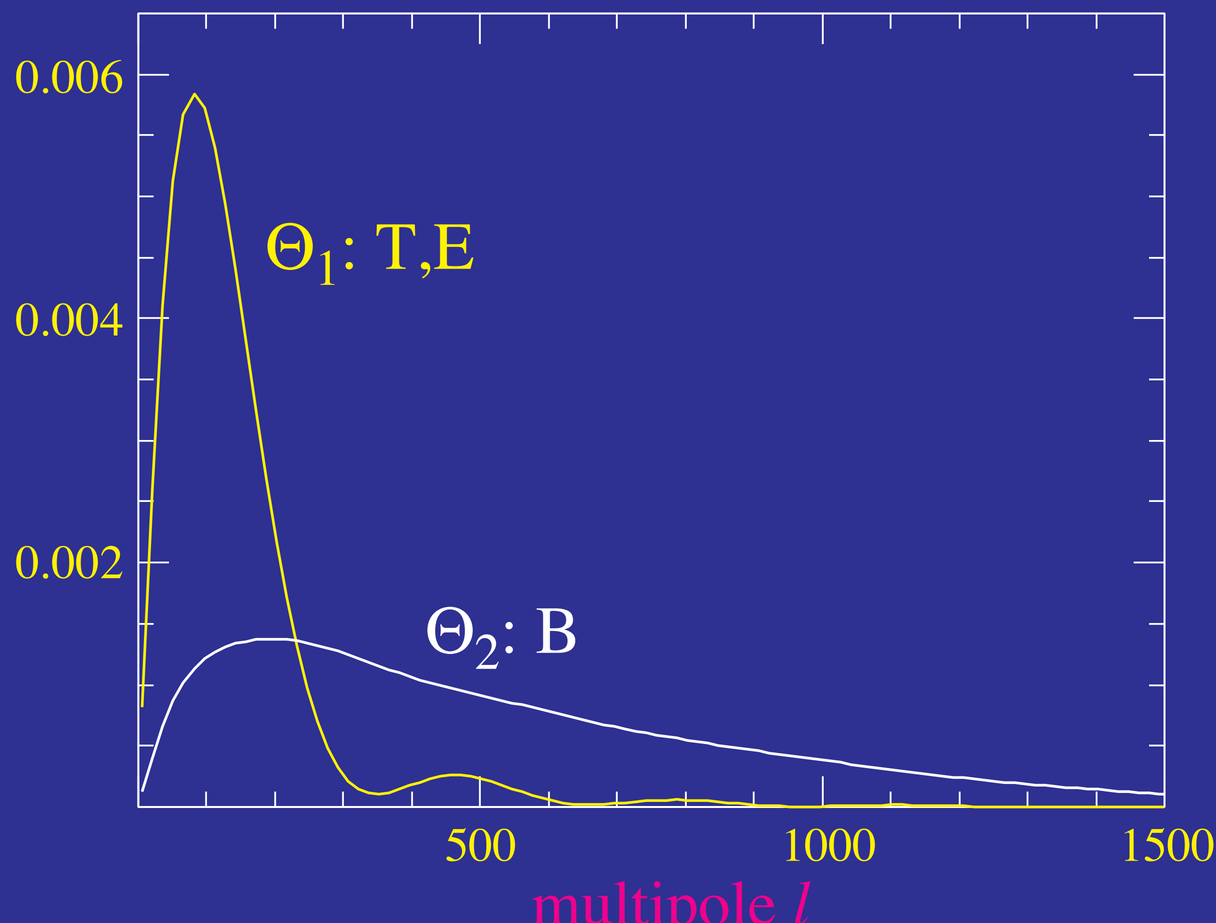


Smith, Hu & Kaplinghat (2006)

# Mass Reconstruction

# Quadratic Estimator

- Taylor expand mapping

$$
\begin{aligned}
T(\hat{\mathbf{n}}) &= \tilde{T}(\hat{\mathbf{n}} + \nabla\phi) \\
&= \tilde{T}(\hat{\mathbf{n}}) + \nabla_i \phi(\hat{\mathbf{n}}) \nabla^i \tilde{T}(\hat{\mathbf{n}}) + \ldots
\end{aligned}
$$

- Fourier decomposition $\longrightarrow$ mode coupling of harmonics

$$
\begin{aligned}
T(\mathbf{l}) &= \int d\hat{\mathbf{n}}\, T(\hat{\mathbf{n}}) e^{-il\cdot\hat{\mathbf{n}}} \\
&= \tilde{T}(\mathbf{l}) - \int \frac{d^2\mathbf{l}_1}{(2\pi)^2} (\mathbf{l} - \mathbf{l}_1) \cdot \mathbf{l}_1 \, \tilde{T}(\mathbf{l}_1) \phi(\mathbf{l} - \mathbf{l}_1)
\end{aligned}
$$

- Consider fixed lens and Gaussian random CMB realizations: each pair is an estimator of the lens at $\mathbf{L} = \mathbf{l}_1 + \mathbf{l}_2$ (Hu 2001):

$$
\langle T(\mathbf{l}) T'(\mathbf{l}') \rangle_{\rm CMB} \approx \left[ \tilde{C}_{l_1}^{TT} (\mathbf{L} \cdot \mathbf{l}_1) + \tilde{C}_{l_2}^{TT} (\mathbf{L} \cdot \mathbf{l}_2) \right] \phi(\mathbf{L}) \quad (\mathbf{l} \neq -\mathbf{l}')
$$

# Reconstruction from the CMB

- Generalize to polarization: each quadratic pair of fields estimates the lensing potential (Hu & Okamoto 2002)

$$\langle x(\mathbf{l}) x'(\mathbf{l}') \rangle_{\rm CMB} = f_\alpha(\mathbf{l}, \mathbf{l}') \phi(\mathbf{l} + \mathbf{l}') \,,$$

  where $x \in$ temperature, polarization fields and $f_\alpha$ is a fixed weight that reflects geometry
- Each pair forms a noisy estimate of the potential or projected mass - just like a pair of galaxy shears
- Minimum variance weight all pairs to form an estimator of the lensing mass
- Generalize to inhomogeneous noise, cut sky and maximum likelihood by iterating the quadratic estimator (Seljak & Hirata 2002)

# High Signal-to-Noise B-modes

- Cosmic variance of CMB fields sets ultimate limit for $T,E$
- $B$-polarization allows mapping to finer scales and in principle is not limited by cosmic variance of $E$ (Hirata & Seljak 2003)

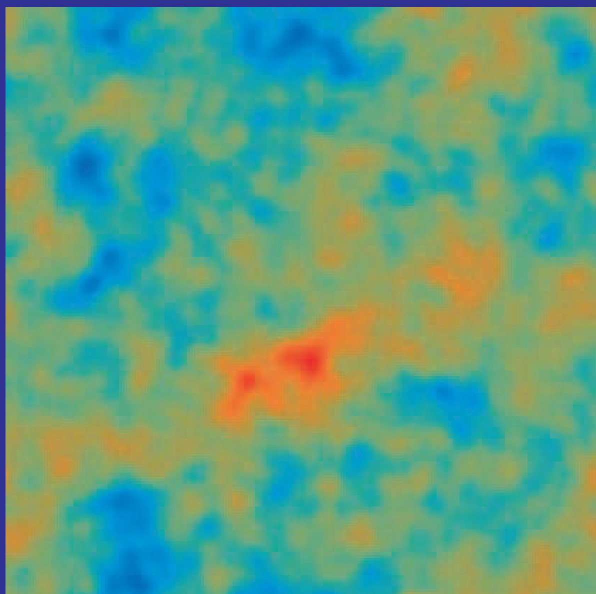

mass

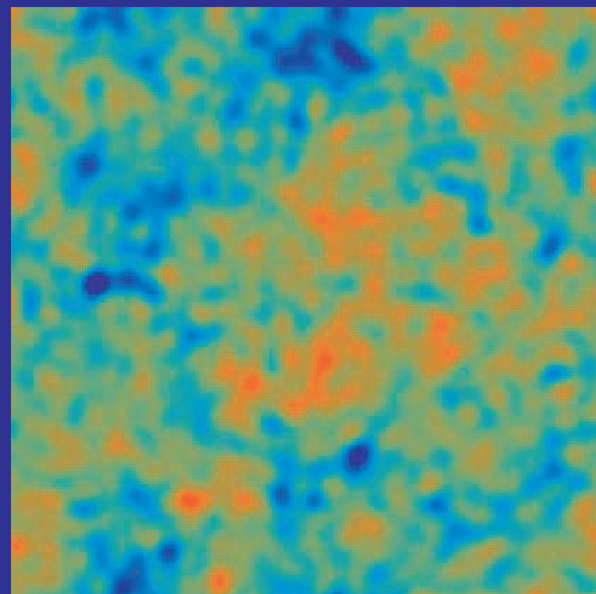

temp. reconstruction

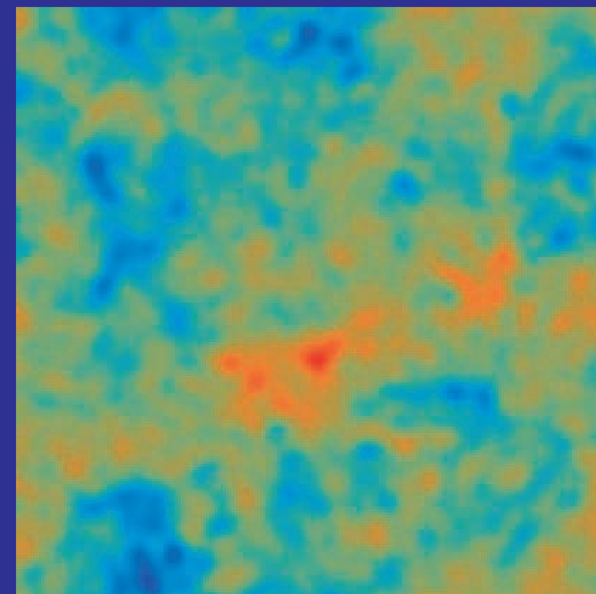

EB pol. reconstruction

100 sq. deg; 4' beam; 1μK-arcmin

Hu & Okamoto (2001)

# Matter Power Spectrum

- Measuring projected matter power spectrum to cosmic variance limit across whole linear regime 0.002< k < 0.2 *h*/Mpc

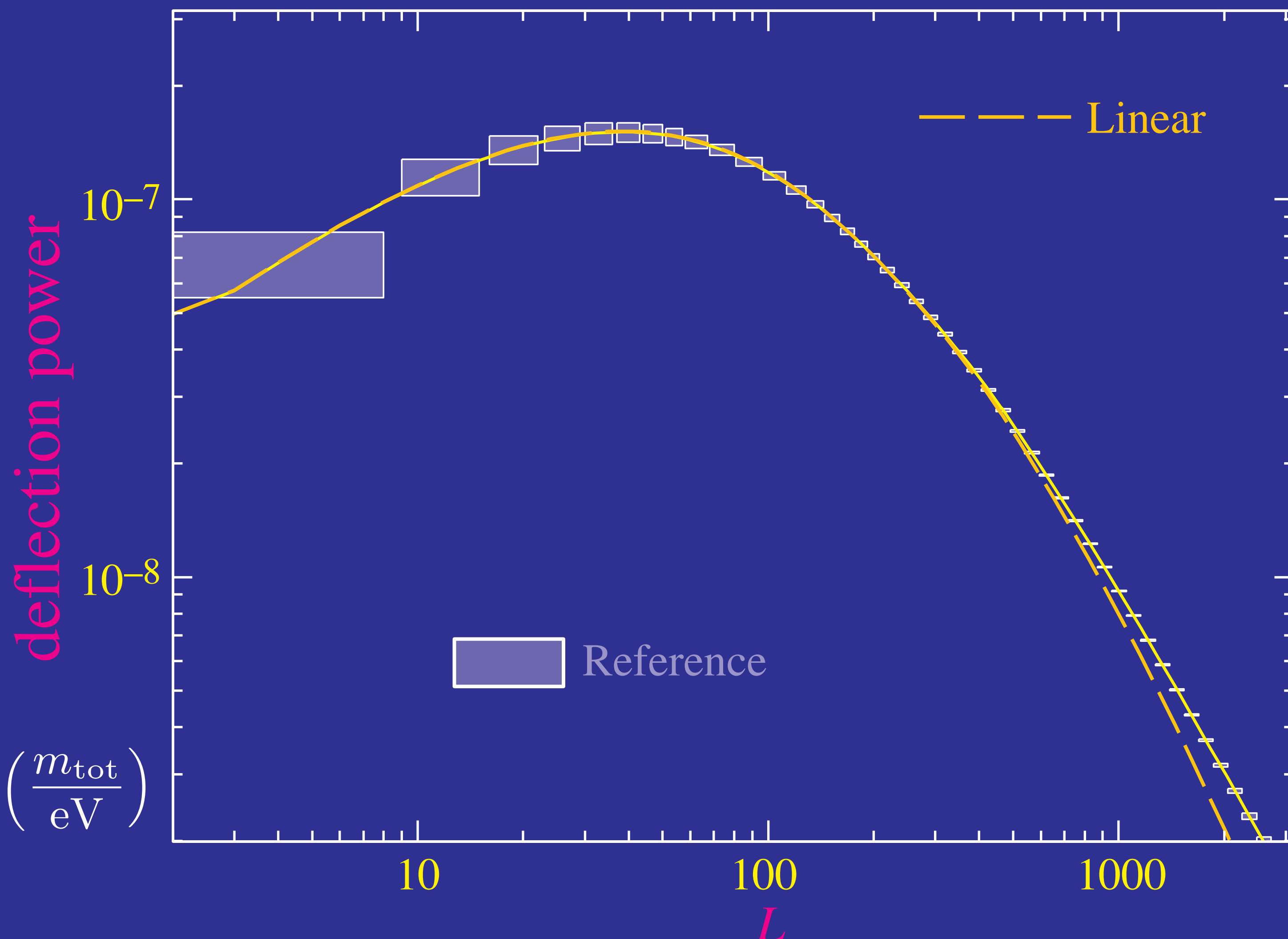


$$\frac{\Delta P}{P} \approx -0.6 \left( \frac{m_{\rm tot}}{\rm eV} \right)$$

Hu & Okamoto (2001)

# Matter Power Spectrum

- Measuring projected matter power spectrum to cosmic variance limit across whole linear regime $0.002 < k < 0.2\ h/\mathrm{Mpc}$

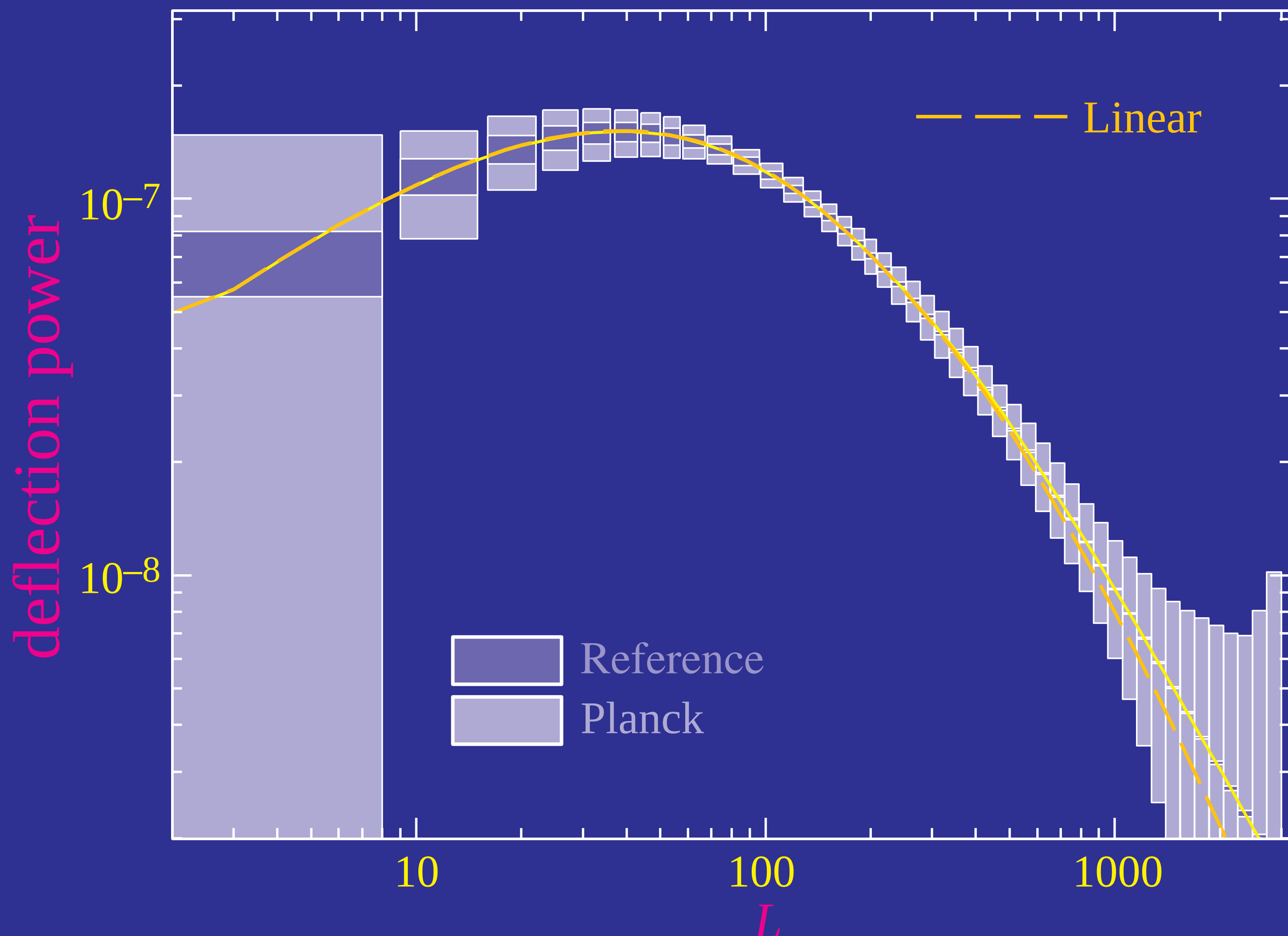


Hu & Okamoto (2001)

# Reconstruction in the Halo Regime

- Reconstruction techniques noisy but nearly unbiased *if* gradients from lensed image and other contaminates filtered out

(Hu, DeDeo, Vale 2007)

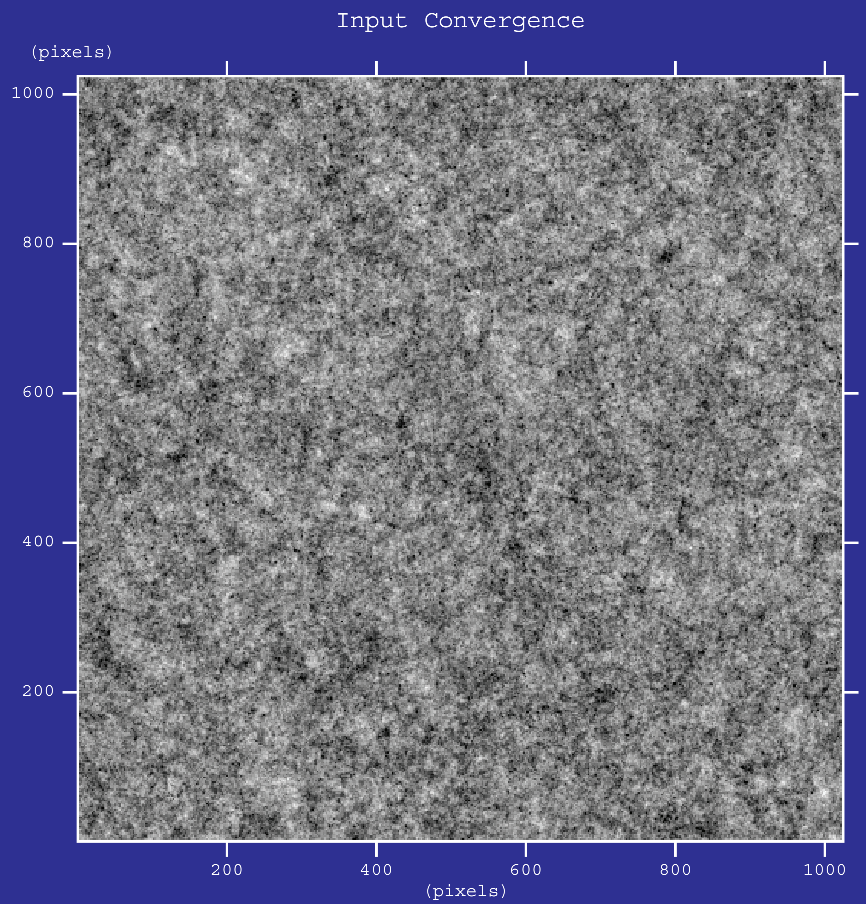


Input κ

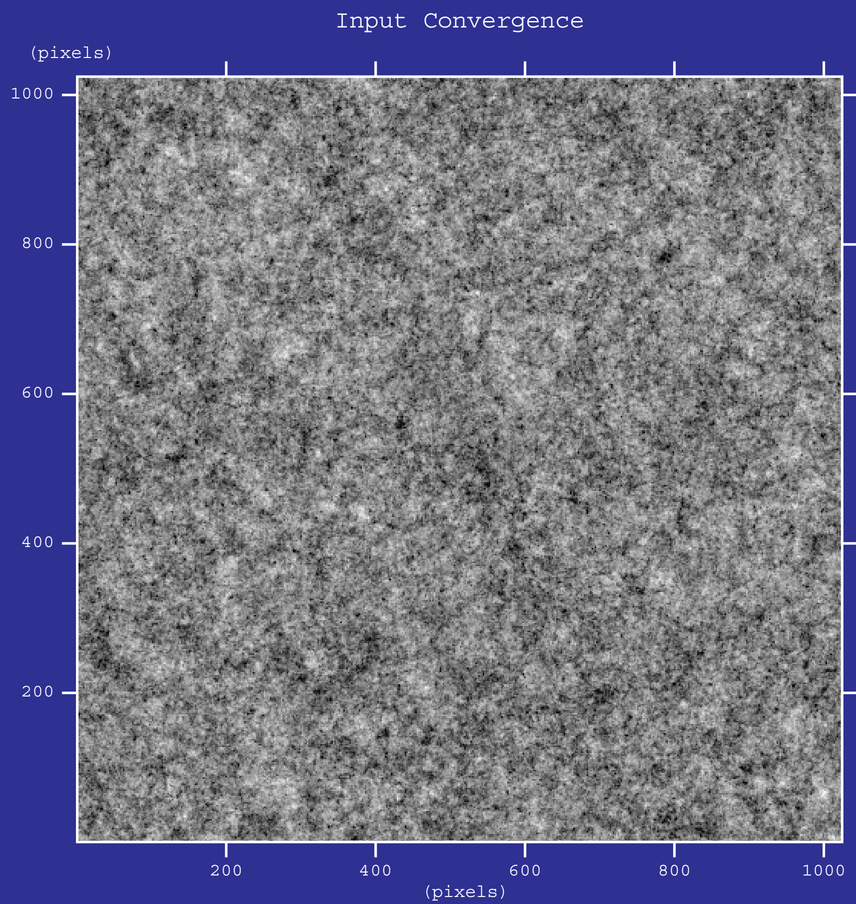


Vale (2007, unpublished); Zahn (in prep)

# Reconstruction in the Halo Regime

- Reconstruction techniques noisy but nearly unbiased *if* gradients from lensed image and other contaminates filtered out

(Hu, DeDeo, Vale 2007)

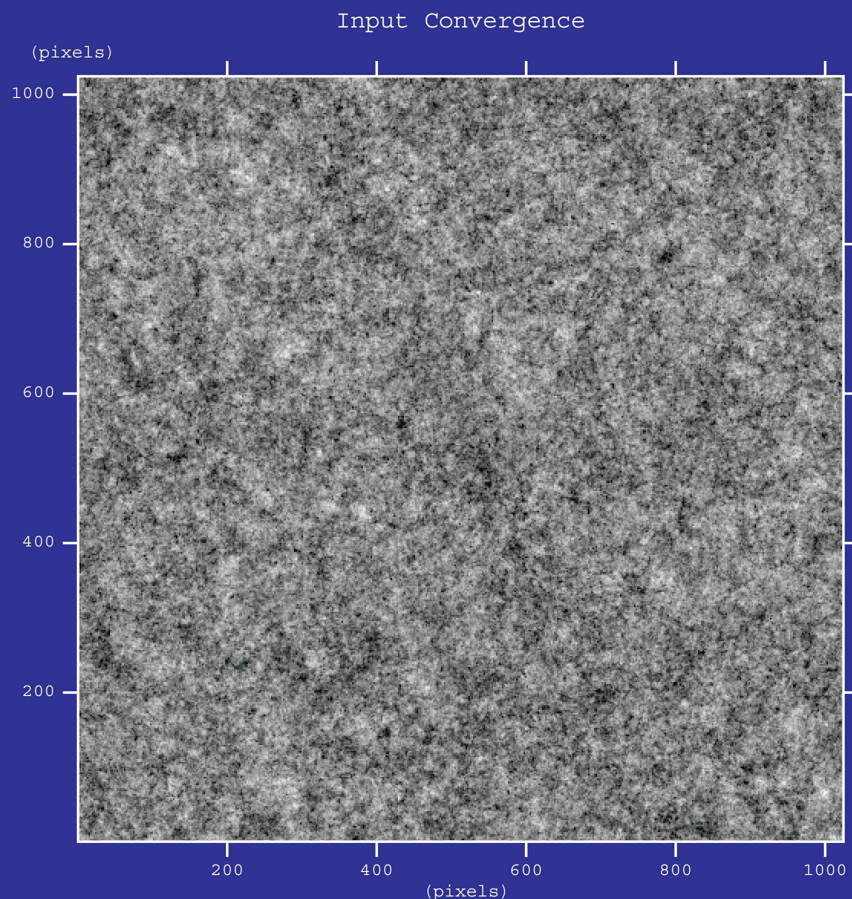


Input κ

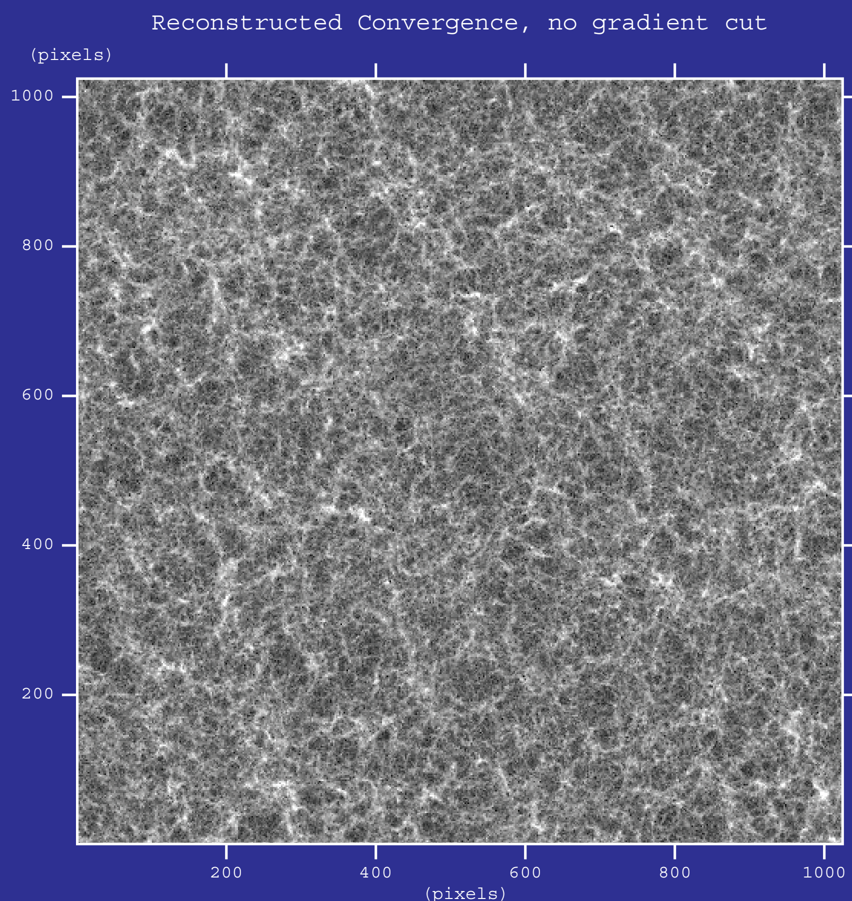


Vale (2007, unpublished); Zahn (in prep)

# Reconstruction in the Halo Regime

- Reconstruction techniques noisy but nearly unbiased *if* gradients from lensed image and other contaminates filtered out

(Hu, DeDeo, Vale 2007)

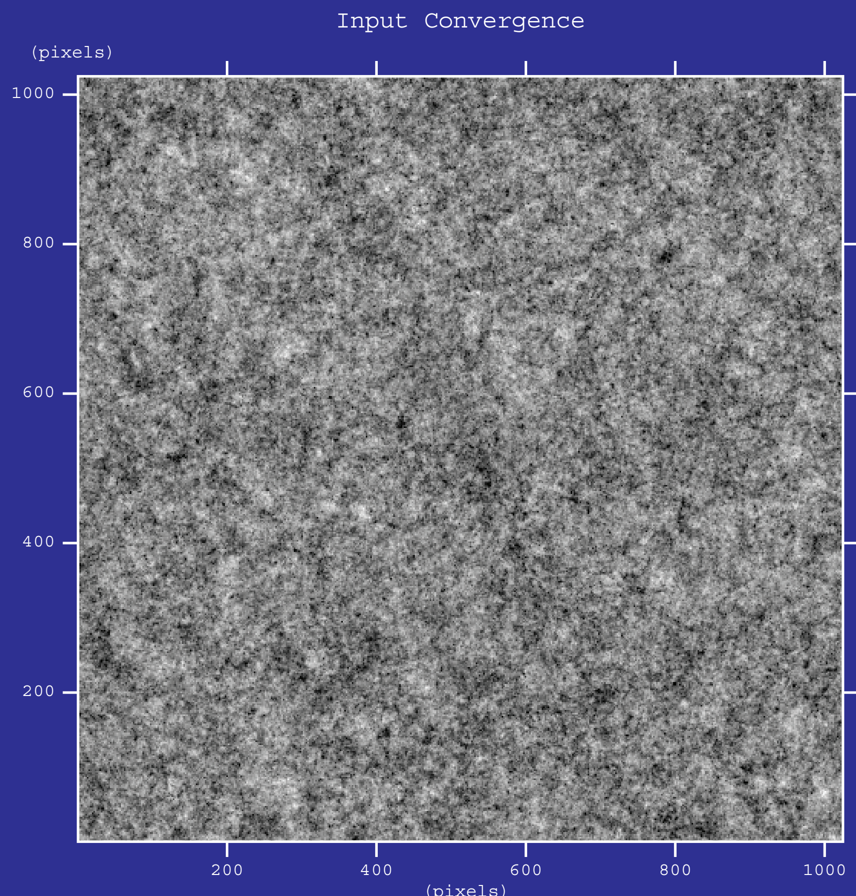


Input κ

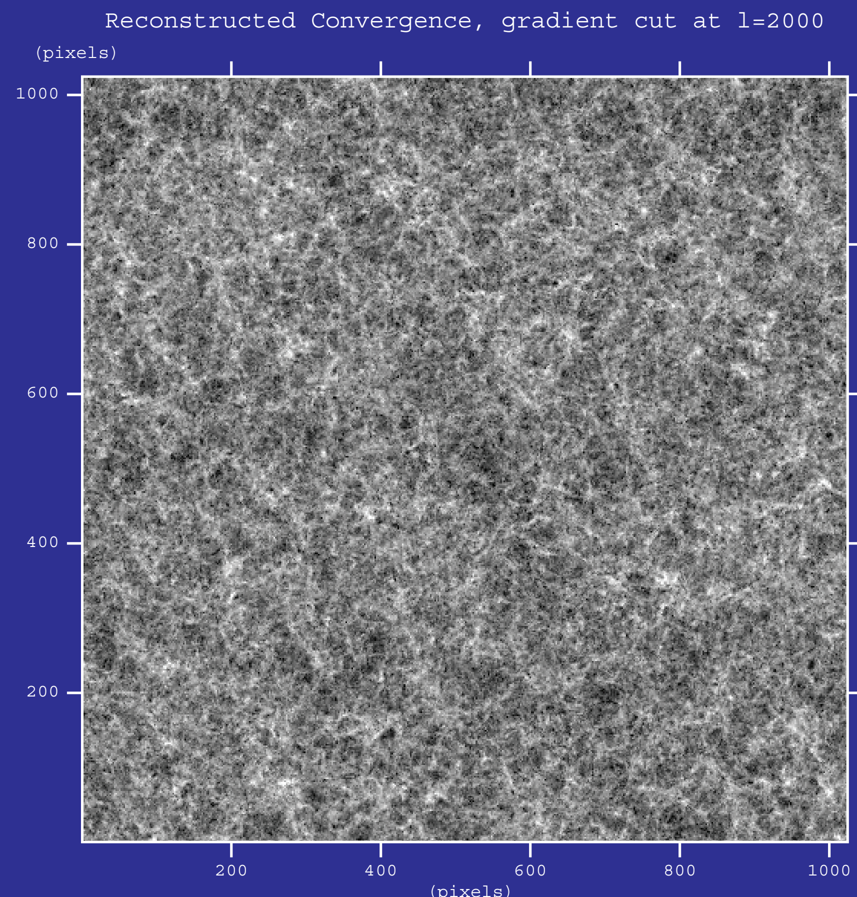


Vale (2007, unpublished); Zahn (in prep)

# Cluster Lensing

- CMB lensing reconstruction measures cluster lensing statistically through average profiles or the cluster-mass correlation function